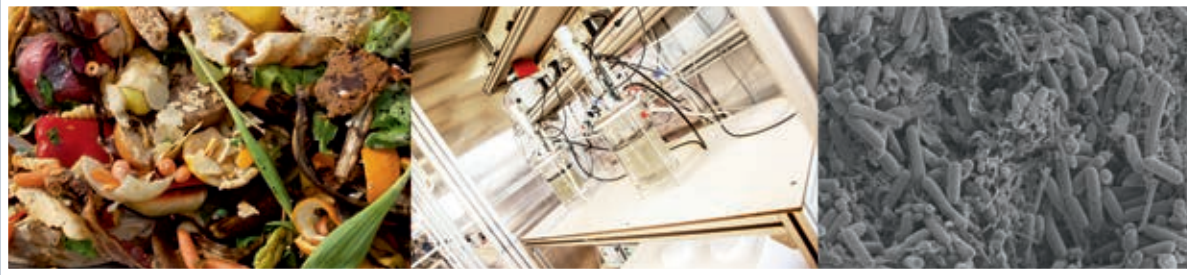# Control strategies for ethanol-based chain elongation processes

Mark Roghair

Control strategies for ethanol-based chain elongation processes

Mark Roghair

Control strategies for ethanol-based chain elongation processes

Mark Roghair

Thesis

submitted in fulfillment of the requirements for the degree of doctor
at Wageningen University
by the authority of the Rector Magnificus,
Prof. Dr A.P.J. Mol,
in the presence of the
Thesis Committee appointed by the Academic Board
to be defended in public
on Friday 16 November 2018
at 4 p.m. in the Aula.

Table of contents

ABSTRACT

Chain elongation with open cultures is an emerging biotechnological process for the conversion of residual biomass to precursors for fuels and chemicals. Like anaerobic digestion, chain elongation is catalyzed by an anaerobic open-culture (i.e. reactor microbiome). The open culture chain elongation process upgrades low-value volatile fatty acids (VFAs from e.g. acidified organic waste) with an electron donor (such as ethanol) into high-value medium chain fatty acids (MCFAs), such as n-caproate. Although fermenting with open-cultures has many advantages, they do typically bring also undesired competing processes which degrade substrates and products. A selective control (i.e. inhibition) of these competing processes will lead to a more effective chain elongation process. The goal of this thesis was to control competing processes in ethanol-based chain elongation. Special attention was given to control the competing process excessive ethanol oxidation (EEO). EEO degrades ethanol, which is a valuable substrate, but does not contribute directly to chain elongation.

In this thesis, it was shown that EEO is dependent on hydrogenotrophic methanogenesis. The overall reaction can be referred to as syntrophic ethanol oxidation. By limiting the CO_2 loading rate to a chain elongation process, syntrophic ethanol oxidation was also limited. Next to CO_2 loading rate, it was found that a long HRT in a continuous chain elongation process also resulted in a limited rate of syntrophic ethanol oxidation. A major advantage of this strategy over a limited CO_2 loading rate is that the n-caproate concentration can become very high. Later on, with inhibition assays, it was shown that these high n-caproate concentrations were inhibitory to syntrophic ethanol oxidation. As such, accumulation of n-caproate in chain elongation bioreactors inhibits syntrophic ethanol oxidation which leads to a more selective and ethanol-efficient chain elongation process.

In this thesis, also the discovery of granular sludge formation in a chain elongation process was presented. The granules did contribute to MCFA production; though the formation of these granules seemed to coincide with high-rate syntrophic ethanol oxidation. Although chain elongation can effectively produce n-caproate from organic residues, ethanol and base use can be further reduced to lower operational costs and environmental impact. An outlook is provided, therefore, on how to further minimize ethanol-use and base-use to further increase the effectiveness of chain elongation processes.

CHAPTER 1

General Introduction

1.1 Biomass residues as alternative resource for fuels and chemicals

Due to a growing world population and wealth, the demand for fuels and chemicals is increasing. Fuels and chemicals are conventionally produced from petrochemical resources (e.g. kerosene from fossil oil [1]), food crops (e.g. bioethanol from sugarcane [2]) and oil crops (e.g. biodiesel from palm oil [3]). Using these resources for production of fuels and chemicals, however, has major drawbacks. Whereas petrochemical resources are finite and cause global warming, using arable land space for applications other than food production results in enhanced loss of water resources and biodiversity [4] [5]. It is therefore evident that tomorrow's fuels and chemicals have to be produced from renewable resources which do not compete for arable land space. Fortunately, these alternative resources do exist: biomass residues that are less suitable for food and feed, such as wheat straw, food scraps, sewage sludge and potato peels (Figure 1.1), have great potential as alternative resource for fuels and chemicals and are abundantly available. Within the European Union, 88 million tonnes of food waste were generated in 2012, including agricultural residues, residues from the food industry, supermarket food waste and food scraps from restaurants and households [6]. Recycling such residues into renewable fuels and chemicals reduces both the dependency of petrochemical resources and land-use for non-food applications.

The conversion of biomass residues into bio based fuels and chemicals fits within the philosophy of a circular economy. In a circular economy, residual streams and used products don't become waste but are used again as valuable resources. This is more sustainable than a linear economy, in which natural resources are consumed while residual streams and used products are typically incinerated, disposed of, or used as land fill, leading to depletion of natural resources and environmental pollution. The European commission defined a circular economy as an economy in which "*the value of products, materials and resources is maintained in the economy for as long as possible, and the generation of waste minimized*" [11]. By converting biomass residues into a fuel or into a chemical instead of incinerating for heat and/or electricity production, more value is maintained. Moreover, a waste stream is hereby reduced, thus resembling the key feedstock for a circular (biobased) economy.

Figure 1.1: Examples of biomass residues that can serve as renewable feedstock for production of fuels and chemicals. a) Straw, b) food scraps, c) sewage sludge, d) potato peels. Images are adapted from ref [7], [8], [9] and [10].

1.2 Feedstock composition determines which conversion route is suitable

The conversion of biomass residues into biobased fuels and chemicals is a kind of biorefining, which is defined as "*the sustainable processing of biomass into a spectrum of bio-based products (food, feed, chemicals, and/or materials) and bioenergy (biofuels, power and/or heat)*" [12]. As such, biorefining is analogous to oil refining, which is based on the conversion of fossil oil into a spectrum of products and energy. Biomass, however, cannot readily substitute for fossil oil because it has different characteristics. Whereas fossil oil consists primarily of carbon and hydrogen atoms, biomass also consists of oxygen atoms. Besides, biomass residues often contain water and nutrients, are typically heterogeneous and are usually recalcitrant to conversion [13]. These characteristics make it challenging to efficiently convert biomass residues into a valorised product. For an energy-efficient conversion, the conversion route must suit the composition of the feedstock. Residues with high water content, for example, such as food scraps and sewage sludge, are not effective

for dry thermochemical conversions (gasification and pyrolysis) because this would cost much energy to evaporate the water. Wet residues, therefore, are more suitable to be converted through wet processes such as anaerobic digestion or hydrothermal liquefaction. Lignocellulosic biomass residues, such as corn stover and wheat straw, have a low water content and are therefore more suitable for dry thermochemical processing. A disadvantage of thermochemical processes, however, is that they destroy the compost value of biomass and thereby deplete the soil of organic matter. Possible conversion routes of both wet and dry residual biomass into fuels and chemicals are presented in Figure 1.2.

Possible conversion routes of residual biomass into bio based fuels and chemicals
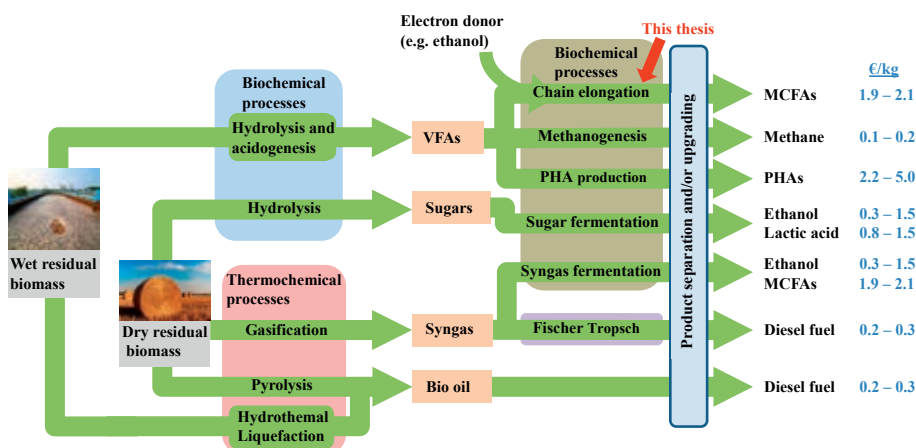
Figure 1.2: Possible conversion routes of wet and dry residual biomass to bio based fuels and chemicals via intermediates (i.e. platform chemicals) or via bio oil. Ethanol is a well-known electron donor for chain elongation and, as shown, can be derived from residual biomass in various ways. Pretreatment steps are not shown. Price ranges are derived from ref [16] and www.alibaba.com (February 2018) for bulk orders. VFAs: volatile fatty acids. MCFAs: medium chain fatty acids. PHAs: Polyhydroxyalkanoates.

Conversion routes from residual biomass to bio based fuels and chemicals typically involve a breakdown of the biomass into small intermediate molecules (i.e. platform chemicals) and a subsequent conversion of these intermediates into the desired products (Figure 1.2). To date, three platforms are distinguished: 1) sugar platform, 2) syngas platform and 3) carboxylate platform [14]. Apart from these platforms, residual biomass can also be converted into bio oil through pyrolysis (dry biomass) or hydrothemal liquefaction (wet biomass). Bio oil could eventually be upgraded to transportation fuels [15].

1.3 MCFA production from wet residual biomass through anaerobic open-culture chain elongation

This thesis focusses on the conversion of wet residual biomass into medium chain fatty acids (MCFAs), such as caproate, through the carboxylate platform. In the carboxylate platform, wet biomass is hydrolyzed and acidified into volatile fatty acids (VFAs), such as acetate, propionate and butyrate, as intermediates [14]. This process is performed by an anaerobic open-culture reactor microbiome, a consortium of microorganisms that is controlled by process conditions and not by genetics. VFAs can be further converted into biogas by the same or by a subsequent microbiome. This is also known as anaerobic digestion. Although anaerobic digestion is a common way to treat wet residual biomass [17], the resulting methane within the biogas has typically limited applications (heat / electricity / vehicle fuel [17]) and a low economic value which makes this solution not very profitable. Producing higher-value products than methane, therefore, such as MCFAs, is gaining increasing interest. MCFAs have a relatively high economic value (Figure 1.2) and can be used for a wide variety of applications such as aviation fuels, lubricants, feed additives and dyes [18]. Moreover, like methane, MCFAs too can be produced through anaerobic open-culture reactor microbiomes. The advantage of these open-culture processes is that they can handle a mixture of residual streams under mild conditions and that they do not need sterilisation of feedstock and reactor [14]. Moreover, additions of toxic and expensive bioactive chemicals (e.g. antibiotics or 2-bromoethanesulfonate) are also not necessary.

The proposed conversion of residual biomass into MCFAs proceeds through two open-culture processes which can be combined (example in [19]) or performed separately (example in [27]). First, as is inherent to the carboxylate platform, residues are hydrolysed and acidified, resulting in production of VFAs and lactate. Second, these VFAs are converted together with an electron donor, such as ethanol, into MCFAs through chain elongation. This conversion is performed by chain elongating micro-organisms (e.g. *Clostridium kluyveri*) that use the reverse β-oxidation pathway (Eq 1.1) [21]. The electron donor for chain elongation is preferably also derived from residual biomass such as lignocellulosic bioethanol (reviewed in [22]). However, todays' ethanol is typically produced from food (first generation bioethanol) or petrochemical resources (synthetic ethanol).

Overall stoichiometry of the reverse β-oxidation pathway:
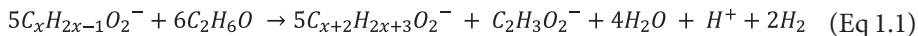
$$5C_xH_{2x-1}O_2^- + 6C_2H_6O \rightarrow 5C_{x+2}H_{2x+3}O_2^- + C_2H_3O_2^- + 4H_2O + H^+ + 2H_2 \quad \text{(Eq 1.1)}$$

Chain elongation with open cultures is an emerging application that can handle many organic feedstocks: it has been demonstrated with synthetic waste [23] [24] [25] [26] and with organic residues such as acidified organic fraction of municipal solid waste [27], acidified garden- and kitchen waste [28], with undistilled fermentation broth from the bioethanol industry [19] [29] and with acid whey waste from the dairy industry [30]. Open-culture chain elongation is typically performed under mesophilic conditions (30 °C), and at either near-neutral pH (e.g. ref [24] [25]) or at slightly acidic pH (e.g. ref [19] [29] [31]). Various reactor configurations have been used; including an upflow anaerobic filter [24], a continuous stirred tank reactor [32] and a bioreactor with in-line product extraction [19]. Although electron donors such as lactate [20] and methanol [33] have been successfully used, ethanol is the preferred electron donor for high-rate chain elongation [18]. In recent years, researchers have demonstrated MCFA production rates with ethanol-based chain elongation up to 57 g$_{\text{MCFA}}$/L/d [25]. Also, open-culture chain elongation can be very selective as MCFA selectivities of up to 94 % on an electron basis have been reported [25]. Open-culture chain elongation can also reach high product concentrations of up to 23.4 g/L caproate [34] while using lactate as electron donor. Overall, the technology has made great leaps in the past decade. Currently, a demonstration factory is being developed, processing approximately 40 tonnes food scraps per day, by ChainCraft in Amsterdam, the Netherlands (www.chaincraft.nl).

1.4 Challenges in ethanol-based chain elongation; controlling competing processes

Because we use an open-culture process for chain elongation, other functional groups of microorganisms than chain elongating microorganisms are usually present and active too [27]. These other functional groups of microorganisms can degrade the substrates and products into undesired metabolites. As such, their presence and activity results in a limited MCFA selectivity and/or in an inefficient use of substrates. Understanding the role of these competing processes and how they can be suppressed is essential for an efficient and selective MCFA production

process. This suppression is preferably performed without the use of bioactive chemicals, such as 2-bromoethanesulfonate or iodoform as methanogenic inhibitor.

Although we recognize several competing processes (acetotrophic methanogenesis, anaerobic oxidation of fatty acids, hydrogenotrophic methanogenesis, excessive ethanol oxidation), in this thesis we particularly focus on one process; excessive ethanol oxidation (EEO). EEO degrades ethanol into acetate and hydrogen (Eq 1.2). It is important to suppress EEO because 1) it does not produce MCFAs directly and therefore it reduces the efficiency and 2) EEO releases a proton which requires extra base addition and thus operating expenses. Recently, our group evaluated the production of 1 kg caproate from organic waste by ethanol-based chain elongation with a life cycle assessment. A dominant cause of environmental impact was the use of both ethanol and base [35]. As such, to lower the environmental impact of ethanol-based chain elongation, their consumption should be reduced in the development of this technology. However, because EEO results in an extra supply of acetate, it may be an important process in the conversion of an ethanol-rich feedstock into MCFAs through ethanol upgrading (ethanol oxidation into acetate and subsequent chain elongation into even-numbered fatty acids).

Excessive ethanol oxidation (EEO):
$$C_2H_6O + H_2O \rightarrow C_2H_3O_2{}^- + H^+ + 2H_2 \hspace{3cm} \text{(Eq 1.2)}$$

EEO is considered to be performed by ethanol-oxidizing microorganisms which do not perform chain elongation. Earlier work demonstrated that EEO depends on hydrogenotrophic methanogenesis [29]. By limiting hydrogenotrophic methanogenic activity through a limited CO_2 availability, the hydrogen partial pressure increases which thermodynamically inhibits EEO [27] [29]. EEO, however, has not been quantified in chain elongation processes. In addition, the effect of EEO on ethanol upgrading was not studied before. Furthermore, alternative control strategies than CO_2 availability to suppress EEO have not been identified to date.

1.5   Goals and thesis outline

The goal of this thesis was to control competing processes in ethanol-based chain elongation with open cultures. This was performed by investigating a process observation (granular chain elongation sludge formation) and by investigating several control strategies (CO_2 loading rate, HRT and n-caproate concentration) on the rate of chain elongation, EEO and other (possible) competing processes.

In the next chapter, Chapter 2, we present the discovery of granular sludge formation in a chain elongation process. Granular sludge formation typically results in increased sludge retention in the reactor, which potentially leads to an increased volumetric MCFA productivity and improved process efficiency.

In Chapter 3, the quantitative effect of CO_2 loading rate on a continuous chain elongation process was investigated. Hereby, we studied not only the rate of MCFA production and EEO but also the different carbon fluxes that lead to MCFA production. Alongside, the microbial community was studied at different CO_2 loading rates.

In Chapter 4, the effect of hydraulic retention time (HRT) on a chain elongation process was investigated. A continuous chain elongation process was fed with hydrolyzed and acidified (real) food waste and additional ethanol and operated at long (4 d) and short (1 d) HRT. Both conditions were compared and evaluated based on an extensive set of performance indicators.

In Chapter 5, the effect of n-caproate concentration on the specific activity of chain elongation and competing processes was investigated with batch inhibition assays. In addition, two types of microbial biomass sludges were compared to study the potential adaptation of microbiomes to high MCFA concentrations.

In Chapter 6, a general discussion is presented about control strategies to suppress the competing processes in chain elongation. In addition, it is shown how much ethanol is inevitably used for ethanol upgrading. Finally, an outlook is provided on how to further minimize ethanol-use and base-use to further increase the effectiveness of chain elongation bioreactors.

Anaerobic Bioreactor

- Propionate
- Ethanol

- Caproate
- Heptanoate

Granular Chain Elongation Sludge
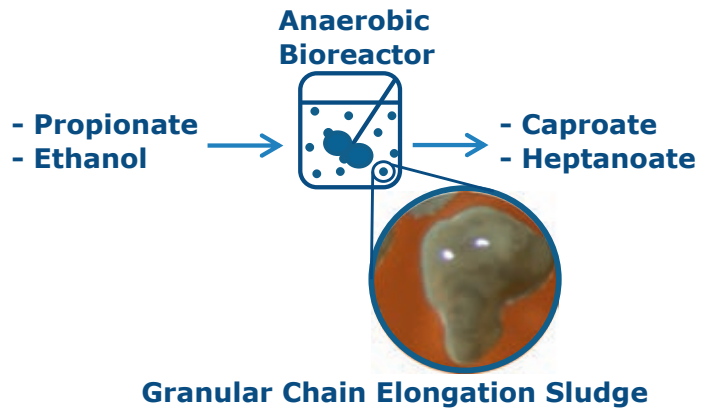
CHAPTER 2

Granular Sludge Formation and Characterization in a Chain Elongation Process

Abstract

Chain elongation is an open-culture biotechnological process which converts short chain fatty acids and an electron donor to medium chain fatty acids (MCFAs). With this letter, we present the first observation of granular sludge formation in a chain elongation process. This discovery was made in a continuously stirred anaerobic reactor producing caproate (10.8 $g \cdot L^{-1} \cdot d^{-1}$) and heptanoate (1.8 $g \cdot L^{-1} \cdot d^{-1}$) as main MCFAs. Concurrently granular and suspended sludge were shaped and attributed to 85 % and 15 % respectively of the total sludge. Both sludge types showed equal product distributions and contributed similarly to MCFA production. Granules had irregular shapes, diameters up to ~1.5 mm, settling velocities of 4 to 36 $m \cdot h^{-1}$ and contained micro-organisms with various shapes. The in-situ settler retained sludge in the bioreactor resulting in a SRT of 4.7 days at an HRT of 17 hours. Granular sludge based chain elongation can be optimized as a high rate biotechnological process.

2.1 Introduction

Chain elongation is an emerging open-culture biotechnological process that facilitates production of chemicals from renewable resources. It uses short chain fatty acids and an electron donor to form medium chain fatty acids (MCFAs) such as caproic acid, heptanoic acid and caprylic acid [18]. These MCFAs can be used as building blocks for a wide variety of applications such as solvents, fuels, lubricants, food additives, plastics and dyes [14]. Chain elongation can use organic degradable residual streams (e.g. organic fraction of municipal solid waste) as primary feedstock once these residues are hydrolysed and acidified [27]. The production of MCFAs is done by micro-organisms using the reverse β-oxidation pathway for chain elongation [36]. In recent years, researchers have demonstrated MCFA production rates with chain elongation up to 57 g·L^{-1}·d^{-1} [25]. Retaining the active micro-organisms (i.e. sludge) is crucial to reach high rates as they are responsible for the conversion [37] [38]. Sludge retention in chain elongation has been applied using polyurethane cubes as sludge carrier material within an up-flow anaerobic filter [24] [25]. Another approach for sludge retention was demonstrated by choosing anaerobic sequencing batch reactors [19] [29].

For other high-rate open-culture biotechnological processes (e.g. anaerobic wastewater treatment coupled to methane production and Anammox), sludge retention is typically mediated by a granular sludge based process [37] [38]. The fast settle-ability of granules does allow retention of the active biocatalyst in the bioreactor whereas the feedstock is supplied at continuous flow. It is already known that hydrogen producing granules in an Upflow Anaerobic Sludge Blanket (UASB) reactor can form caproate from sucrose during hydrogen fermentation [39]. To date however, former studies did not apply a specific combination of reactor configuration and process conditions that leads to granulation in a chain elongation process. Therefore, formation of granular sludge in chain elongation studies has never been reported before. Here we present the discovery of granulation during chain elongation. The objective of this study was to characterize the discovered granules on key properties (morphology, specific activity, size distribution, settle ability) and alongside clarify its impact on the chain elongation process.

2.2   Materials and methods

2.2.1   Reactor setup and operation

A Continuously Stirred Anaerobic Reactor (CSAR) (Applikon, Schiedam, the Netherlands) with a working volume of 1.0 L was used in this study. A schematic drawing of the reactor setup can be found in Figure S2.1 (Supporting information). The temperature was controlled at 30 °C. Agitation, pH, pump rates and CO_2 supply were regulated with an ADI 1010 Biocontroller (Applikon, Schiedam, the Netherlands). Reactor content was mixed at 100 rpm with two Rushton turbines (6 blades) and a marine impeller (3 blades). Mixing was further assured with 3 vertical baffles in the reactor. The pH was controlled at pH 6.8 by addition of 2M NaOH. Influent and effluent flows were controlled by peristaltic pumps (Watson and Marlow 403U, UK). A vertically positioned tube (4 mm inner diameter, 29.5 cm length) served as an in-situ settler and was connected to the effluent pump. A mass-flow controller (Brooks Instruments 5850S, the Netherlands) supplied CO_2 at $2.5 \text{ L·L}^{-1}\text{·d}^{-1}$ as chain elongating microorganisms such as *Clostridium kluyveri* require CO_2 for growth [40]. The off-gas of the reactor was cooled using a condenser at 4 °C. Exhaust gas flow was determined with a gas flow meter (Ritter, Germany). The influent was stored in a 20 L tank at 4 °C. The headspace of the influent tank was continuously flushed with N_2 gas to maintain anaerobic conditions. The initial influent medium consisted of 7.7 g·L^{-1} propionic acid, 11.5 g·L^{-1} ethanol, salts, yeast extract, vitamins and trace metals (Supporting information). The reactor was inoculated in batch mode. The inoculum originated from a continuous chain elongation reactor and contained suspended sludge in which MCFA producers, hydrogenotrophic methanogens and possibly also acetotrophic methanogens were present [27]. After 8 days of batch mode, the reactor operation mode was set to continuous with an HRT of 24 h. On day 19 the HRT was set to 17 h. On day 68, ethanol loading rate was doubled to prevent ethanol depletion. The SRT was calculated from the VSS determined in the activity test; it was assumed that the effluent contained primarily suspended sludge, which was supported by visual observations.

2.2.2   Sampling and analysis

Liquid and gas samples were taken through a rubber septum using a syringe with needle. Fatty acids (C2-C8) and ethanol were determined in liquid samples whereas CO_2 and CH_4 were determined in gas samples taken from the headspace. Sludge samples for the activity test (day 110), for making scanning electron microscopic

(SEM) images (day 110), for the settling velocity assay (day 110), and for the granule size distribution assay (day 119) were taken from the reactor under steady state conditions. Methods with regard to the activity test, SEM imaging, granule settling velocity assay, granule size-distribution assay and analytical procedures are given in the Supporting information.

2.3 Results and discussion

2.3.1 First observation of granular sludge formation

Microbial granulation was discovered in a lab-scale CSAR performing chain elongation from propionate, ethanol and CO_2. A graphical summary of reactor performance can be seen in Figure S2.2. The reactor was inoculated with suspended sludge. MCFA production started on day 7. After 84 days a steady state was reached and maintained for 27 days (day 84-97 and day 105-119). In this period the main MCFAs produced were caproate (10.8 ± 0.5 g·L^{-1}·d^{-1}) and heptanoate (1.8 ± 0.1 g·L^{-1}·d^{-1}) at concentrations of 7.4 ± 0.2 g·L^{-1} and 1.2 ± 0.1 g·L^{-1} respectively. These reactor performances are in the same range as recently reviewed [18]. Caprylate (0.2 g·L^{-1} ± 0.1 at 0.3 ± 0.1 g·L^{-1}·d^{-1}) was formed without the use of acetate as substrate; a phenomenon not observed in chain elongation studies to date. The substrates ethanol and propionate were not depleted and were present at 3.7 g·L^{-1} ± 1.4 and 2.1 g·L^{-1} ± 0.2 respectively.

After 9 days of continuous operation the earliest observation of granules (by eye visible) was made. Besides granules also suspended sludge was seen in the reactor. Further examination with a macroscope revealed that the granules had irregular shapes, a light-grey color and a smooth and shiny surface (Figure 2.1a and b). SEM images (Figure 2.1c and d) showed that the granules consisted of various microorganisms as different microbial cell shapes (i.e. rods, cocci, filamentous) were observed. Extracellular polymeric substances (EPS) were also observed on the granules by SEM analysis (Figure 2.1d). The granules were characterized on size and settling velocity (Figure 2.2a and b). Most of the granules had a diameter between 0.4 and 1.0 mm but granule diameters up to ~1.5 mm were also observed. The mean granule diameter (0.7 mm) was smaller compared to granules from full scale UASB reactors (0.8 – 2.2 mm) [41]. The mean settling velocity of the formed granules in the present study (15.3 m·h^{-1}) was found to be lower compared to full scale reactor granules (53 – 99 m·h^{-1}) [41]. Granules were persistently observed up

to the end of the experiment at day 120. This is the first report of granulation in chain elongation.
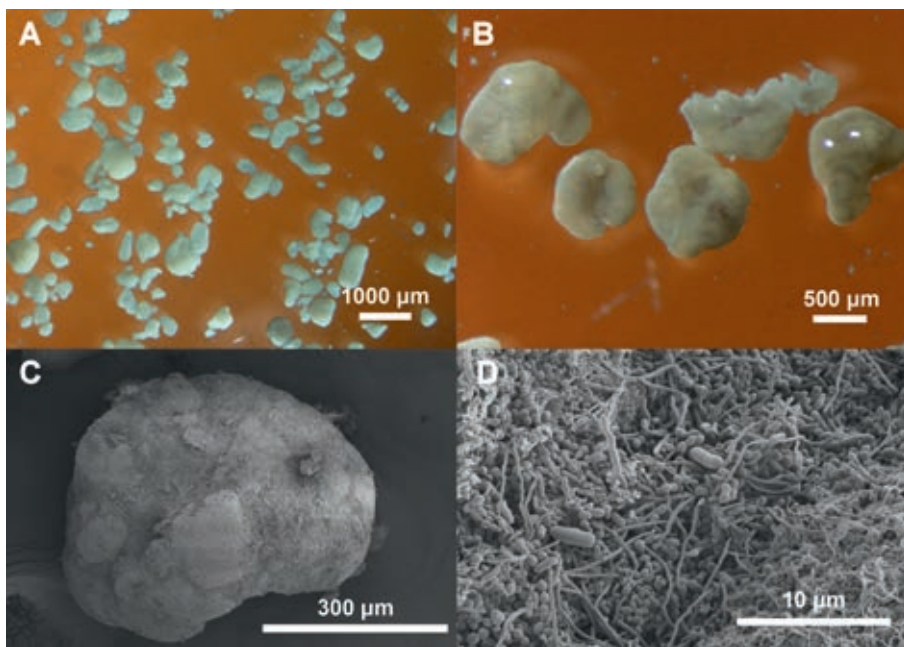
Figure 2.1: A) Overview of a sludge sample with granules, B) a close-up of several granules, C) a single granule by SEM imaging, D) surface of a granule by SEM imaging.

2.3.2 Sludge composition, specific activity and product distribution

The impact of granular sludge on reactor performance was quantified with an activity test. The activity test showed that the granules were active in chain elongation but also in methanogenesis (Figure 2.3). Suspended sludge showed a 5.5 times higher specific activity (6.6 mol C products·g $VSS^{-1}·d^{-1}$) compared to granular sludge (1.2 mol C products·g $VSS^{-1}·d^{-1}$). The difference in specific activity between granular and suspended sludge can be explained by diffusion limitation occurring in the granules [42]. Because of this phenomenon, granules could enable different micro conditions compared to suspended sludge, making different pathways feasible. The distribution of products was therefore determined for both types of sludge. These were found to be similar (Figure 2.3) and this indicates that the same pathways and relative carbon fluxes were applicable in granular and suspended biomass. No chain elongation activity was observed in bottles that were not inoculated (i.e. negative control) and this indicates that chain elongation must
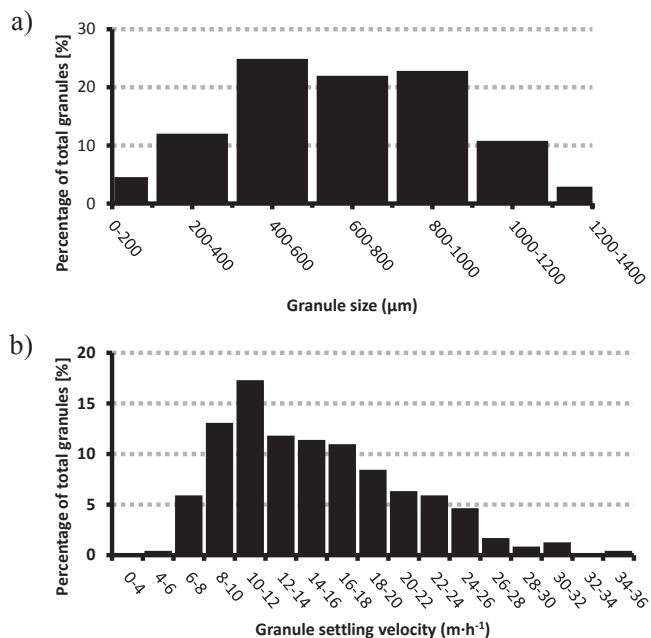
Figure 2.2: a) Granule size distribution, b) granule settling velocity distribution.

have been enabled by sludge samples from the reactors (data not shown). Granules (1.41 g VSS·L^{-1}; 85 %) were more abundant in the reactor compared to suspended sludge (0.24 g VSS·L^{-1}; 15 %). By combining the granular VSS concentrations with specific activity values we could estimate that granular sludge produced ~52 % of all products in the reactor. The higher concentration of granular sludge in combination with lower specific activity makes the net production rate of granular sludge equal to suspended sludge. Although we clarified hereby the impact of the granules under steady state conditions, we could however not relate the first visual observation of granules to a performance improvement.

The activity test showed that the granules had a specific methanogenic activity (SMA) of 13 mmol CH$_4$·g VSS^{-1}·d^{-1}. However, this value is likely underestimated because the headspace composition was only determined at the start and at the end of the activity test and linearity of the cumulative methane production over time was not substantiated. Nevertheless, the SMA of granules was in the same range compared to mesophilic methanogenic granules, which has an SMA of 9 – 39 mmol CH$_4$·g VSS^{-1}·d^{-1} [41]. Methane could have been produced by both hydrogenotrophic methanogens and by acetotrophic methanogens. However, earlier it was explained by Grootscholten et al. (2012) that acetotrophic

methanogenic activity can be limited in chain elongation at neutral pH values [24]. They suggested that the combination of hydraulic shear force and a low HRT respectively detach and wash-out the slow-growing acetotrophic methanogens. A similar effect may have been applicable in the present study. Although hydraulic shear was not induced by an up-flow mixing regime like the study of Grootscholten et al. (2012), we applied a stirring speed of 100 rpm that induced significant shear and the HRT was sufficiently low (17 h) to washout suspended biomass. The methane production rate in the reactor was in the same order of magnitude as the CO_2 uptake rate (data not shown) and this indicates that methane was primarily produced by hydrogenotrophic methanogens. However, to further elucidate the competing processes within the granular biomass, microbial analysis and activity measurements are needed at a granular level.
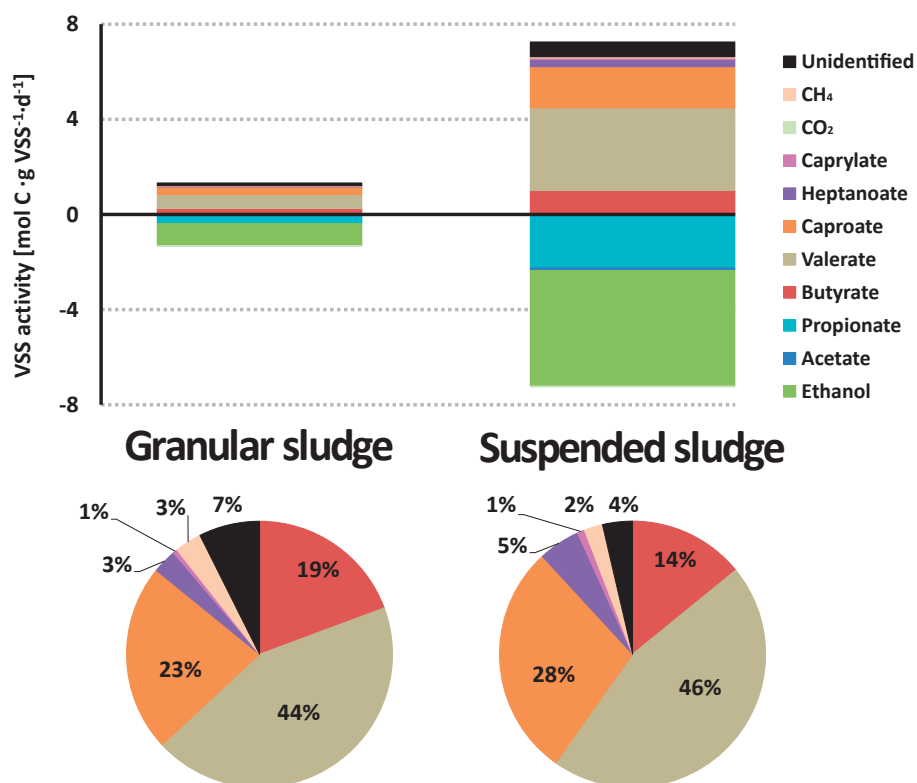
Figure 2.3: (Top) Specific activity of granular and suspended sludge, (Bottom) product distribution (mol C product / mol C total formed products) of granular sludge and suspended sludge. Specific activity values of liquid components were calculated based on the first 42 hours of the activity test. Specific activity values of gaseous products were determined over the whole period of the batch test (138 h) and could therefore have been underestimated.

2.3.3 Granulation and sludge retention

Microbial granulation in biotechnological processes is a complex phenomenon in which physical, microbial and thermodynamic aspects are involved [43]. Although an elaboration on fundamental aspects on microbial granulation is out of the scope of this study, we discuss three operational parameters that likely contributed to granulation and sludge retention in the present experiment: 1) hydrodynamic shear force, 2) presence of nucleation points and 3) continuous selection of heavier sludge particles.

The rotation of the impellers (100 rpm in a 1 L CSAR) causes shear and this could have triggered granulation. It is even reported that hydrodynamic shear force is required in the formation of granules [44]. The shear force in the reactors must have been sufficient to induce granulation but mild enough to prevent disintegration of granules. However, granulation is not common in continuously stirred reactors as nearly all granular sludge types are produced in column-type or liquid-upflow reactors or sequencing batch reactors [44]. On the other hand, other authors have also reported granulation in continuous stirred reactors [45] [46] and some concluded that also axial flow-mixing can have a positive effect on sludge granulation [47]. Grootscholten et al. (2013) did not report granulation in a similar chain elongation study using an upflow anaerobic filter with the same process conditions (T = 30 °C, pH = 6.8, HRT = 17 h) and with the same influent composition (synthetic medium containing propionate and ethanol) [26]. It is however possible that, if granulation occurred in their experiment, granules were destroyed by the peristaltic recirculation pump. It is therefore evident that, next to process conditions, also reactor configuration is a crucial aspect in sludge granulation.

A second likely contributing factor for granulation was the presence of suspended solids in the form of precipitates from salts, which were present in the influent. The attachment of cells to these salts that act as nucleation points is considered as the first step in granulation [43]. The concentration of suspended solids must have been sufficiently low as too high concentrations of suspended solids would lead to slow growth of granules. On the other hand, spontaneous formation of nuclei by clusters of microorganisms cannot be excluded. This is because some methanogens (e.g. *Methanosarcina* spp.) are able to form nuclei by excreting EPS onto which other methanogens (e.g. *Methanothrix* spp.) with good adhering capacities can

attach [43]. EPS formation could indeed have played a role in granulation in the present experiment since these substances were also observed on the granules by SEM imaging as mentioned before. To what extent shear force and nucleation points did determine the actual granulation has to be investigated.

An important aid for granular sludge accumulation (i.e. sludge retention) in the present study was the presence of the vertical up-flow effluent tube. This tube acted as an in-situ settler because it was placed inside the reactor configuration and the effluent-flow direction (up) was opposite to the settling direction (down). As a result, heavier sludge particles were continuously selected on their settling ability whereas dispersed sludge was washed out. The average up-flow velocity from the reactor to the effluent pump was $\pm$ 4.7 m·h^{-1}. The settling velocity of the granules was higher (in the range of 4 – 36 m·h^{-1}, Figure 2.2b) than the up-flow velocity in the effluent tube (Figure S2.1). This shows that the granules accumulated due to the selection pressure of the vertical tubular settler. The resulting SRT (4.7 d) was a factor ~7 higher than the HRT (17 h) during steady state.

Granular sludge-based chain elongation can be further optimised as a high rate biotechnological process. By increasing the up-flow velocity of the settler, a further pressure in out-selecting fast settling granules could be possible, which does allow a higher flow of feedstock. Earlier work showed that acidogenic hydrogen producing granules in an UASB produced caproate up to 7 g·L^{-1}·d^{-1} from sucrose [39]. The seed sludge was derived from a full-scale UASB and contained suspended sludge with an average diameter of 100 – 150 μm, which grew rapidly after inoculation. Their 3-year experiment showed the robustness at lab-scale; though the granules were not further examined on specific activity or stability. Additional batch tests also confirmed that granules from a methanogenic UASB reactor can be active in chain elongation up to 1.2 g caproate·L^{-1}·d^{-1} (Own measurements, data not shown). This shows that granular chain elongation activity is warranted in UASB configurations as well as within our CSAR. By further optimising process conditions, further selection of fast settling granules, and better understanding of the granulation process the MCFA volumetric productivity and its process efficiency can be improved.

2.4   Conclusions

This study demonstrated for the first time the formation of granular chain elongation sludge. This discovery was made in a reactor producing caproate (10.8 g·L^{-1}·d^{-1}) and heptanoate (1.8 g·L^{-1}·d^{-1}) as main MCFAs. Granular sludge (1.41 g VSS·L^{-1}) and suspended sludge (0.24 g VSS·L^{-1}) showed equal product distributions and contributed similarly to MCFA production. Granules had irregular shapes, diameters up to ~1.5 mm, settling velocities of 4 to 36 m·h^{-1} and contained micro-organisms with various shapes. Granules were persistently present for over 100 days of operation and were retained in the reactor due to the selection pressure of the in-situ settler. Granular sludge-based chain elongation can be further optimised as a high rate biotechnological process in UASBs and other granular sludge-based reactors.

2.5   Supporting Information

Reactor setup
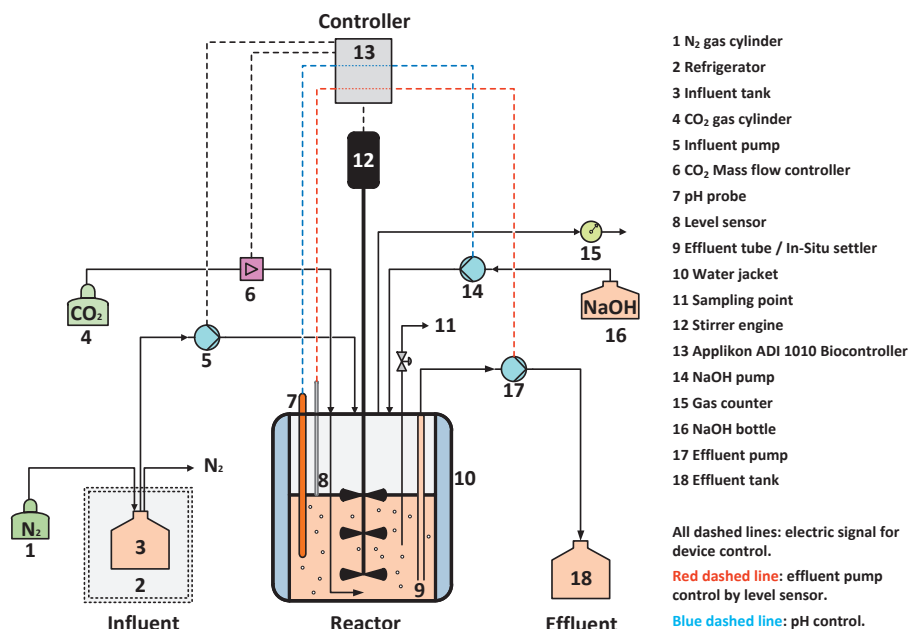
Figure S2.1: Schematic drawing of the Continuously Stirred Anaerobic Reactor (CSAR). Vertical baffles inside the reactor and the condenser are not shown.

Influent medium composition

The influent medium consisted of 7.7 g·L^{-1} propionic acid (≥99.5 % Sigma Aldrich, USA), 11.5 or 23 g·L^{-1} ethanol (absolute, Merck, Germany), salts, yeast extract (Merck, Germany), vitamins and trace metals. These compounds were dissolved in demi-water that was de-oxygenated with N$_2$-gas. The concentrations of the salts were 0.15 g·L^{-1} KCl, 0.2 g·L^{-1} CaCl$_2$·2H$_2$O, 3.6 g·L^{-1} (NH$_4$)H$_2$PO$_4$, 0.2 g·L^{-1} MgSO$_4$·7H$_2$O, and 0.33 g·L^{-1} MgCl$_2$·6H$_2$O. The concentration of yeast extract was 1.0 g·L^{-1}. Vitamins and trace metals were applied using 1000x stock solutions and the final medium concentrations were according to the design medium of Phillips et al [48]. The trace metal stock solution was modified by adding 6.2 g·L^{-1} EDTA to the stock solution and the pH was adjusted to 1.0 by adding 37 % HCl after all trace metals were added. The final pH of the media was adjusted to 6.8 by adding 5M NaOH.

Activity test

The role of the formed granules was studied in an activity test. A sludge sample was taken from the reactor and three sludge types (to be used as inoculum) were prepared in an anaerobic hood:

1. Granular sludge: Granules were allowed to settle in a 50mL falcon tube and were washed 3 times with activity test medium.

2. Suspended sludge: After the granules were settled, the supernatant (that didn't contain visible granules) was taken. This fraction was considered as suspended biomass.

3. No sludge: No sludge was added. This experiment was used as a negative control to verify whether the obtained inocula from the reactors were essential for chain elongation activity.

The VSS was determined of the washed granules and of suspended sludge. Batch flasks (125 mL total volume) with 50 mL liquid (45 mL medium + 5 mL inoculum) were used for the activity tests. Although the final VSS concentrations were different among granular and suspended sludge, the same inoculum volume (5 mL) was used to 1) ensure the same initial substrate concentrations and 2) to remain the same ratio of granular VSS and suspended VSS as was found in the reactor. The composition of the medium for the activity test was 5.5 $g \cdot L^{-1}$ ethanol, 2.0 $g \cdot L^{-1}$ acetic acid and 3.7 $g \cdot L^{-1}$ propionic acid. Salts, vitamins, trace metals and yeast extract had the same concentrations as the influent medium as described before. The pH of the medium was adjusted to 6.8 using 2M NaOH. The medium was flushed with N_2-gas to make it completely anaerobic and ethanol was added after that to avoid ethanol stripping.

After inoculation, the headspace was filled with 20 % CO_2 and 80 % N_2 until a pressure of 1.3 ± 0.1 bar was reached. Thereafter, the bottles were incubated at 30 °C at 100 rpm on a rotary shaker (Edmund Bühler, Germany). Liquid samples were analysed for ethanol and fatty acids (C2-C8) whereas gas samples from the headspace were analysed for CO_2 and CH_4.

Specific activities of liquid products were calculated based on the highest rate during the batch test (i.e. the first 42 hours). Specific activities for gaseous compounds (e.g. CO_2 and CH_4) were based on the whole period of the batch test (138 h) and on the initial and final headspace composition. Rates divided by the measured VSS gave specific rates. Product distribution was based on net formed products at the end of the batch test. All activity experiments were carried out in triplicates.

Analytical procedures

Ethanol and fatty acids (C2-C8) were determined by gas chromatography (GC) [23]. For ethanol measurements, the temperature program started at 75 °C (6 min), followed by a temperature ramp of 5 °C·min^{-1} until 130 °C and a subsequent temperature ramp of 49 °C·min^{-1} until 160 °C (8.5 min). The composition of the headspace gas (CH_4 and CO_2) was analysed by GC [49]. Volatile suspended solids (VSS) were calculated from the difference in weight between a completely dried sample and an incinerated sample, divided by the sample volume. For VSS, 30 mL sample volume was filtered through a Whatman GF/F filter (0.7 μm). Prior to filtration, the filters were pre-treated at 450 °C to oxidize any organic matter on the filter. After complete filtration, the reservoir was rinsed with demi water and this liquid was allowed to drain through the filter. The filter was then dried until constant weight at 105 °C and was subsequently incinerated at 550 °C until constant weight.

Granule characterization

SEM imaging

Granules were pre-treated for scanning electron microscope (SEM) - imaging in several steps. First the granules were fixated with 4 % (v/v) glutaraldehyde (30 min) and subsequently with 4 % (v/v) osmium tetroxide (30 min). After every fixation step the granules were rinsed with demi water (3 x 10 min). The fixated granules were dehydrated in a series of acetone solutions (10, 30, 50, 70, 90 and 100 % (v/v), 10 min each) from which 100 % was done twice. After dehydration, the granules were dried using critical point drying. The pre-treated granules were fit on SEM sample holders by carbon adhesive tabs (EMS, Washington, USA) and were sputter-coated with 15 nm iridium. Samples were morphologically analyzed at 2 kV, 6.3 pA, and WD 4 mm at room temperature in a field emission SEM (Magellan 400, FEI, Eindhoven, the Netherlands). Images were digitally recorded.

Granule size distribution

Images of granules were captured with a Nikon SMZ-800 macroscope equipped with a Nikon DS-5M-L1 digital color camera system. Granule diameters were digitally measured using Eclipse Net software (Nikon). This was done for 241 granules.

Granule settling velocity distribution

Granule settling velocity was determined using a 1 L laboratory cylinder which was distance-marked over 30 cm. The time that each granule settled 30 cm was measured with a stopwatch. This was done for 237 granules.

Reactor performance
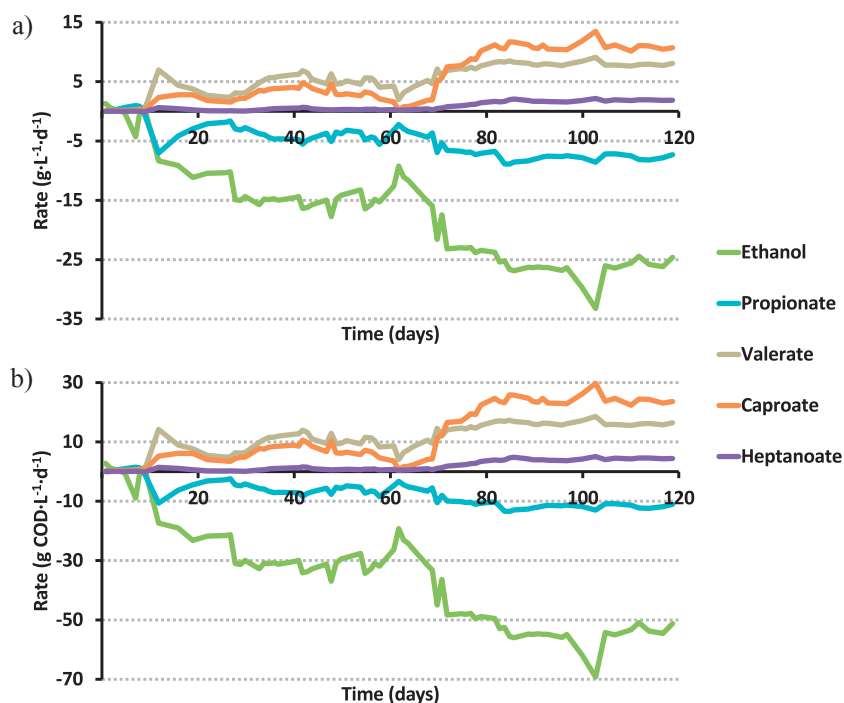
Figure S2.2: Production and consumption rates within the reactor. Rates are indicated in $g \cdot L^{-1} \cdot d^{-1}$ (a) and in $g \ COD \cdot L^{-1} \cdot d^{-1}$ (b). The ethanol-loading rate was doubled on day 68 to prevent ethanol depletion. Steady state intervals were day 84-97 and day 105-119. T = 30 °C, pH = 6.8, HRT = 17 h, V = 1 L.

CO$_2$

Acetate

Ethanol

Propionate

n-C4
n-C6
n-C8

n-C5
n-C7

CO$_2$

Acetate

Ethanol

Propionate

n-C4
n-C6
n-C8

n-C5
n-C7

Ethanol
upgrading

VFA
upgrading
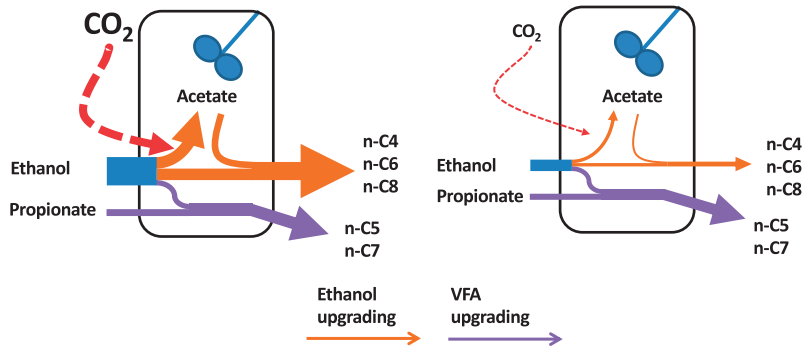
CHAPTER 3

Controlling Ethanol Use in Chain Elongation by CO_2 Loading Rate

Abstract

Chain elongation is an open-culture biotechnological process which converts volatile fatty acids (VFAs) into medium chain fatty acids (MCFAs) using ethanol and other reduced substrates. The objective of this study was to investigate the quantitative effect of CO_2 loading rate on ethanol usages in a chain elongation process. We supplied different rates of CO_2 to a continuously stirred anaerobic reactor, fed with ethanol and propionate. Ethanol was used to upgrade ethanol itself into caproate and to upgrade the supplied VFA (propionate) into heptanoate. A high CO_2 loading rate (2.5 $L_{CO2} \cdot L^{-1} \cdot d^{-1}$) stimulated excessive ethanol oxidation (EEO; up to 29 %) which resulted in a high caproate production (10.8 $g \cdot L^{-1} \cdot d^{-1}$). A low CO_2 loading rate (0.5 $L_{CO2} \cdot L^{-1} \cdot d^{-1}$) reduced EEO (16 %) and caproate production (2.9 $g \cdot L^{-1} \cdot d^{-1}$). Heptanoate production by VFA upgrading remained constant (~1.8 $g \cdot L^{-1} \cdot d^{-1}$) at CO_2 loading rates higher than or equal to 1 $L_{CO2} \cdot L^{-1} \cdot d^{-1}$. CO_2 was likely essential for growth of chain elongating microorganisms while it also stimulated syntrophic ethanol oxidation. A high CO_2 loading rate must be selected to upgrade ethanol (e.g. from lignocellulosic bioethanol) into MCFAs whereas lower CO_2 loading rates must be selected to upgrade VFAs (e.g. from acidified organic residues) into MCFAs while minimizing use of costly ethanol.

3.1   Introduction

Medium chain fatty acids (MCFAs) are straight-chain mono-carboxylic acids with 6 to 10 carbon atoms. These molecules can serve as precursors for production of fuels and other chemicals [14]. Conventional methods to produce MCFAs use vegetable oils (palm kernel oil, coconut oil and castor oil) from oil seed crops [50] [51]. Growing these crops for production of fuels and chemicals, however, competes with human food production (i.e. arable land) and is associated with loss of water resources and biodiversity [4] [5]. Organic residues from agriculture or food industry are interesting alternative feedstocks for the production of MCFAs because they are renewable, abundantly available and their application does not compete with human food production. In addition, these residues must often be treated to prevent environmental pollution. An emerging open-culture biotechnological process that facilitates valorization of organic residues into MCFAs is chain elongation. Chain elongation is a secondary fermentation process within the carboxylate platform [14]. It is known to ferment volatile fatty acids (VFAs; acetate, propionate and butyrate) as electron acceptor together with ethanol as electron donor into MCFAs through the reverse β-oxidation pathway. In this pathway, 1 mole of ethanol is anaerobically oxidized into acetate for every 5 chain elongation reactions, yielding one ATP via substrate level phosphorylation (Eq 3.1 and Table S3.1).

Reverse β-oxidation pathway:
$$5C_xH_{2x-1}O_2^- + 6C_2H_6O \rightarrow 5C_{x+2}H_{2x+3}O_2^- + C_2H_3O_2^- + 4H_2O + H^+ + 2H_2 \quad \text{(Eq 3.1)}$$
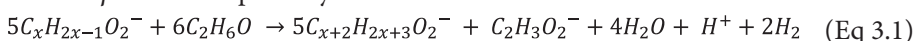
Chain elongation has been demonstrated with synthetic medium [23] [24] [25] [26], with organic residues such as acidified garden- and kitchen waste [28], acidified organic fraction of municipal solid waste [27] and with undistilled fermentation broth from the bioethanol industry [19] [29].

VFAs for chain elongation can be obtained by hydrolysis and acidification (primary fermentation) of organic residues, making them inexpensive substrates. Although electron donors such as methanol [33] or lactate [20] have been successfully used, ethanol is the preferred electron donor for high-rate chain elongation [18]. Ethanol can be introduced in three ways: 1) it can be present within the feedstock itself, 2) it can be produced *in situ* from the feedstock (e.g. by fermentation of sugars) or 3)

it can be procured off site and added to the chain elongation reactor [18]. Ethanol, however, is a costly substrate. Knowledge on the mechanisms of the use of ethanol is therefore essential to establish an ethanol-efficient chain elongation process.

In a chain elongation process, ethanol is primarily used by chain elongating microorganisms (e.g. *Clostridium kluyveri* [23] [52]) through the reverse β-oxidation pathway. Since we use an open culture process, however, typically several competing biochemical processes occur as a result of consumption of supplied substrates or produced intermediates. For example, increased ethanol oxidation to acetate at a ratio different from the 5:1 ratio has also been observed in chain elongation cultures [27]. This is caused by direct oxidation of ethanol and is also known as excessive ethanol oxidation (EEO; Eq 3.2 and Table S3.1). EEO is considered to be performed by ethanol-oxidizing microorganisms which do not perform chain elongation, but these microorganisms have not been identified yet. Although it could be possible that EEO is performed by chain elongating microorganisms through a more flexible 5:1 ratio in the reverse β-oxidation pathway, we assume in this study that this ratio does not change and that EEO is performed through direct oxidation of ethanol. Another process that proceeds in chain elongation cultures is hydrogenotrophic methanogenesis (Eq 3.3 and Table S3.1). This process does not consume VFAs, ethanol or MCFAs directly [19] [27] but it consumes a part of the produced components within the open culture.

Excessive ethanol oxidation (EEO):
$$C_2H_6O + H_2O \rightarrow C_2H_3O_2^- + H^+ + 2H_2 \qquad \text{(Eq 3.2)}$$

Hydrogenotrophic methanogenesis:
$$4H_2 + CO_2 \rightarrow CH_4 + 2H_2O \qquad \text{(Eq 3.3)}$$

Ethanol use in chain elongation is not straightforward because ethanol is not only used to elongate (i.e. upgrade) VFAs into MCFAs but also because it can be used to upgrade ethanol itself into MCFAs. To identify the different uses of ethanol, we distinguish two types of carbon fluxes which lead to the production of MCFAs: VFA upgrading (Eq 2a and 2b, Table S3.1) and ethanol upgrading (Eq 1a-1e, Table S3.1). VFA upgrading is chain elongation of VFAs (through the reverse β-oxidation pathway) which are derived from primary fermentation and which are not derived from *in situ* ethanol oxidation into acetate. Ethanol upgrading is a combination

of 1) *in situ* ethanol oxidation into acetate (through both EEO and the reverse *β*-oxidation pathway) and 2) subsequent chain elongation of this *in situ* produced acetate into even-numbered fatty acids (through the reverse *β*-oxidation pathway). Both VFA upgrading and ethanol upgrading are not self-contained biochemical processes or pathways. Rather, whereas VFA upgrading is a result from only a part of the reverse *β*-oxidation pathway, ethanol upgrading is a result from a combination of *in situ* ethanol oxidation and the reverse *β*-oxidation pathway. Because EEO, ethanol upgrading and VFA upgrading are simultaneous and intertwined fluxes, previous studies could not quantify via which route MCFAs were produced (e.g. [25] [27]). As such, it was not determined how much ethanol was effectively used for MCFA production.

CO_2 affects both chain elongating microorganisms and ethanol oxidizers. The well described chain elongating bacterium *C. kluyveri* requires CO_2 for anabolic reactions [40]. CO_2 has also been shown to influence EEO. When the CO_2 concentration is sufficiently low, hydrogenotrophic methanogenic activity is suppressed, and the resulting higher hydrogen concentration inhibits EEO [27] [29]. Because CO_2 influences EEO and because the resulting acetate could stimulate the carbon flux of ethanol upgrading, CO_2 loading rate may be an important control parameter in the conversion of an ethanol-rich feedstock into MCFAs through ethanol upgrading. To date, there are no studies that describe the effect of CO_2 on chain elongation while specifically distinguishing ethanol upgrading and VFA upgrading. In addition, the concurring archaeal community involved in methane formation has not been characterized.

The objective of this study was to investigate the quantitative effect of CO_2 loading rate on ethanol use in a chain elongation process. Ethanol upgrading and VFA upgrading were studied by supplying different loading rates of gaseous CO_2 to a continuously stirred anaerobic reactor with granular and suspended chain elongation sludge [53]. By using propionate as VFA instead of acetate, a distinction between the carbon flux of ethanol upgrading (represented by even-numbered fatty acids) and the carbon flux of VFA upgrading (represented by odd-numbered fatty acids) was conceived. In addition, the microbial community was analyzed to compare the microbial communities at different CO_2 loading rates.

3.2 Materials and methods

3.2.1 Experimental set-up, procedure and analysis

This study used a continuously stirred anaerobic reactor as described by Roghair et al. (2016) [53]. In short, a continuous reactor (Volume 1 L) with granular and suspended chain elongation sludge was operated at 30 °C, 1 atm, pH 6.8 (by addition of 2M NaOH), stirred at 100 rpm with a hydraulic retention time (HRT) of 17 h. Gaseous CO_2 was supplied with a mass-flow controller (Brooks Instruments 5850S, the Netherlands). The reactor was continuously fed with a synthetic medium that contained propionate (10.9 g·L^{-1}·d^{-1}) and ethanol. During the study, different CO_2 loading rates were applied: 2.5 L$_{CO2}$·L^{-1}·d^{-1} (day 0 to 124), 1 L$_{CO2}$·L^{-1}·d^{-1} (day 124 to 187), 0.5 L$_{CO2}$·L^{-1}·d^{-1} (day 187 to 211), 0 L$_{CO2}$·L^{-1}·d^{-1} (day 211 to 224) and again 1 L$_{CO2}$·L^{-1}·d^{-1} (day 224 to 240). The first 119 days of the reactor operation has been presented in a previous study [53]. Steady state data of this previous study (2.5 L$_{CO2}$·L^{-1}·d^{-1}) is presented here again to place it in the context of steady state intervals from this study.

Ethanol loading rates were 16.3 g·L^{-1}·d^{-1} (at 1, 0.5 and 0 L$_{CO2}$·L^{-1}·d^{-1}) and 32.5 g·L^{-1}·d^{-1} (at 2.5 L$_{CO2}$·L^{-1}·d^{-1}). The ethanol loading rate at 1.0, 0.5, and 0 L$_{CO2}$·L^{-1}·d^{-1} was twice as low as compared to the initial CO_2 loading rate (2.5 L$_{CO2}$·L^{-1}·d^{-1}). This was performed to prevent ethanol toxicity because with lower CO_2 loading rates, ethanol consumption rates decreased, resulting in increased ethanol concentrations. Ethanol concentrations during selected steady state intervals were in a range in which chain elongation is known to occur and were between 0.7 ± 0.5 g·L^{-1} (1 L$_{CO2}$·L^{-1}·d^{-1}) and 8.7 ± 0.7 g·L^{-1} (no CO_2 loading rate). The reactor was in steady state when net production and consumption rates of fatty acids and ethanol were similar (maximum relative standard deviation of 20 %) over a period of at least 5 days (7 HRTs). Caprylate was excluded from this criterion because this compound was produced in insignificant amounts. Results that we present and discuss are based on steady states unless mentioned otherwise. Standard deviations are based on at least four measurements.

Analytical procedures for fatty acids (C2-C8), alcohols (C2-C3) and for determination of the headspace composition (CO_2 and CH_4) were the same as described previously [53]. Propanol was measured on the same column as ethanol although this was not formerly mentioned. In addition, hydrogen in the headspace

was determined by GC [54]. Liquid samples were taken from the reactor content 3-5 times per week whereas gas samples from the headspace were taken once per week.

Samples for microbial community analysis were taken on day 1, 2 and 3 (pooled together; initial bacterial community), day 110 (2.5 $L_{CO2} \cdot L^{-1} \cdot d^{-1}$), day 219, 222 and 224 (pooled together; 0 $L_{CO2} \cdot L^{-1} \cdot d^{-1}$) and on day 238 (1 $L_{CO2} \cdot L^{-1} \cdot d^{-1}$). These samples were divided into granular and suspended sludge fractions by allowing granules to settle. After separation, suspended sludge fractions eventually did not contain visible granules and granular sludge fractions were washed 3 times with 1x phosphate-buffered saline to remove residual suspended sludge. Bacterial community analysis was performed on all samples using high-throughput 16S rRNA gene sequencing. Archaeal community analysis was performed on one sample, suspended sludge at 2.5 $L_{CO2} \cdot L^{-1} \cdot d^{-1}$, by using 16S rRNA gene cloning. This sample was selected based on the highest methane production rate in the operational period. Details on the materials and methods for microbial community analysis (DNA extraction, bacterial community analysis and archaeal community analysis) are reported in the supporting information.

3.2.2 Calculations on carbon fluxes for carbon flux analysis

Calculations on carbon fluxes are shown in Table S3.2. These calculations are based on net production and consumption rates (under steady state conditions) and on the stoichiometric equations in Table S3.1. Total ethanol use was divided into 1) excessive ethanol oxidation, 2) ethanol oxidation through the reverse β-oxidation pathway and 3) ethanol use for elongation of fatty acids through the reverse β-oxidation pathway. Total CO_2 use was divided into 1) CO_2 use by hydrogenotrophic methanogenesis and 2) unidentified CO_2 use (i.e. biomass).

Carbon selectivity is based on product formed divided by total substrates consumed.

3.2.3 Calculations on change in Gibbs free energy for thermodynamic analysis

Thermodynamic calculations were performed as described by Kleerebezem et al. (2010) using their provided ΔG_f^0 and ΔH_f^0 values for individual components [55]. Temperature corrections to 30 °C were made using the Gibbs-Helmholtz

equation. Thermodynamic limits for hydrogen partial pressures (pH_2) of EEO and the reverse β-oxidation pathway were determined in the same way as was performed by Ge et al. (2015) [56].

3.3 Results

3.3.1 Bioreactor performance at different CO_2 loading rates

CO_2 loading rate was shown to be an effective control parameter in chain elongation. CO_2 was essential for caproate, heptanoate and caprylate (MCFA) production and it especially stimulated ethanol upgrading to caproate. Caprylate production was insignificant and hence the effect of CO_2 on caprylate production was not shown in this study. A graphical summary of the effect of CO_2 loading rate on reactor performance can be seen in Figure 3.1 (rate in $g \cdot L^{-1} \cdot d^{-1}$) and Figure S3.1 (rate in mmol $C \cdot L^{-1} \cdot d^{-1}$). Mean steady state values of reactor concentrations, rates and carbon selectivity values can be seen in Table S3.3-S3.7.
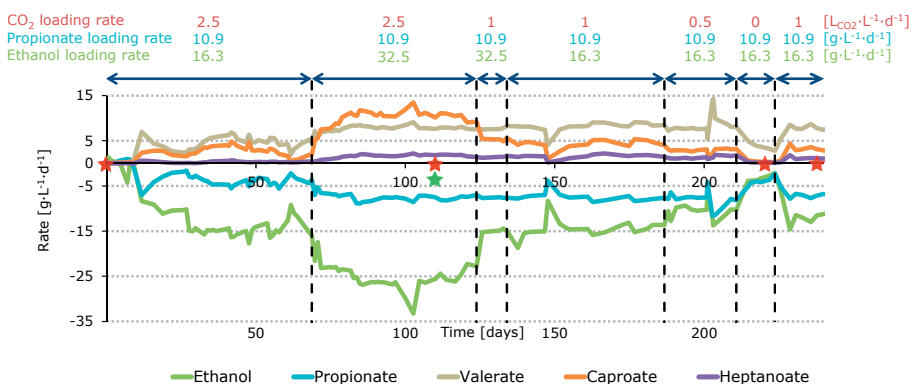
Figure 3.1: Graphical summary of the effect of CO_2 loading rate on reactor performance with net production and consumption rates over time. At the red stars, samples for bacterial community analysis were taken. At the green star, a sample for archaeal community analysis was taken. T = 30 °C, pH = 6.8, HRT = 17 h, V = 1 L.

The reactor was started with a high CO_2 loading rate (2.5 $L_{CO2} \cdot L^{-1} \cdot d^{-1}$). Through the first stage, the reactor did not reach a steady state. Yet, it was noticed that ethanol became depleted which likely limited MCFA production rates. The ethanol loading rate, therefore, was increased on day 68 from 16.3 to 32.5 $g \cdot L^{-1} \cdot d^{-1}$.

Thereafter, a steady state of 27 days was observed as was presented previously [53]. Here, caproate was produced at 10.8 ± 0.5 g·L^{-1}·d^{-1} at a concentration of 7.4 ± 0.2 g·L^{-1} while heptanoate was produced at 1.8 ± 0.1 g·L^{-1}·d^{-1} at a concentration of 1.2 ± 0.1 g·L^{-1}. Caproate must have been produced by ethanol upgrading because other even-numbered fatty acids (acetate or butyrate) were not fed to the reactor. Heptanoate must have been produced by VFA upgrading starting with propionate because 1) propionate was the only VFA that was fed to the reactor and 2) chain elongation of propionate results in production of heptanoate [26].

On day 124, we decreased the CO_2 loading rate from 2.5 to 1 L$_{CO2}$·L^{-1}·d^{-1} after which a steady state of 8 days was observed (steady state characteristics are not shown). Here, caproate was produced at a ~two times lower rate (5.3 ± 0.3 g·L^{-1}·d^{-1}) while heptanoate was produced at a slightly lower rate (1.4 ± 0.2 g·L^{-1}·d^{-1}) compared to the steady state at 2.5 L$_{CO2}$·L^{-1}·d^{-1}. Because ethanol was consumed at a lower rate, its concentration increased from 3.7 ± 1.4 g·L^{-1} to 11.6 ± 0.8 g·L^{-1}. To prevent potential ethanol toxicity (e.g. [57]), we decreased the ethanol loading rate from 32.5 to 16.3 g·L^{-1}·d^{-1} on day 134. Thereafter, a steady state was observed of 40 d in which caproate (4.6 ± 0.6 g·L^{-1}·d^{-1}) and heptanoate (1.7 ± 0.3 g·L^{-1}·d^{-1}) were produced at similar rates as before the decrease in ethanol loading rate. This shows that a change in ethanol loading rate and concentration does not substantially influence reactor performance as long as ethanol is not depleted.

On day 187, the CO_2 loading rate was further decreased from 1 to 0.5 L$_{CO2}$·L^{-1}·d^{-1} after which we observed another steady state of 13 days. Here, caproate was produced at a 73 % lower rate (2.9 ± 0.2 g·L^{-1}·d^{-1}) while heptanoate was produced at a 35 % lower rate (1.2 ± 0.2 g·L^{-1}·d^{-1}) compared to the steady state at 2.5 L$_{CO2}$·L^{-1}·d^{-1}. On day 211, we cut off the CO_2 supply (0 L$_{CO2}$·L^{-1}·d^{-1}). From then on, the microbiome failed in effective chain elongation as we noticed low and decreasing MCFA production rates (< 0.5 g·L^{-1}·d^{-1}). Because rates kept on decreasing the reactor did not reach a steady state. To prevent a total collapse, the CO_2 loading rate was increased from 0 to 1 L$_{CO2}$·L^{-1}·d^{-1} on day 224. This resulted in a revival of the microbiome as we observed, later on, similar steady state rates as before with the same CO_2 loading rate. A summary on net production and consumption rates of fatty acids and ethanol at different CO_2 loading rates in shown in Figure 3.2a. An overview and characteristics of the steady states is shown in Table 3.1.
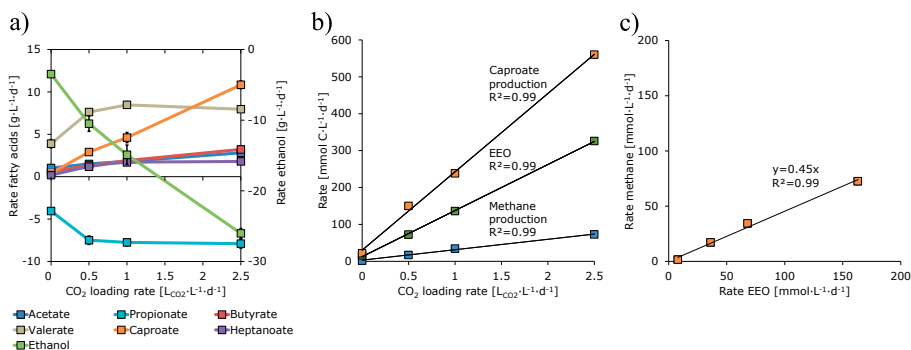
Figure 3.2: a) Net production and consumption rates of fatty acids and ethanol at different CO_2 loading rates (bars indicate standard deviations but are often too small to be visual), b) carbon flux of EEO, caproate production and methane production at different CO_2 loading rates, c) rate of methane vs EEO. Presented values at 0 $L_{CO2}·L^{-1}·d^{-1}$ are not steady state values but averages. Regression line = —

3.3.2 Excessive ethanol oxidation and the fate of propionate

The highest rate of EEO was observed when the CO_2 loading rate was 2.5 $L_{CO2}·L^{-1}·d^{-1}$ (7.5 $g·L^{-1}·d^{-1}$; Table 3.1). EEO (1.7 $g·L^{-1}·d^{-1}$) could be reduced with 77 % when the CO_2 loading rate was decreased to 0.5 $L_{CO2}·L^{-1}·d^{-1}$ but was still observed when CO_2 was not supplied. A part of the acetate produced by EEO was used as electron acceptor for ethanol upgrading. In the period with the highest rate of ethanol upgrading (2.5 $L_{CO2}·L^{-1}·d^{-1}$), this acetate consumption for ethanol upgrading was 7.9 $g·L^{-1}·d^{-1}$. Because the reverse β-oxidation pathway could maximally produce 4 $g·L^{-1}·d^{-1}$ (51 %), the remaining 49 % acetate that served as electron acceptor for ethanol upgrading must have been produced by EEO. Ethanol upgrading was therefore found to be clearly mediated by EEO.

Propanol production (0.5 – 1.2 $g·L^{-1}·d^{-1}$) was observed throughout the entire study and was likely formed by reduction of propionate with hydrogen. Propanol can still be used as electron donor for chain elongation of acetate if not for propionate elongation. Because all consumed propionate was used for propanol production and chain elongation to heptanoate and valerate (with a carbon closure of 95 – 102 %) it is unlikely that propanol served as electron donor for MCFA production or that propionate was oxidized into acetate. As such, the carbon flux of ethanol upgrading and VFA upgrading were not complicated by propanol elongation or propionate oxidation.

Table 3.1: Overview and characteristics of steady states. Concentrations, rates and carbon selectivities are reported in Table S3-S7.

CO$_2$ loading rate	Propionate / Ethanol loading rate	Steady state interval	Mean product formation rate			Mean EEO	Mean headspace gas composition			CO$_2$ in liquid [i]
			Caproate [g·L⁻¹·d⁻¹]	Heptanoate [g·L⁻¹·d⁻¹]	CH$_4$ [mmol·L⁻¹·d⁻¹]	[g·L⁻¹·d⁻¹] (% of total ethanol use)	pCH$_4$ [%]	pH$_2$ [%]	pCO$_2$ [%]	
[L$_{CO2}$·L⁻¹·d⁻¹]	[g·L⁻¹·d⁻¹]	[d]								[mmol·L⁻¹]
High [2.5]	10.9 / 32.5	84-97, 105-119	10.8	1.8	72.6	7.5 (28.8 %)	91.9	0.03	4.6	1.42
Medium [1.0]	10.9 / 16.3	155-187	4.6	1.7	34.3	3.1 (21.0 %)	92.2	0.08	2.3	0.71
Low [0.5]	10.9 / 16.3	188-201	2.9	1.2	17.1	1.7 (15.9 %)	87.9	0.20	1.1	0.34
None [0.0]	10.9 / 16.3	N.A. [ii]	0.4	0.2	1.5	0.4 (10.5 %)	49.3	41.6	0.07	0.03
Medium [1.0]	10.9 / 16.3	229-240	3.3	1.2	29.6	2.5 (20.7 %)	93.1	0.08	1.4	0.44

[i] Calculated from the gaseous CO$_2$ concentration in the headspace by Henry's law at 1 atm and 30 °C [58].
[ii] Not applicable because there was no steady state observed. Presented values at 0 L$_{CO2}$·L⁻¹·d⁻¹ are averages.

3.3.3 Microbial community: abundance of *Clostridiales* and *Methanobrevibacter acididurans*

The bacterial community was analyzed using high throughput 16S rRNA amplicon sequencing to identify changes at different CO_2 loading rates in the chain elongation process. This was performed for both the granular and suspended sludge fraction. The *Clostridiales* order consistently dominated the bacterial community irrespective of CO_2 loading rate or sludge type (Figure 3.3 and Figure S3.3). *Clostridiales* had the highest relative abundance in all reactor samples (53 – 77 %), followed by *Bacteroidales* (3 – 18 %) and *Erysipelotrichales* (1 – 12 %). Most *Clostridiales* were identified as members of the *Clostridiaceae* family. Dominance of *Clostridiaceae*, with *C. kluyveri* as well-known member and model species for chain elongation, has been frequently observed [23] [52].

CO_2 loading rate [$L_{CO2} \cdot L^{-1} \cdot d^{-1}$] →		High [2.5]		Medium [1.0]		None [0.0]	
Order ↓	IBC	Granular	Suspended	Granular	Suspended	Granular	Suspended
Bacteroidales	20	11	10	3	18	8	8
Bacillales	3	0	0	0	1	0	0
Lactobacillales	11	1	7	1	9	2	5
Clostridiales	62	71	71	75	53	64	77
Erysipelotrichales	0	12	7	8	4	12	1
Selenomonadales	0	2	1	10	4	11	5
Burkholderiales	1	0	1	0	6	0	1
Desulfovibrionales	1	3	2	3	4	2	2
Other	1	0	0	1	2	1	1

Figure 3.3: Heatmap of bacterial community at different CO_2 loading rates in granular and suspended sludge. Numbers indicate percentage relative abundance. "Other" are specified in Figure S3.3. The ethanol loading rate at 2.5 $L_{CO2} \cdot L^{-1} \cdot d^{-1}$ was 32.2 $g \cdot L^{-1} \cdot d^{-1}$ whereas the ethanol loading rate at 1.0 and 0.0 $L_{CO2} \cdot L^{-1} \cdot d^{-1}$ was 16.3 $g \cdot L^{-1} \cdot d^{-1}$. IBC = initial bacterial community.

Minor changes in the bacterial community were observed during the operational period which do not seem to link with the CO_2 loading rate. An increase in relative abundance (compared to the initial bacterial community) was observed for several operational taxonomic units. *Erysipelotrichales* and *Selenomonadales* increased in relative abundance as compared to the initial bacterial community, especially in the granular sludge fraction. *Desulfovibrionales* increased in relative abundance as compared to the initial bacterial community in both granular and suspended sludge fractions.

The archaeal community in suspended sludge at 2.5 $L_{CO2} \cdot L^{-1} \cdot d^{-1}$ was analyzed by 16S rRNA gene cloning and Sanger sequencing. 95 out of 96 clones showed

highest identity with *Methanobrevibacter acididurans* (97-99 % sequence identity; Table S3.8). This means that we have specifically identified a hydrogenotrophic methanogen in a chain elongation process whereas no acetotrophic methanogens were detected.

3.4   Discussion

3.4.1 Ethanol upgrading: CO_2 stimulates excessive ethanol oxidation and caproate production

In our study, we identified three dominant biochemical processes that convert the supplied substrates and/or produced intermediates: 1) chain elongation (through the reverse *β*-oxidation pathway; Eq 3.1) [21], 2) excessive ethanol oxidation (EEO; Eq 3.2) [27], and 3) hydrogenotrophic methanogenesis (Eq 3.3) [19] [27]. They were identified based on processes that are known to occur in chain elongation reactors and on a stoichiometric carbon flux analysis of our results. Acetotrophic methanogenesis was not identified in this carbon flux analysis. This was confirmed by our archaeal community analysis in which no acetotrophic methanogens were detected. We consider that each process is performed by a corresponding functional group of microorganisms; chain elongation is performed by chain elongating microorganisms, EEO is performed by ethanol oxidizers and methanogenesis by hydrogenotrophic methanogens.

A Sankey diagram was made to illustrate the role of the three functional groups in the carbon fluxes at high (2.5 $L_{CO2} \cdot L^{-1} \cdot d^{-1}$) and at low (0.5 $L_{CO2} \cdot L^{-1} \cdot d^{-1}$) CO_2 loading rate (Figure 3.4). Although ethanol loading rates were also different at these selected CO_2 loading rates, the resulting mean ethanol concentrations were similar (81.3 mmol·L^{-1} at 2.5 $L_{CO2} \cdot L^{-1} \cdot d^{-1}$ and 70.1 mmol·L^{-1} at 0.5 $L_{CO2} \cdot L^{-1} \cdot d^{-1}$), which makes these conditions comparable. Ethanol upgrading (orange arrows) was mediated by ethanol oxidizers and chain elongating microorganism because both EEO and chain elongation (of even-numbered fatty acids) attributed to this carbon flux. VFA upgrading (purple arrows) was mediated by chain elongating microorganisms because only chain elongation (of odd-numbered fatty acids) attributed to this carbon flux. Methane production was performed by hydrogenotrophic methanogens which presumably operated in syntrophy with ethanol oxidizers (see also explanation on the microbial analysis below).
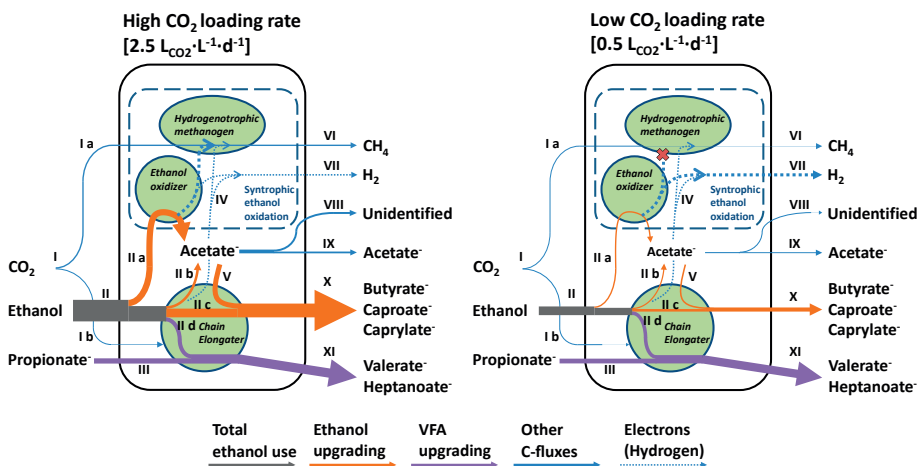
Figure 3.4: Sankey diagram with observed and calculated carbon fluxes at high (2.5 L_{CO2}·L^{-1}·d^{-1}) and low (0.5 L_{CO2}·L^{-1}·d^{-1}) CO_2 loading rate. Widths of arrows are proportional to carbon fluxes. Three functional groups of microorganisms (hydrogenotrophic methanogens, ethanol oxidizers and chain elongating microorganisms) are indicated as green shapes.
I) Total CO_2 use, I a) CO_2 use by methanogens, I b) unidentified CO_2 use (i.e. biomass), II) total ethanol use, II a) excessive ethanol oxidation (EEO), II b) ethanol oxidation through the reverse β-oxidation pathway, II c) ethanol use for elongation of fatty acids through the reverse β-oxidation pathway (even), II d) ethanol use for elongation of fatty acids through the reverse β-oxidation pathway (odd), III) propionate use for VFA upgrading, IV) (interspecies) hydrogen transfer, V) acetate use for ethanol upgrading, VI) methane production, VII) hydrogen production, VIII) unidentified acetate use (i.e. biomass), IX) acetate production, X) butyrate, caproate and caprylate production by ethanol upgrading, XI) valerate and heptanoate production by VFA upgrading.
Calculations on carbon fluxes and numerical values are shown in Table S3.2.

The determined carbon flux analysis provided a linear effect of CO_2 loading rate on caproate production, EEO and on methane production (Figure 3.2a and 3.2b). This shows that these processes were collectively controlled by the CO_2 loading rate in the tested range. This can be explained as follows: CO_2 was the limiting substrate for hydrogenotrophic methanogenic activity because higher CO_2 loading rates resulted in higher rates of CO_2 consumption and higher rates of methane production (Table S3.3-S3.6). A high CO_2 loading rate, therefore, stimulated hydrogenotrophic methanogens which, in turn, provided favorable conditions for ethanol oxidizers by lowering the hydrogen partial pressure (pH$_2$). This explanation is in line with our results because a lower CO_2 loading rate did lead to a higher pH$_2$ (Table 3.1). Because of the lower pH$_2$ at a high CO_2 loading rate, more ethanol was oxidized by EEO and thus more acetate was available as electron acceptor for chain elongation into even-numbered fatty acids (i.e. ethanol upgrading). The concentration of acetate was thus limiting caproate production. Vice versa, a low

CO_2 loading rate limited hydrogenotrophic methanogenic activity which resulted in an increased pH_2. This increased pH_2 made EEO thermodynamically less favorable and this resulted into less available acetate for caproate production. Next to acetate, chain elongating microorganisms were possibly also directly limited by CO_2 (Section 3.4.3). Although the effect of CO_2 on EEO has been shown previously [27] [29], this study demonstrates the effect of CO_2 on ethanol upgrading in a chain elongation process.

The thermodynamic analysis provided the change in Gibbs free energy of various processes at different CO_2 loading rates under actual bioreactor conditions (Figure S3.2). This analysis gives further insights on the determined carbon fluxes. EEO was thermodynamically feasible at 0.5, 1 and 2.5 $L_{CO2} \cdot L^{-1} \cdot d^{-1}$ ($\Delta Gr'$ < -20 kJ·reaction^{-1}) but was thermodynamically inhibited at 0 $L_{CO2} \cdot L^{-1} \cdot d^{-1}$ ($\Delta Gr'$ > -20 kJ·reaction^{-1}). This was due to the pH_2, which was at least 200 times lower when CO_2 was supplied (0.5, 1 and 2.5 $L_{CO2} \cdot L^{-1} \cdot d^{-1}$) compared to when CO_2 was not supplied (0 $L_{CO2} \cdot L^{-1} \cdot d^{-1}$; Table 3.1). EEO (0.4 g·L^{-1}·d^{-1}), however, was still observed at 0 $L_{CO2} \cdot L^{-1} \cdot d^{-1}$. This reaction could have been enabled at aberrant local conditions (i.e. lower pH_2); for example, inside a granule by hydrogenotrophic methanogens [59]. This process could also have been executed by chain elongating micro-organisms through a more flexible reverse β-oxidation pathway. However, as mentioned before, we assume that the reverse β-oxidation pathway is not flexible and that EEO is executed by ethanol oxidizers which do not perform chain elongation. The reverse β-oxidation pathway (ethanol oxidation coupled to 5 x propionate elongation) was thermodynamically feasible at all applied CO_2 loading rates ($\Delta Gr'$ < -20 kJ·reaction^{-1}). Other reverse β-oxidation reactions (ethanol oxidation coupled to 5 x acetate, butyrate or valerate elongation) were also feasible since their thermodynamic values were in the same order of magnitude (data not shown). We calculated that the reverse β-oxidation pathway is still feasible even when the pH_2 is extremely high (1000 bar). This shows that the reverse β-oxidation pathway is thermodynamically not hindered by the CO_2 loading rate and by its corresponding pH_2.

We also used the thermodynamic analysis to confirm whether the *in situ* produced acetate was a result of ethanol oxidation and not from other processes such as propionate oxidation (Eq 5, Table S3.1) or homoacetogenesis (Eq 6, Table S3.1). Our calculations show that both of these processes were thermodynamically

inhibited when CO_2 was supplied ($\Delta Gr' > -20$ kJ·reaction^{-1}). True, these processes could still have occurred at aberrant local conditions. However, even if they occurred, it would have been at negligibly low rates. Propionate oxidation could be neglected because, as mentioned before, propionate was primarily used for production of propanol, valerate and heptanoate. Also based on stoichiometrics, homoacetogenesis could be neglected because the unidentified CO_2 use (that could have contributed to homoacetogenesis) was at most 33 mmol C ·L^{-1}·d^{-1}; only ~2 % of the total carbon flux. Even this value, though, is overestimated because a part of the unidentified CO_2 use was likely used for growth of chain elongating microorganisms (Section 3.4.3).

Grootscholten et al. (2013) also reported increased caproate production rates in a chain elongation process after increasing the CO_2 concentration by doubling the amount of K_2CO_3 in the influent from 4 to 8 g·L^{-1} [25]. Although they did not attribute this observation specifically to ethanol upgrading, increased caproate production was likely a result of this carbon flux. However, because acetate was also present in their influent medium, increased caproate production could (partly) also have been the result of chain elongation of fed acetate (i.e. VFA upgrading). In a later stage of their fermentation study they applied gaseous CO_2 (4.8 L$_{CO2}$·L^{-1}·d^{-1}), but that did not result in improved caproate production rates, implying that ethanol upgrading was not limited by CO_2 anymore. Eventually, they concluded that their system was limited by (one of the components in) yeast extract. This shows that high-rate ethanol upgrading only proceeds when sufficient growth factors and nutrients are available.

Both EEO and hydrogenotrophic methanogenesis increased with increasing CO_2 loading rate (Figure 3.2b). The rates of these processes are plotted against each other in Figure 3.2c. The slope of the plot shows that for every mole of ethanol oxidized by EEO, 0.45 mole of methane is produced. This value is close to the stoichiometric ratio of 0.5 mole methane produced per mole ethanol oxidized in syntrophic ethanol oxidation (Table S3.1), indicating that EEO is a result of the identified syntrophic process.

Electrons (in the form of hydrogen) that did not end up as methane were likely used to reduce propionate into propanol (up to 20 mmol·L^{-1}·d^{-1}) or left the reactor as hydrogen in exhaust gas (up to 1.1 mmol·L^{-1}·d^{-1}). In syntrophic ethanol oxidation,

EEO and hydrogenotrophic methanogenesis are interdependent: an ethanol oxidizer needs a hydrogenotrophic methanogen that keeps the pH_2 sufficiently low (<14 % at standard conditions for $\Delta G_r^{0\prime}$ < 0 kJ·reaction^{-1}) to proceed EEO whereas a hydrogenotrophic methanogen cannot survive without a hydrogen producer [60]. Electrons can be transferred from an ethanol oxidizer to a hydrogenotrophic methanogen via interspecies hydrogen or formate transfer [61]. Ethanol oxidizers and hydrogenotrophic methanogens are not the only potential syntrophic partners because chain elongating microorganisms also oxidize ethanol and produce hydrogen (Eq 3.1). Chain elongating microorganisms, however, can theoretically oxidize ethanol at a much higher pH_2 compared to ethanol oxidizers (as discussed before) which makes the reverse β-oxidation pathway, from a thermodynamic perspective, independent of a hydrogen consuming syntrophic process.

In our microbial community analysis, we observed that all detected OTUs that belonged to the *Desulfovibrionales* order belonged to the sulfate-reducing genus *Desulfovibrio*. *Desulfovibrio vulgaris* can shift its lifestyle from sulfate reducer to ethanol oxidizer in the absence of sulfate [62]. It is therefore likely that *D. vulgaris* (EEO) performed syntrophic ethanol oxidation with the identified hydrogenotrophic methanogen *M. acididurans*. *M. acididurans* is an acid-tolerant hydrogenotrophic methanogen that can be active at pH 5 - 7 [63]. Presence of acid-tolerant methanogens such as *M. acididurans* explains methanogenic activity in reactors with high concentrations of fatty acids such as sour digesters or, in this case, chain elongation reactors.

Syntrophic ethanol oxidation could be related to the formation of granular sludge, which was observed in the first period of the reactor run [53]. These granules were persistently present in the reactor up to the end of the study at day 240. Syntrophic co-cultures of an ethanol oxidizer and a hydrogenotrophic methanogen, have previously been shown to co-aggregate [64], indicating that such syntrophic partnerships may have contributed to granulation in our study. Syntrophic consortia benefit from granulation because intermicrobial distances are short which leads to an efficient interspecies hydrogen transfer [65]. Based on the activity test in our previous study, we calculated that EEO in granular sludge (25.2 ± 1.5 % of total ethanol use) was similar compared to suspended sludge (19.3 ± 3.6 %). This shows that both sludge types can be used for ethanol upgrading.

3.4.2 VFA upgrading: CO_2 stimulates heptanoate production up to 1 $L_{CO2}\cdot L^{-1}\cdot d^{-1}$

Heptanoate production by VFA upgrading remained constant (~1.8 $g\cdot L^{-1}\cdot d^{-1}$) at CO_2 loading rates higher than or equal to 1 $L_{CO2}\cdot L^{-1}\cdot d^{-1}$ (Figure 3.2a). Caproate production by ethanol upgrading, however, was always faster and proportional to the CO_2 loading rate in the tested range (0 – 2.5 $L_{CO2}\cdot L^{-1}\cdot d^{-1}$). This observation can be explained by assuming that propionate (electron acceptor for VFA upgrading) and acetate (electron acceptor for ethanol upgrading) compete for the same enzyme system (in chain elongating microorganisms) which could have a higher affinity for acetate. This explanation is supported by our results which show that the rate of ethanol upgrading (butyrate + caproate + caprylate; 131.9 $mmol\cdot L^{-1}\cdot d^{-1}$) was 44 % higher than the rate of VFA upgrading (valerate + heptanoate; 91.7 $mmol\cdot L^{-1}\cdot d^{-1}$) while acetate and propionate had similar concentrations (~30 $mmol\cdot L^{-1}$; at 2.5 $L_{CO2}\cdot L^{-1}\cdot d^{-1}$). The role of electron acceptors on ethanol upgrading and VFA upgrading could be further elucidated by for instance substituting acetate or butyrate with propionate in a similar experiment. Because of the higher apparent affinity for acetate and because acetate is always produced via the reverse β-oxidation pathway, it is a challenge to achieve a high selectivity for odd numbered fatty acids in chain elongation. This study, however, shows that selectivity for odd numbered fatty acids can be increased to some extent by limiting ethanol upgrading: Combined selectivity for valerate and heptanoate at 2.5 $L_{CO2}\cdot L^{-1}\cdot d^{-1}$ was 31 % (Table S3.3) and could be increased up to 56 % by lowering the CO_2 loading rate to 0.5 $L_{CO2}\cdot L^{-1}\cdot d^{-1}$ (Table S3.5). This shows that the odd-even product ratio in chain elongation can be controlled by limiting syntrophic ethanol oxidation via CO_2 loading rate. So far, continuous odd-numbered fatty acid production by chain elongation was also studied by Grootscholten et al. (2013) [26]. Their maximum selectivity for valerate and heptanoate was similar (57 %). To what extent selectivity for odd numbered fatty acids can be further increased remains open for future investigation.

3.4.3 CO_2 is essential for both ethanol upgrading and VFA upgrading

Low and decreasing rates of ethanol upgrading and VFA upgrading were observed when CO_2 was not supplied to the reactor (day 211 to 224). This shows that chain elongation cannot be established as a high rate process without a source of CO_2. Grootscholten et al. (2014) already mentioned that chain elongation without CO_2 may not be possible [27], although experimental data on complete elimination of (a source of) CO_2 has not been shown to date.

An evident explanation why chain elongation could not be established without CO_2, is that CO_2 is used in anabolic reactions (protein synthesis for growth) by the key chain elongating bacterium *C. kluyveri*. *C. kluyveri*, requires both CO_2 and acetate for growth [40]. Growth of *C. kluyveri* was shown to be proportional to the CO_2 uptake and the dissolved CO_2 concentration up to ~3 mmol·L^{-1} [40]. This concentration is more than twice as high as compared to the highest observed CO_2 concentration in this study (Table 3.1), which could imply that growth of such chain elongating microorganisms (and thus chain elongation-activity) may have been limited by CO_2 availability during the entire study. Although presence of *C. kluyveri* could not be confirmed to species level in the bacterial community, it is evident from our results that CO_2 is essential for MCFA production by both ethanol upgrading and VFA upgrading.

At 0 L_{CO_2}·L^{-1}·d^{-1}, hydrogenotrophic methanogenic activity was almost entirely suppressed and this resulted in a buildup of hydrogen until 41.6 % (Table 3.1). Although this hydrogen may have reduced the growth rate of chain elongating microorganisms such as *C. kluyveri* (e.g. [66]), it is unlikely that this caused the total collapse of the process. A co-culture of *C. kluyveri* and *Clostridium autoethanogenum* was able to perform chain elongation at an initial pH_2 of ≥100 % [67]. Furthermore, earlier work with open cultures demonstrated MCFA production rates up to 28.6 mmol C·L^{-1}·d^{-1} at an initial pH_2 of 150 % [23]. Angenent et al. (2016) recently explained why chain elongation through the reverse β-oxidation pathway still proceeds at high pH_2, albeit at lower rate, by means of a stoichiometric and thermodynamic model [18]. This shows that chain elongation does not collapse at increased hydrogen concentrations. A systematic investigation on the effect of pH_2 on chain elongation, however, remains open for future studies.

When CO_2 was not supplied, we still measured a CO_2 concentration of 0.07 % in the headspace (0.03 mmol·L^{-1}). This was possibly a result of fermentation of yeast extract or decaying biomass which could have contributed to chain elongating activity observed. Another chain elongation study showed that fermentation of yeast extract (1 g; 34 mmol C) results in production of acetate (11 mmol C), butyrate (3 mmol C) and CO_2 (4 mmol C; data not shown) [33]. This means that yeast extract could have contributed to 4-7 % of total formed products and to CO_2 production with an equivalent of ~0.1 L_{CO_2}·L^{-1}·d^{-1} in the present study.

At 0 $L_{CO2} \cdot L^{-1} \cdot d^{-1}$, we could not identify a steady state because rates were decreasing. For example, the valerate production rate was 4.5 $g \cdot L^{-1} \cdot d^{-1}$ on day 216 and 3.2 $g \cdot L^{-1} \cdot d^{-1}$ on day 222. To prevent the likelihood of a further collapse of the process, it was decided to supply the reactor with CO_2 again with 1 $L_{CO2} \cdot L^{-1} \cdot d^{-1}$ on day 224. As a result, chain elongation activity increased and had similar steady state values as before at the same CO_2 loading rate (Table S3.7 and S3.4). This does not only confirm that CO_2 is the crucial control parameter, but also that CO_2-dependent activity (i.e. chain elongation and syntrophic ethanol oxidation) is repairable.

3.5   Outlook: CO_2 control in chain elongation with residual substrates

Depending on the anticipated type of chain elongation process, ethanol upgrading is either desired (should be stimulated) or not (should be minimized). Our results show that a high CO_2 loading rate must be selected when ethanol upgrading is desired whereas a low CO_2 loading rate must be selected when ethanol upgrading is undesired.

Ethanol upgrading can be desired when the value of caproate is relatively high compared to ethanol [19] [29]. Currently, purified caproic acid (1.00 €·kg⁻¹; 19.36 €·kmol C⁻¹) has a higher value per carbon atom than ethanol (0.52 €·kg⁻¹; 11.98 €·kmol C⁻¹) [68]. To produce 1 kg caproic acid (€1), 1.19 kg ethanol is needed (€0.62) so ethanol upgrading is therefore from a feedstock to product point of view economically feasible. Moreover, the potential of using (lignocellulosic) bioethanol as feedstock for the biotechnological conversion into other higher-value biobased platform chemicals has already been considered [69]. Caproate could eventually also be used for production of 1-hexene (via 1-hexanol) for jet and diesel fuels [70]. In this way, car fuel is converted into aviation fuel. Agler et al. (2012) mentioned that ethanol upgrading from undistilled fermentation broth could be useful to circumvent distillation of ethanol which is energetically expensive [19]. When an ethanol upgrading process is desired, the CO_2 loading rate should be high enough to sufficiently stimulate syntrophic ethanol oxidation. When the CO_2 loading rate is too high however, this could become detrimental because the CO_2 loading rate is inversely related with the pH_2 (Table 3.1). When the pH_2 becomes too low, anaerobic oxidation of MCFAs is thermodynamically feasible [56]. This

was likely the case when Grootscholten et al. (2014) increased the CO_2 loading rate to a chain elongation reactor from 2.4 to 4.8 $L_{CO_2} \cdot L^{-1} \cdot d^{-1}$ which resulted in acetate accumulation instead of chain elongation [27]. To what extent ethanol upgrading can be further increased without oxidation of products remains to be investigated. Possibly, one can control ethanol upgrading by supplying CO_2 while controlling the pH_2 at 0.007 %. In theory, this does thermodynamically prevent oxidation of both VFAs and MCFAs under standard conditions ($\Delta Gr' > 0$ kJ·reaction^{-1}). CO_2 does not necessarily need to be supplied externally because it can also be produced through primary fermentation reactions (e.g. fermentation of sugars). This allows the conversion of a sugar rich feedstock into MCFAs in only one reactor vessel without external CO_2 supply. However, there is an argument to prefer to separate primary fermentation from chain elongation and to supply CO_2 externally because this allows easier control of the pH_2 during chain elongation [27].

Ethanol upgrading is not desired when (costly and procured) ethanol must be used efficiently. This means that 1) ethanol should primarily be used for VFA upgrading and 2) EEO should be minimized. Ethanol upgrading is also not desired when a higher odd numbered MCFA (e.g. heptanoate) fraction is wanted because ethanol upgrading always results in even-numbered MCFA production. Ethanol upgrading is less efficient than VFA upgrading because ethanol upgrading requires more ethanol to produce MCFAs than VFA upgrading. For example, ethanol upgrading requires three moles of ethanol to produce 1 mole of caproate whereas VFA upgrading requires only 1.2 (starting from butyrate) or 2.4 (starting from acetate) moles of ethanol. Ge et al. (2015) therefore mentioned that ethanol use is reduced when primary fermentation is directed towards butyrate instead of acetate as electron acceptor for chain elongation [56].

If ethanol upgrading is undesired, CO_2 loading rate should be sufficiently low to limit EEO. When working with residual substrates, however, CO_2 loading rate may be more challenging to control than in this study in which a synthetic medium and gaseous CO_2 with a mass flow controller was used. This is because residual substrates may contain initial dissolved CO_2, or CO_2 is produced *in situ* from the residues. For example, Ge et al. (2015) fed undistilled fermentation broth from the bioethanol industry to a chain elongation reactor without external CO_2 supply [56]. They still observed a CO_2 concentration of ~0.4 % which could be derived from primary fermentation reactions. Although this CO_2 likely enabled chain elongation

activity in their study, its supply was not controlled during the process. To avoid *in situ* CO_2 production in chain elongation, a two-stage conversion (primary fermentation followed by chain elongation) can be considered [27]. Still, effluent from a primary fermentation reactor can contain high concentrations of CO_2 (up to 39 % in the headspace; 10 mmol·L^{-1}) [71]. This means that, if ethanol upgrading is undesired, the CO_2 concentration in this effluent must be reduced prior to feeding it to the chain elongation stage. This could be performed by supplying hydrogen to the primary fermentation stage to facilitate homoacetogenesis to produce acetate [72] or hydrogenotrophic methanogenesis to produce methane [73], resulting in consumption of CO_2. As an alternative, the CO_2 concentration could be reduced by stripping with nitrogen or upgrading it with acetate into butyrate using a bioelectrochemical system [74]. Evidently, producing acetate or butyrate is advantageous since it has a higher value than methane. Limiting EEO (by limiting hydrogenotrophic methanogenesis) could also be performed in a different way than adjusting the CO_2 loading rate. For example, Agler et al. (2014) demonstrated that activity of hydrogenotrophic methanogens decreased with increasing concentrations of undissociated butyric acid [29]. This indicates that EEO may also be limited by toxicity of fatty acids under conditions with residual substrates.

ACKNOWLEDGEMENTS

3.6   Supporting Information

Table S3.1: Overview of dominant and considered processes and their corresponding reaction equations. $\Delta G_r^{0'}$ values were calculated at standard conditions (25 °C, pH 7.0, liquid components at 1M and gaseous components at 1 atm).

Processes	Organism(s)	Reaction equation	Coupled processes	$\Delta G_r^{0'}$ kJ/reaction	
1) Processes involved in the carbon flux of ethanol upgrading					
1a) Excessive ethanol oxidation	Ethanol oxidizers	$C_2H_6O + H_2O \rightarrow C_2H_3O_2^- + H^+ + 2H_2$		9.6	
1b) Ethanol oxidation	Chain elongaters	$C_2H_6O + H_2O \rightarrow C_2H_3O_2^- + H^+ + 2H_2$	x1	9.6	
1c) Chain elongation of acetate to butyrate	Chain elongaters	$C_2H_3O_2^- + C_2H_6O \rightarrow C_4H_7O_2^- + H_2O$ [i]	x5	-38.6	
1d) Chain elongation of butyrate to caproate	Chain elongaters	$C_4H_7O_2^- + C_2H_6O \rightarrow C_6H_{11}O_2^- + H_2O$ [i]	x5	-38.8	
1e) Chain elongation of caproate to caprylate	Chain elongaters	$C_6H_{11}O_2^- + C_2H_6O \rightarrow C_8H_{15}O_2^- + H_2O$ [i]	x5	-38.8	Processes involved in the reverse β-oxidation pathway
2) Processes involved in the carbon flux of VFA upgrading					
2a) Chain elongation of propionate to valerate	Chain elongaters	$C_3H_5O_2^- + C_2H_6O \rightarrow C_5H_9O_2^- + H_2O$ [i]	x5	-38.6	
2b) Chain elongation of valerate to heptanoate	Chain elongaters	$C_5H_9O_2^- + C_2H_6O \rightarrow C_7H_{13}O_2^- + H_2O$ [i]	x5	-37.1	
3) Processes involved in syntrophic ethanol oxidation					
3a) (Excessive) ethanol oxidation	Chain elongaters & Ethanol oxidizers	$C_2H_6O + H_2O \rightarrow C_2H_3O_2^- + H^+ + 2H_2$ [ii]		9.6	
3b) Hydrogenotrophic methanogenesis	Hydrogenotrophic methanogens	$2H_2 + 0.5CO_2 \rightarrow 0.5CH_4 + H_2O$		-65.3	
3c) Syntrophic ethanol oxidation		$C_2H_6O + 0.5\ CO_2 \rightarrow C_2H_3O_2^- + H^+ + 0.5\ CH_4$	Overall	-55.7	
5) Propionate oxidation	Propionate oxidizers	$C_3H_5O_2^- + 2H_2O \rightarrow C_2H_3O_2^- + 3H_2 + CO_2$		71.7	
6) Homoacetogenesis	Homoacetogens	$2CO_2 + 4H_2 \rightarrow C_2H_3O_2^- + H^+ + 2H_2O$		-95.0	

[i] This process is done through the reverse β-oxidation pathway and is considered as VFA upgrading when the starting electron acceptor is produced from the organic feedstock (through primary fermentation) as well as when it is externally fed to the reactor. This process is considered as ethanol upgrading when the starting electron acceptor is *in situ* produced through ethanol oxidation (into acetate).
[ii] This process is not only done through the reverse β-oxidation pathway but also through direct oxidation of ethanol (excessive ethanol oxidation; EEO)

Materials and methods for microbial community analysis

DNA extraction

Genomic DNA was extracted from granular and suspended sludge fractions (500 µl sludge per sample) using a Fast DNA SPIN kit for soil (MP Biomedicals, Solon, OH), according to the manufacturers' protocol. Bead beating was performed using a FastPrep instrument (MP Biomedicals).

Bacterial community analysis

Samples for bacterial community analysis were labelled according to the corresponding CO_2 loading rate and sludge type (see overview in Figure 3.3); the initial bacterial community was labelled as 'IBC' (I). At high CO_2 loading rate (2.5 $L_{CO2} \cdot L^{-1} \cdot d^{-1}$), granular sludge was labelled as '2.5 granular' (R1go) and suspended sludge was labelled as '2.5 suspended' (R1lo). At medium CO_2 loading rate (1.0 $L_{CO2} \cdot L^{-1} \cdot d^{-1}$), granular sludge was labelled as '1.0 granular' (R1g) and suspended sludge was labelled as '1.0 suspended' (R1l). At no CO_2 loading rate (0.0 $L_{CO2} \cdot L^{-1} \cdot d^{-1}$), granular sludge was labelled as '0.0 granular' (R1gx) and suspended sludge was labelled as '0.0 suspended' (R1lx). Mock communities were also added in the analysis as previously used [75]. Extracted DNA was subjected to amplification of the V1–V2 region of the 16S rRNA gene using primers 27F-DegS [76] and an equimolar mix of reverse primers 338R-I and 338R-II [77] that were extended with 18 bp Universal Tags (Unitags). All amplification and purification steps were done as described previously [78]. All PCR reactions were done in a Thermocycler (G-storm, Essex, UK). After purification, DNA was quantified using a Nanodrop 1000 spectrophotometer (Thermo Fisher Scientific, Waltham, MA). Purified PCR products were pooled in an equimolar mix, adapter-ligated and sequenced using the MiSeq platform (GATC-Biotech, Konstanz, Germany). Analysis of the sequenced data was done using NG-Tax, an in-house pipeline [75]. Operational taxonomic units (OTUs) were assigned with the NG-Tax default settings which are extensively described by Ramiro-Garcia et al. (2016) [75]. In short, barcoded-primer and chimera filtering was done and only read pairs with perfectly matching primers and barcodes were kept. OTU picking was done using a 97 % cutoff value and a OTU table was generated using a minimum relative abundance threshold of 0.1 %. This resulted in 23556 reads for the IBC sample, 160591 reads for sample '2.5 granular' (R1go), 38223 reads for sample '2.5 suspended' (R1lo), 59806 reads for sample '1.0 granular'(R1g), 208183 reads for sample '1.0 suspended' (R1l), 112817 reads for sample '0.0 granular' (R1gx), and 64301 reads for sample '0.0 suspended'

(R1lx). The relative abundances per OTU were then calculated from the amount of reads of the OTU relative to the total amount of reads in the sample. Taxonomic assignment was done against the non-clustered, non-redundant SILVA 16S rRNA reference database [79] using the uclust algorithm [80]. Microbial composition plots were made with a workflow that is based on Quantitative Insights Into Microbial Ecology (QIIME) v1.8.0 [81]. The project was deposited to the SRA archive of the European Nucleotide Archive (ENA) with the study accession number PRJEB19881 (ERP021948) (http://www.ebi.ac.uk/).

Archaeal community analysis

For archaeal community profiling, extracted DNA was used for clone library construction. To amplify almost full-length archaeal 16S rRNA genes for cloning, the primer A109f (ACKGCTCAGTAACACGT) [82] and universal reverse primer 1492R (GYTACCTTGTTACGACTT) [83] were used. PCR amplification was done with a GoTaq polymerase kit (Promega, Madison, WI) and using a LabCycler Gradient (SensoQuest, Göttingen, Germany). The PCR program consisted of a pre-denaturing step of 30 s at 98 °C, followed by 25 cycles of 98 °C for 10 s, 56 °C for 20 s, and 72 °C for 20 s. Lastly, a post-elongation step of 10 min at 72 °C was done. PCR products were purified using a PCR Clean & Concentrator kit (Zymo Research Corporation, Irvine, CA) and ligated into the pGEM-T Easy plasmid vector (pGEM-T Easy vector system I; Promega), and transformed into *Escherichia coli* XL1-Blue competent cells (Stratagene/Agilent Technologies, Santa Clara, CA). Both ligation and transformation were performed according to the manufacturer's instructions. Afterwards, PCR was done using primers SP6 (ATTTAGGTGACACTATAG) and T7 (TAATACGACTCACTATAGGG) to amplify the cloned 16S rRNA plasmid inserts. The PCR program consisted of a pre-denaturing step of 2 min at 95 °C, followed by 25 cycles of 95 °C for 30 s, 55 °C for 40 s, and 72 °C for 1.3 min. Lastly, a post-elongation step of 5 min at 72 °C was done. PCR products were checked on an agarose gel and were sent for sequencing using the Sanger platform at GATC-Biotech (Konstanz, Germany). Forward and reverse partial sequences were assembled into full length 16S rRNA genes and trimmed for vector sequences and low quality sequences using the DNA sequence assembler of DNA Baser software (Heracle BioSoft SRL, Romania). Obtained full length 16S rRNA gene sequences were compared with 16S rRNA sequences (bacteria and archaea) using the NCBI BLAST search algorithm (http://blast.ncbi.nlm.nih.gov/Blast.cgi). The project was deposited to the European Nucleotide Archive (ENA) with study accession numbers LT855569-LT855663 (http://www.ebi.ac.uk/).

Table S3.2: Calculations on carbon fluxes and numerical values at high CO_2 loading rate (2.5 $L_{CO_2} \cdot L^{-1} \cdot d^{-1}$) and at low CO_2 loading rate (0.5 $L_{CO_2} \cdot L^{-1} \cdot d^{-1}$).

Process number	Description	Calculation on carbon flux	Carbon flux [mmol C·L^{-1}·d^{-1}]	
			2.5 $L_{CO_2} \cdot L^{-1} \cdot d^{-1}$ [i]	0.5 $L_{CO_2} \cdot L^{-1} \cdot d^{-1}$ [i]
I	Total CO_2 use	$1 \cdot |r_{CO_2}|$	100	20
I a	CO_2 use by methanogens	$1 \cdot r_{CH4}$	73	17
I b	Unidentified CO_2 use (i.e. biomass)	$1 \cdot (I - I\ a)$	27	3
II	Total ethanol use	$2 \cdot |r_{Ethanol}|$	1130	456
II a [ii]	Excessive ethanol oxidation (EEO)	II - II b - II c - II d	326	72
II b [iii]	Ethanol oxidation through the reverse β-oxidation pathway	$1/5 \cdot (II\ c + II\ d)$	134	64
II c [iv]	Ethanol use for elongation of fatty acids through the reverse β-oxidation pathway (even)	$2 \cdot (r_{Butyrate} + 2 \cdot r_{Caproate} + 3 \cdot r_{Caprylate})$	459	134
II d [iv]	Ethanol use for elongation of fatty acids through the reverse β-oxidation pathway (odd)	$2 \cdot (r_{Valerate} + 2 \cdot r_{Heptanoate})$	211	185
III	Propionate use for VFA upgrading	$3 \cdot (r_{Valerate} + r_{Heptanoate})$	275	251
IV	(Interspecies) hydrogen transfer			
V	Acetate uptake for ethanol upgrading	$2 \cdot (r_{Butyrate} + r_{Caproate} + r_{Caprylate})$	264	81
VI	Methane production	$1 \cdot r_{CH4}$	73	17
VII	Hydrogen production			
VIII	Unidentified acetate use (i.e. biomass)	II a + II b - V - IX	102	5
IX	Acetate production	$2 \cdot r_{Acetate}$	94	50
X	Butyrate, caproate and caprylate production	$4 \cdot r_{Butyrate} + 6 \cdot r_{Caproate} + 8 \cdot r_{Caprylate}$	723	215
XI	Valerate and heptanoate production	$5 \cdot r_{Valerate} + 7 \cdot r_{Heptanoate}$	486	436

[i] The ethanol loading rate at 2.5 $L_{CO_2} \cdot L^{-1} \cdot d^{-1}$ was 32.2 g·L^{-1}·d^{-1} whereas the ethanol loading rate at 0.5 $L_{CO_2} \cdot L^{-1} \cdot d^{-1}$ was 16.3 g·L^{-1}·d^{-1}. Yet, carbon fluxes are comparable because ethanol concentrations were similar.

[ii] Excessive ethanol oxidation (EEO) is the use of ethanol that is not done by the reverse β-oxidation pathway (II b, II c & II d).

[iii] Ethanol oxidation into acetate by the reverse β-oxidation pathway is 1/5th times ethanol use for elongation of fatty acids (II c + II d).

[iv] Ethanol that is used for elongation of fatty acids by reverse β-oxidation pathway is a function of elongation steps per net produced fatty acid. This is 1 step for butyrate and valerate, 2 steps for caproate and heptanoate and 3 steps for caprylate.

r_x values are net production or consumption rates in mmol·L^{-1}·d^{-1}.
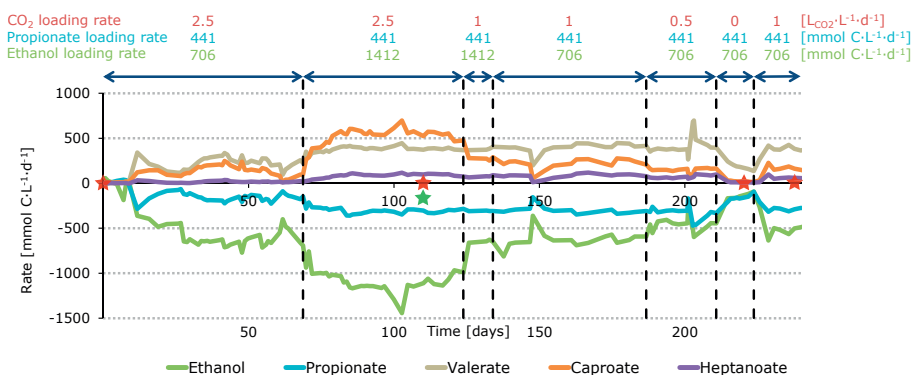
Figure S3.1: Graphical summary of the effect of CO_2 loading rate on reactor performance with net production and consumption rates over time. At the red stars, samples for bacterial community analysis were taken. At the green star, a sample for archaeal community analysis was taken. T = 30 °C, pH = 6.8, HRT = 17 h, V = 1 L.

Mean steady state values of reactor concentrations, rates and carbon selectivities

Table S3.3: Mean steady state values at 2.5 $L_{CO2} \cdot L^{-1} \cdot d^{-1}$; day 84-97, 105-119.

Compound	Concentration [mmol·L⁻¹]	Rate [mmol·L⁻¹·d⁻¹]	Selectivity [mol C %]
Ethanol	81.3 ± 30.1	-565 ± 15.3	N.A.
Propanol	9.1 ± 1.4	14.1 ± 3.0	2.7
Acetate	31.8 ± 1.5	46.9 ± 2.2	6.1
Propionate	28.4 ± 2.3	-106.6 ± 7.3	N.A.
Butyrate	24.9 ± 1.9	36.5 ± 2.5	9.4
Valerate	52.9 ± 1.1	77.9 ± 2.3	25.1
Caproate	63.4 ± 1.6	93.3 ± 3.9	36.1
Heptanoate	9.3 ± 0.5	13.8 ± 1.1	6.2
Caprylate	1.5 ± 0.4	2.1 ± 0.7	1.1
CO_2	4.6 ± 0.2 %	-99.8 ± 5.3	N.A.
CH_4	91.9 ± 0.2 %	72.6 ± 0.2	4.7
H_2	0.03 ± 0.01 %		N.A.
Unidentified			8.5

Table S3.4: Mean steady state values at 1.0 $L_{CO2} \cdot L^{-1} \cdot d^{-1}$; day 155-187.

Compound	Concentration [mmol·L⁻¹]	Rate [mmol·L⁻¹·d⁻¹]	Selectivity [mol C %]
Ethanol	15.6 ± 10.2	-323.3 ± 29.8	N.A.
Propanol	4.8 ± 1.5	7.7 ± 2.2	2.3
Acetate	21.5 ± 2.8	30.1 ± 3.9	6.0
Propionate	30.0 ± 3.0	-104.6 ± 5.6	N.A.
Butyrate	15 ± 0.7	21.6 ± 1.1	8.7
Valerate	57.4 ± 2.3	82.9 ± 3.9	41.6
Caproate	26.8 ± 2.6	39.7 ± 5.2	23.9
Heptanoate	8.8 ± 1.4	12.8 ± 2	9.0
Caprylate	0.7 ± 0.1	1.0 ± 0.3	0.8
CO_2	2.3 ± 0.2 %	-36.9 ± 3.7	N.A.
CH_4	92.2 ± 0.6 %	34.3 ± 0.2	3.4
H_2	0.08 ± 0.04 %		N.A.
Unidentified			4.2

Table S3.5: Mean steady state values at 0.5 $L_{CO2} \cdot L^{-1} \cdot d^{-1}$; day 188-201.

Compound	Concentration [mmol·L⁻¹]	Rate [mmol·L⁻¹·d⁻¹]	Selectivity [mol C %]
Ethanol	70.1 ± 25.6	-227.8 ± 23.5	N.A.
Propanol	12.9 ± 1.0	19.7 ± 2.2	7.6
Acetate	18.5 ± 1.4	25.0 ± 4.5	6.4
Propionate	30.9 ± 2.0	-101.1 ± 6.7	N.A.
Butyrate	11.0 ± 0.6	14.8 ± 1.2	7.6
Valerate	54.3 ± 1.4	74.6 ± 2.2	47.9
Caproate	18.6 ± 1.8	25.0 ± 1.5	19.3
Heptanoate	6.6 ± 0.7	9.0 ± 0.9	8.1
Caprylate	0.6 ± 0.2	0.7 ± 0.5	0.8
CO_2	1.1 %	-19.9	N.A.
CH_4	87.9 %	17.1	2.2
H_2	0.2 %		N.A.
Unidentified			0.2

Selectivity (mol C %) = mol C product/mol C total consumed substrates · 100
N.A. = Not Applicable
Concentrations of gaseous compounds (CO_2, CH_4, H_2) are shown as % in headspace at 1 atm.

Table S3.6: Mean values at 0 $L_{CO_2} \cdot L^{-1} \cdot d^{-1}$; day 216-222 (No steady state).

Compound	Concentration [mmol·L⁻¹]	Rate [mmol·L⁻¹·d⁻¹]	Selectivity [mol C %]
Ethanol	188.5 ± 15.7	-75.6 ± 10	N.A.
Propanol	8.9 ± 1.2	12.3 ± 1.5	11.7
Acetate	12.2 ± 0.8	17.1 ± 0.8	10.9
Propionate	67.7 ± 3.3	-54.6 ± 3.3	N.A.
Butyrate	5.0 ± 0.7	6.9 ± 0.9	8.7
Valerate	27.8 ± 4.0	38.1 ± 4.7	60.4
Caproate	3.0 ± 0.9	3.6 ± 0.8	6.9
Heptanoate	1.3 ± 0.4	1.4 ± 0.1	3.2
Caprylate	0.4 ± 0.1	0.5 ± 0.5	1.2
CO_2	0.07 ± 0.01 %	0 ± 0	N.A.
CH_4	49.3 ± 3.9 %	1.5 ± 0.1	0.5
H_2	41.6 ± 5.1 %		N.A.
Unidentified			-3.4

Table S3.7: Mean steady state values at 1.0 $L_{CO_2} \cdot L^{-1} \cdot d^{-1}$; day 229-240.

Compound	Concentration [mmol·L⁻¹]	Rate [mmol·L⁻¹·d⁻¹]	Selectivity [mol C %]
Ethanol	56.7 ± 15	-267.2 ± 28.1	N.A.
Propanol	6.4 ± 0.7	9.5 ± 1.6	3.3
Acetate	27.9 ± 2.5	42.5 ± 4.6	9.8
Propionate	39.3 ± 2.9	-97.2 ± 6.2	N.A.
Butyrate	12.9 ± 0.4	19.7 ± 0.7	9.1
Valerate	51.9 ± 1.9	78 ± 5.1	45.1
Caproate	18.9 ± 1.9	28.7 ± 4.9	19.9
Heptanoate	6.1 ± 1.1	9.2 ± 2.4	7.4
Caprylate	0.7 ± 0.1	1.0 ± 0.3	0.9
CO_2	1.4 ± 0.01 %	-38.7 ± 0.3	N.A.
CH_4	93.1 ± 0.5 %	29.6 ± 0.1	3.4
H_2	0.1 ± 0.005 %		N.A.
Unidentified			0.9

Selectivity (mol C %) = mol C product/mol C total consumed substrates · 100
N.A. = Not Applicable
Concentrations of gaseous compounds (CO_2, CH_4, H_2) are shown as % in headspace at 1 atm.
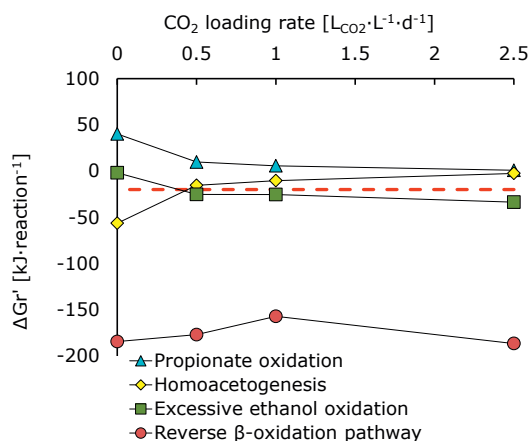
Figure S3.2: Results of thermodynamic analysis: change in Gibbs free energy of propionate oxidation (Eq 5, Table S3.1), homoacetogenesis (Eq 6, Table S3.1), excessive ethanol oxidation (EEO; Eq 1a, Table S3.1), reverse β-oxidation pathway (ethanol oxidation coupled to 5x propionate elongation; Eq 1b + 2a, Table S3.1) at different CO_2 loading rates under actual bioreactor conditions (pH = 6.8, T = 30 °C, steady state concentrations of substrates and products). The red line indicates the thermodynamic feasible limit of -20 kJ·reaction^{-1} for microorganisms [60].
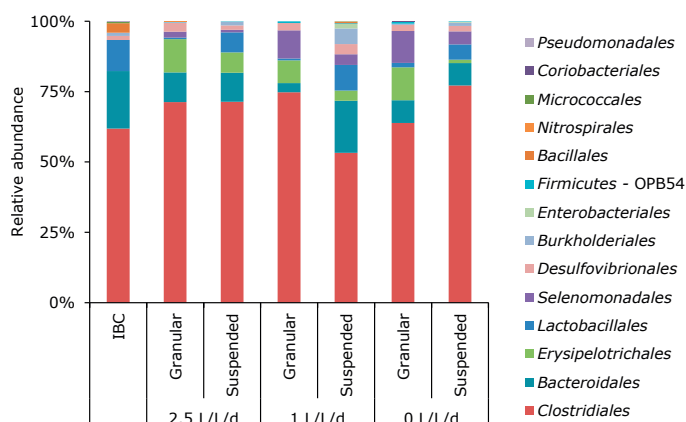
Figure S3.3: Results of bacterial community analysis: order level composition of bacterial community at different CO_2 loading rates in granular and suspended sludge. IBC = initial bacterial community.

Table S3.8: Results of archaeal community analysis: phylogenetic affiliation of the cloned 16S rRNA gene sequences from the archaeal community in suspended sludge at 2.5 L_{CO_2}·L^{-1}·d^{-1}.

Closest cultured relative	No. of clones	Sequence identity [%]
Methanobrevibacter acididurans	58	99
Methanobrevibacter acididurans	31	98
Methanobrevibacter acididurans	6	97
Failed clones	1	
Total no. of clones	96	

136 g NaOH

419 g VS
Food waste

AFW

1013 g Ethanol
307 g NaOH

Long HRT

1000 g MCFAs

**Hydrolysis &
acidogenesis**
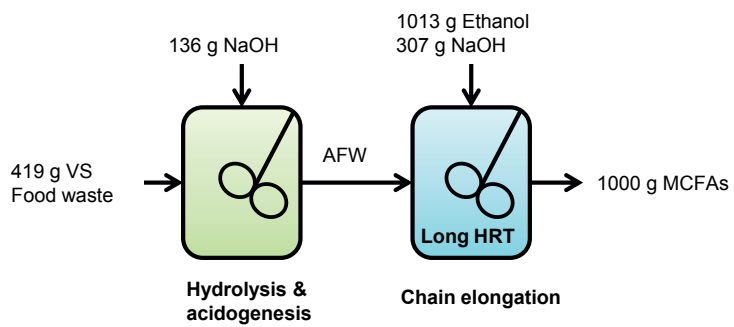
Chain elongation

CHAPTER 4

Development of an Effective Chain Elongation Process

Abstract

Introduction: Continuous chain elongation with organic residues becomes effective when the targeted medium chain fatty acids (MCFA(s)) are produced at high concentrations and rates, while excessive ethanol oxidation and base consumption are limited. The objective of this study was to develop an effective continuous chain elongation process with hydrolyzed and acidified food waste and additional ethanol.

Results: We fed acidified food waste (AFW) and ethanol to an anaerobic reactor while operating the reactor at long (4 d) and at short (1 d) hydraulic retention time (HRT). At long HRT, n-caproate was continuously produced (5.5 g/L/d) at an average concentration of 23.4 g/L. The highest n-caproate concentration was 25.7 g/L which is the highest reported n-caproate concentration in a chain elongation process to date. Compared to short HRT (7.1 g/L n-caproate at 5.6 g/L/d), long HRT resulted in 6.2 times less excessive ethanol oxidation. This led to a two times lower ethanol consumption and a two times lower base consumption per produced MCFA at long HRT compared to short HRT.

Conclusions: Chain elongation from AFW and ethanol is more effective at long HRT than at short HRT not only because it results in a higher concentration of MCFAs but also because it leads to a more efficient use of ethanol and base. The HRT did not influence the n-caproate production rate. The obtained n-caproate concentration is more than twice as high as the maximum solubility of n-caproic acid in water which is beneficial for its separation from the fermentation broth. This study does not only set the record on the highest n-caproate concentration observed in a chain elongation process to date, it notably demonstrates that such high concentrations can be obtained from AFW under practical circumstances in a continuous process.

4.1   Introduction

Organic residual streams, like food waste, have great potential as alternative resource for production of fuels and chemicals because they are renewable and because they do not compete with the human food chain [84]. The challenge is to convert these mixed residues into the desired products and purify them in an energy-efficient and economically viable process. An emerging technology that facilitates conversion of (derivatives of) organic residues into (precursors of) fuels and chemicals is chain elongation. Chain elongation is an anaerobic open-culture biotechnological process that converts volatile fatty acids (VFAs) and an electron donor into more valuable medium chain fatty acids (MCFAs) [18]. The conversion of VFAs into MCFAs with ethanol as electron donor is done by chain elongating micro-organisms (e.g. *Clostridium kluyveri*) that use the reverse β-oxidation pathway. In this pathway, 1 additional mole of ethanol is oxidized into acetate for every 5 chain elongation reactions (Eq 4.1) [21].

Reverse β-oxidation pathway:
$$5C_xH_{2x-1}O_2^- + 6C_2H_6O \rightarrow 5C_{x+2}H_{2x+3}O_2^- + C_2H_3O_2^- + 4H_2O + H^+ + 2H_2 \quad \text{(Eq 4.1)}$$
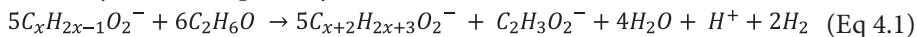
VFAs can be obtained through hydrolysis and acidogenesis of organic residues. Electron donors that are suitable for chain elongation processes, such as ethanol [23], hydrogen [23], methanol [33] and lactic acid [34], can also be produced from organic residues (e.g. lignocellulosic bioethanol). Particularly, MCFAs can be used for production of aviation fuels [70] [85] and for other end-products such as solvents, lubricants, feed additives for poultry [86] and piglets [87], plastics and dyes [18]. The main advantage of chain elongation is that it is catalysed by an anaerobic open-culture reactor microbiome (i.e. sludge). Open-culture microbiomes can tolerate mixtures of residual streams while they convert the residues under mild and non-sterile conditions. Chain elongation, therefore, does not need a chemical catalyst and proceeds under mild and non-sterile conditions. Although inhibition of competing processes is important, it is not necessary to do this by adding bioactive chemicals such as antibiotics or methanogenic inhibitors such as 2-bromoethanesulfonate (e.g. ref [88]). As such, solid residual streams from the chain elongation process itself could be used as soil fertilizer upon composting.

MCFA production from organic residues through biomass hydrolysis, acidogenesis and chain elongation can be executed in a single-stage system [19] as well as in a two-stage system [27]. In a two-stage system, hydrolysis and acidogenesis are done in one stage and chain elongation in a subsequent stage. The advantage of a two-stage system over a single-stage system is that both stages can be optimized independently. Grootscholten et al. (2014) concluded that MCFA production from the organic fraction of municipal solid waste and additional ethanol in a two-stage system resulted in higher MCFA production rates and concentrations compared to a single-stage system [27]. Another advantage of a two-stage system is that it allows easier control of the hydrogen partial pressure (pH$_2$) in the chain elongation stage by e.g. manipulating CO_2 loading rate [27] [88]. The pH$_2$ is important because it can thermodynamically inhibit competing processes such as anaerobic oxidation of MCFAs and anaerobic oxidation of ethanol, also known as excessive ethanol oxidation (EEO; Eq 4.2).

Excessive ethanol oxidation (EEO):
$$C_2H_6O + H_2O \rightarrow C_2H_3O_2^- + H^+ + 2H_2 \qquad \text{(Eq 4.2)}$$

Hydrogenotrophic methanogenesis:
$$2H_2 + 0.5CO_2 \rightarrow 0.5CH_4 + H_2O \qquad \text{(Eq 4.3)}$$
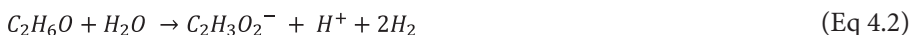
Syntrophic ethanol oxidation:
$$C_2H_6O + 0.5\,CO_2 \rightarrow C_2H_3O_2^- + H^+ + 0.5\,CH_4 \qquad \text{(Eq 4.4)}$$

Suppression of EEO is essential to make efficient use of ethanol because ethanol is a major cost factor. EEO is considered to be performed by ethanol-oxidizing microorganisms which do not perform chain elongation [88]. Earlier work demonstrated that ethanol is oxidized due to hydrogenotrophic methanogenesis (Eq 4.3) [29] and that the overall reaction can be referred to as syntrophic ethanol oxidation [88] (Eq 4.4). By limiting the CO_2 loading rate to a chain elongation process, EEO was reduced from 28.8 % to 15.9 % of total ethanol consumption [88]. No CO_2 addition resulted in low and decreasing MCFA production rates. When working with organic residues, however, CO_2 loading rate may be more difficult to control because CO_2 is also a product of acidogenesis. Even though acidogenesis and chain elongation can be separated, dissolved CO_2 could still complicate the control over the actual CO_2 supply to the chain elongation process.

In such a case, alternative strategies than CO_2 loading rate to suppress EEO are needed. Although EEO can be beneficial for ethanol upgrading processes to n-caproate (*in situ* ethanol oxidation into acetate and subsequent chain elongation into even-numbered fatty acids), one can consider ethanol upgrading as an inefficient use of ethanol per produced MCFA [88]. Furthermore, EEO acidifies the fermentation broth and this requires extra base addition for pH correction. Because the use of both ethanol and base cause major environmental impact over the life cycle of chain elongation processes [35], their consumption should be reduced in the development of this technology.

A high MCFA concentration in chain elongation processes would be beneficial because this improves its separation from the fermentation broth [89]. Grootscholten et al. (2014) achieved a maximum n-caproate concentration of 12.6 g/L in a two-stage MCFA production system from organic waste. Recently, considerably higher concentrations of n-caproate (>20 g/L) have been reported from chain elongation processes which were conducted in batch at near-neutral pH [34] [90]. These studies suggest that such high concentrations can also be reached in a continuous chain elongation process as long as the hydraulic retention time (HRT) is long enough to allow product accumulation. The HRT, however, was also shown to influence the volumetric MCFA productivity as the highest reported MCFA production rate was achieved at a short HRT of 4 h (57 g/L/d) [25]). A high MCFA productivity is desired to make effective use of the bioreactor; though MCFA production by chain elongation (62.4 g COD/L/d [27]) already exceeds the rate of methane production by anaerobic digestion (6.7 - 11.2 g COD/L/d [a]). Chain elongation studies that operated at near neutral pH usually maintained an HRT shorter than 1 d [24] [26] [27] [53] [88]. To date, however, there are no studies that report the effect of a long HRT in combination with a near-neutral pH in a chain elongation process from acidified organic waste and ethanol.

The objective of this study was to develop an effective continuous biological chain elongation process from acidified food waste (AFW) and ethanol to produce n-caproate at a high concentration while EEO is limited. The effect of 2 HRTs (1 and 4 d) was compared and evaluated based on an extensive set of performance indicators including MCFA production rates, MCFA concentrations, MCFA production efficiency, substrate consumption efficiency, rate of EEO and base consumption. Finally, an outlook is given on the potential of the developed bioprocess.

---

[a] Based on 5–6 $m^3/m^3/d$ with a methane content of 50–70 % [91])

4.2 Materials and methods

4.2.1 Preparation of food waste

Food waste was collected from Rotie, a recycling company in Lijnden, the Netherlands. The waste consisted of outdated food scraps and had a total solids (TS) content of 15.5 ± 0.2 % (w/w), a volatile solids (VS) content of 13.8 ± 0.4 % (w/w) and a sodium content of 2.7 ± 0.01 g/L. The waste was stored at -20 °C until further use. Before use as fermentation feed, the waste was thawed at 4 °C, diluted until ~4.0 % VS (w/w) with tap water and the pH was adjusted to 5.5 with 5 M NaOH.

4.2.2 First stage: Hydrolysis and acidogenesis of food waste

Hydrolysis and acidogenesis of food waste was executed in a batch reactor with a working volume of 20 L as described by Chen et al. (2016) [92]. After loading 20 L diluted food waste into the reactor, the reactor content was sparged with N_2 for 10 min to remove oxygen. Thereafter, 200 mL inoculum (derived from a previous hydrolysis and acidogenesis run that used the same substrate and reactor configuration) and 5 mL Antifoam B Emulsion (Sigma-Aldrich, the Netherlands) were added. The reactor was then operated at 35 °C, 1 atm, stirred at 44 rpm while the pH was maintained at 5.5 using a pH sensor (model QP-635-E275-S8, ProSense BV - QiS, Oosterhout, The Netherlands) and 5M NaOH. The slightly acidic pH was selected to inhibit methanogenesis [19] [56]. After 18 days of operation, reactor content (acidified food waste; AFW) was centrifuged (15000 rpm for 15 min) and decanted to remove solids and sieved (1 mm) to remove floating particles (e.g. lipids). This was performed for in total four 20 L batches to generate sufficient AFW as feedstock for the chain elongation stage. The resulting centrifuged and sieved AFW from the four batches was pooled together and stored at 4 °C until further use. The following compounds in the pooled AFW were measured (concentration in g/L): inorganic carbon (0.011), sodium (4.8), ethanol (0.1), butanol (0.2), acetate (8.1), propionate (1.7), isobutyrate (0.6), n-butyrate (9.3), isovalerate (0.4), valerate (0.4) and n-caproate (1.4). The mentioned organic compounds account for a chemical oxygen demand (COD) of 35 g_{O2}/L. AFW had a soluble COD of 37.1 g_{O2}/L (LCK 014 COD, Hach Lange GMBH, Germany).

Average VS consumption in the hydrolysis and acidogenesis stage was determined based on the mean VS content at the beginning of two batches (n = 6) and on

the mean VS content at the end of these two batches (n = 6). Average NaOH consumption in the hydrolysis and acidogenesis stage was determined based on the difference between the mean sodium content of diluted food waste (n = 3) and the mean sodium content of AFW (n = 3)

4.2.3   Second stage: Chain elongation of acidified food waste and ethanol

Chain elongation of AFW and ethanol was performed in one single process using a continuously stirred anaerobic reactor as described by Roghair et al. (2016) [53]. In short, a continuous reactor with a working volume of 1 L was operated at 30 °C, 1 atm, stirred at 100 rpm while the pH was maintained at 6.8 using a pH sensor (Applisens model Z001023551, Schiedam, The Netherlands) and 2M NaOH. Gaseous CO_2 was supplied with a mass-flow controller (Brooks Instruments 5850S, the Netherlands) at 1 L_{CO2}/L/d. The reactor was started with a synthetic medium that contained 13.8 g/L propionic acid (≥99.5 %, Sigma-Aldrich) and 32.2 g/L ethanol (Absolute, VWR). These starting conditions have formerly shown to induce formation of granular sludge [53] and can also be used to distinguish the carbon flux of ethanol upgrading from VFA upgrading [88]. The composition of other components (salts, yeast extract, vitamins and trace elements) were as previously described [53]. The reactor was inoculated in batch mode on day 1 with 50 mL chain elongation sludge from a previous run; the inoculum contained chain elongating micro-organisms, ethanol oxidizers and hydrogenotrophic methanogens [88]. On day 9, the reactor operation mode was set from batch to continuous with an HRT of 4 d. From day 19 onwards, the reactor was fed with AFW to which 32.2 g/L ethanol was added. On day 58, the HRT was set from 4 d to 1 d. On day 103, the HRT was set back from 1 d to 4 d.

Liquid samples were taken from the reactor content and from the influent tank 1-3 times per week. Gas samples were taken from the headspace 1-3 times per week. The reactor was assumed to be in steady state when n-caproate production rates were similar (with a maximum relative standard deviation of 16 %) over a period of at least 7 HRTs. Average concentrations and rates and their corresponding standard deviations were based on at least nine measurements within a steady state. Average NaOH consumption in the chain elongation stage was determined based on the difference between average sodium concentration in the effluent (n = 3 different samples during a steady state) and on the average sodium concentration in the influent tank (n = 3 different samples during a steady state).

4.2.4 Analytical procedures

Alcohols (C2-C6) and fatty acids (C2-C8) were analyzed by gas chromatography using an Agilent 7890B (USA), equipped with HP-FFAP capillary column (l = 25 m, ID = 0.32 mm, film = 0.5 μm). 1 μl from a diluted sample was injected into a liner with glass wool at 250 °C. Vaporized compounds entered the column, along with helium as carrier gas, with a flow rate of 1.25 mL/min (first 3 min) and 2 mL/min (until the end of the run). The oven temperature program was as follows: 60°C for 3 min; 21°C/min up to 140°C; 8°C/min up to 150°C and constant for 1.5 min; 120°C/min up to 200°C and constant for 1.25 min; 120°C/min up to 240°C and constant for 3 min. Compounds were detected with a flame ionization detector at 240 °C, fed with 30 mL/min hydrogen and 400 mL/min air.

Gaseous compounds (N_2, H_2, CO_2, CH_4 and O_2) were analyzed by gas chromatography using an Agilent Varian CP4900 μGC (USA) equipped with a thermal conductivity detector and two parallel columns: a Mol Sieve 5A PLOT column (l = 10 m, ID = 0.32 mm, film = 0.15 μm) and a PoraPlot U column (l = 10 m). The oven temperature was 80 °C for the Mol Sieve 5A PLOT column and 65 °C for the PoraPLOT U column. The carrier gas was argon and had a flow rate of 1.47 mL/min.

Sodium was measured by ion chromatography using a Metrohm Compact IC Flex 930 (Schiedam, the Netherlands) equipped with a pre-column (Metrohm Metrosep RP 2 Guard/3.6), a cation column (Metrosep C 4- 150/4.0) and a conductivity detector. The mobile phase was 3 mM nitric acid.

TS, VS and VSS were determined following Standard Methods [93]. The filter for VSS measurements (Whatman GF/F 0.7 μm) was preheated at 450 °C prior to filtration. Inorganic carbon was measured using a total organic carbon analyser (Shimadzu TOC-VCPH, Japan).

4.2.5 Mathematical expressions

The volumetric production or consumption rate of aqueous compounds is based on the difference between effluent concentration and influent concentration divided by the HRT:

Rate [g/L/d] = (effluent concentration [g/L] – influent concentration [g/L]) / HRT [d]

Excessive ethanol oxidation is the difference between total ethanol consumption and ethanol consumption through the reverse β-oxidation pathway:

Excessive ethanol oxidation (EEO) [g/L/d] = rate total ethanol consumption [g/L/d] – rate ethanol consumption through the reverse β-oxidation pathway [g/L/d] [88]

Ethanol consumption through the reverse β-oxidation pathway (g/L/d) = ethanol use for elongation of fatty acids through the reverse β-oxidation pathway (g/L/d) + ethanol oxidation into acetate through the reverse β-oxidation pathway (g/L/d)

Ethanol use for elongation of fatty acids through the reverse β-oxidation pathway (g/L/d) = (rate n-butyrate [mmol/L/d] + rate valerate [mmol/L/d] + 2 · rate n-caproate [mmol/L/d] + 2 · rate n-heptanoate [mmol/L/d] + 3 · rate n-caprylate [mmol/L/d]) · 46.05 / 1000

Ethanol oxidation into acetate through the reverse β-oxidation pathway (g/L/d) = Ethanol use for elongation of fatty acids through the reverse β-oxidation pathway (g/L/d) · 0.2

Selectivity is defined as product produced relative to substrates consumed on an electron basis [27]:

Selectivity [mol e %] = product formation rate [mol e/L/d] / total substrate consumption rate (mol e /L/d) · 100

Selectivity values that are based on a carbon basis are reported in the Supporting information but are not presented and discussed in the results and discussion section.

Substrate consumption efficiency is defined as substrate consumed relative to the organic loading rate on an electron basis:

Substrate consumption efficiency [mol e %] = (|substrate consumption rate [mol e/L/d]| / organic loading rate [mol e/L/d] · 100

Product production efficiency is defined as product produced relative to the organic loading rate on an electron basis

Product production efficiency [mol e %] = product formation rate [mol e/L/d] / organic loading rate [mol e/L/d] · 100

4.3   Results

4.3.1 Higher MCFA concentrations and selectivities at long HRT than at short HRT

Acidified food waste (AFW) and ethanol were fed to a continuous biological chain elongation process, resulting in production of MCFAs (n-caproate, isocaproate, n-heptanoate and n-caprylate). n-Caproate, the dominant MCFA, was produced (5.5 ± 0.4 g/L/d) at a high steady state concentration of 23.4 ± 1.0 g/L. This was observed at long HRT (4 d) from day 28 through day 58 (Figure 4.1). After the HRT was decreased from 4 d to 1 d (short HRT), another steady state was observed from day 79 through day 103. Here, n-caproate was produced at a similar rate (5.6 ± 0.9 g/L/d) but at a lower concentration (7.1 ± 0.9 g/L). On day 103, the HRT was increased from 1 to 4 d. Again, n-caproate was continuously produced at a high steady state concentration (23.2 ± 1.9 g/L). This was observed from day 114 through day 147. The maximum n-caproate concentration was 25.7 g/L on day 120. Reactor performance of the first steady state at long HRT was similar as the reactor performance of the second steady state at long HRT. This shows that the effect of HRT on reactor performance is reversible. From here on, however, 'long HRT' refers to the first steady state (day 28 – 58). Mean steady state rates, concentrations and selectivities of all identified substrates and products at long and at short HRT are reported in Tables S4.1 and S4.2 respectively. A summary of reactor performance indicators and properties of the steady states at both long and short HRT are reported in Table 4.1 for comparison.

At long HRT, n-heptanoate and n-caprylate were both produced at a low rate (~0.15 g/L/d) and concentration (~0.6 g/L) compared to n-caproate. At short HRT, however, these MCFAs were produced at insignificant amounts (< 0.1 g/L). Isocaproate was produced in trace amounts at both long and short HRT. The selectivity of MCFAs was 81.6 mol e % at long HRT and 46.3 mol e % at short HRT. The remaining consumed carbon ended up as VSS (biomass), VFAs, methane, propanol, and unidentified products as given in Table S4.1 and S4.2. The MCFA productivity at both long and short HRT (~12.5 g COD/L/d) was somewhat higher compared to the typical methane productivity in an anaerobic digester (6.7 - 11.2 g COD/L/d [b]).

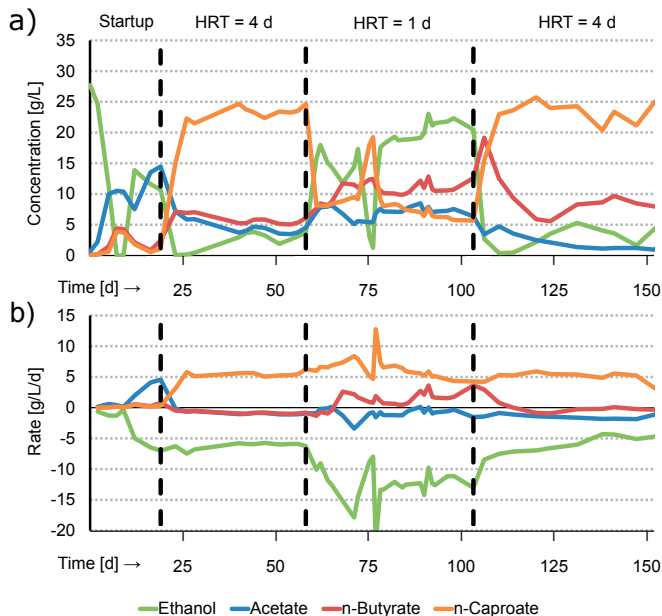[b]   Based on 5–6 $m^3/m^3/d$ with a methane content of 50–70 % [91])

Figure 4.1: Graphical summary of experimental results with concentrations over time (a) and net production and consumption rates over time (b). T = 30 °C, pH = 6.8, V = 1 L, CO_2 loading rate = 1.0 L_{CO_2}/L/d.

4.3.2 Excessive ethanol oxidation, methane production and NaOH consumption

Long HRT did not only result in higher MCFA concentrations and selectivities compared to short HRT, it also resulted in less EEO and in less sodium hydroxide (NaOH) consumption per MCFA produced. EEO occurred at a 6.3 times lower rate at long HRT (0.9 ± 0.4 g/L/d) than at short HRT (5.6 ± 1.4 g/L/d). This process was also relative to the total ethanol consumption rate lower at long HRT (14.7 ± 5.5 %) than at short HRT (45.0 ± 9.7 %).

Methane production was 3.4 times lower at long HRT (12.8 ± 2.6 mmol/L/d) than at short HRT (43.8 ± 2.5 mmol/L/d). A previous study showed that hydrogenotrophic methanogenesis and EEO are coupled and that the overall reaction can be referred to as syntrophic ethanol oxidation [88]. In syntrophic ethanol oxidation, the stoichiometric ratio between methane production and ethanol oxidation is 0.5 mol/mol (Eq 4.4). The present study shows a similar ratio at long HRT (0.7 ± 0.3) and at short HRT (0.4 ± 0.1) which implies that EEO, like in the previous study, was a result of syntrophic ethanol oxidation. Less EEO also led to fewer NaOH consumption for pH correction because EEO is an acidifying process that releases

a proton (Eq 4.2). NaOH consumption per produced MCFA was two times lower at long HRT (0.92 ± 0.04 mol$_{NaOH}$/mol$_{MCFA}$) than at short HRT (1.93 ± 0.31 mol$_{NaOH}$/mol$_{MCFA}$). These results not only show that EEO can be limited at long HRT but also that consumption of NaOH is hereby reduced.

4.3.3 Consumption of VFAs and ethanol

Acetate, propionate and ethanol were consumed at both long and short HRT. However, whereas butyrate was consumed at long HRT (-0.9 ± 0.1 g/L/d), it was produced at short HRT (1.6 ± 1.1 g/L/d). This resulted in a lower n-butyrate concentration in the reactor at long HRT (5.6 ± 0.6 g/L) than at short HRT (10.8 ± 1.0 g/L). A net consumption of n-butyrate instead of production indicates that caproate production is more efficient in ethanol-use. This is because n-butyrate consumption (i.e. elongation) requires less ethanol than acetate elongation to caproate or ethanol upgrading. Whereas ethanol upgrading requires 3 moles of ethanol to produce 1 mole of n-caproate, VFA upgrading requires only 1.2 moles of ethanol from n-butyrate or 2.4 moles of ethanol from acetate [88]. Indeed, the chain elongation process at long HRT was more efficient in ethanol-use than at short HRT. Approximately two times less ethanol was consumed per produced MCFA at long HRT (0.87 ± 0.07 mol C/mol C) than at short HRT (1.83 ± 0.31 mol C/mol C). The VFA consumption per produced MCFA at both long (0.29 ± 0.04 mol C/mol C) and short HRT (0.20 ± 0.07 mol C/mol C) were found to be similar.

The concentration of ethanol in the reactor (and thus also in the effluent) was much lower at long HRT (2.8 ± 1.1 g/L) than at short HRT (20.1 ± 1.6 g/L). The ethanol consumption efficiency, therefore, defined as consumed ethanol relative to supplied ethanol, was higher at long HRT (98.6 ± 5.4 mol e %) than at short HRT (40.3 ± 3.5 mol e %). A high ethanol consumption efficiency (or a low ethanol concentration in the effluent) is desired because any unconsumed ethanol requires an additional recovery or treatment step after the chain elongation stage which makes the overall process more expensive. The VFA consumption efficiency was also higher at long HRT (45.8 ± 6.9 mol e %) than at short HRT (7.2 ± 2.3 mol e %). Although VFAs are not as costly as ethanol, it is evident that a higher VFA consumption efficiency is preferred because the remaining VFAs (e.g. after selective extraction of the MCFAs) also have to be recovered or treated with a waste water treatment system.

4.3.4 VSS

The mean VSS concentration in the reactor at long HRT (0.34 ± 0.23 g/L) was similar compared to the mean VSS concentration in the reactor at short HRT (0.33 ± 0.03 g/L). These reactor concentrations were in the same order of magnitude as the VSS concentrations in the effluent (0.43 ± 0.32 g/L at long HRT and 0.35 ± 0.20 g/L at short HRT), implying that the reactor was ideally stirred with no biomass retention (i.e. CSTR). Formation of granular sludge, however, was observed like in the earlier experiment with the same set-up while using a synthetic medium [53]. The earliest observation of granules (by eye visible) was on day 82, at short HRT. Granules disappeared within a few days after the HRT was increased on day 103. Because the formation of granular sludge coincided with high-rate syntrophic ethanol oxidation (at short HRT) it is likely that this syntrophic process attributed to sludge granulation. Syntrophic processes may benefit from granulation because granules could facilitate a more efficient interspecies hydrogen transfer due to the decreased intermicrobial distances [65].

The mean VSS concentration in the influent was 0.25 ± 0.06 g/L. From the mentioned values the VSS production rate and VSS specific growth rate were calculated (Table 4.1). Although one could expect a four times lower growth rate at long HRT (0.07 ± 0.16 g/g/d) than at short HRT (0.54 ± 1.0 g/g/d), there was no significant difference due to the large standard deviations.

Table 4.1: Performance indicators and properties of the chain elongation process at long and at short HRT

Performance indicator	Unit	Long HRT [4 d]	Short HRT [1 d]
Steady state characteristics			
Steady state interval	d	28 – 58	79 – 103
Number of HRTs	-	7.5	24.3
Products			
n-Caproate concentration	g/L	23.4 ± 1.0	7.1 ± 0.9
n-Caproate rate	g/L/d	5.5 ± 0.4	5.6 ± 0.9
n-Caproate selectivity	mol e %	76.5 ± 5.0	44.6 ± 7.8
MCFA selectivity	mol e %	81.6 ± 5.0	46.3 ± 8.0
Methane rate	mmol/L/d	12.8 ± 2.6	43.8 ± 2.5
Substrates			
Ethanol loading rate	g/L/d	6.1 ± 0.2	30.6 ± 1.3
Ethanol concentration	g/L	2.8 ± 1.1	20.1 ± 1.6
Ethanol rate	g/L/d	-6.0 ± 0.3	-12.3 ± 1.1
EEO	g/L/d	0.9 ± 0.4	5.6 ± 1.4
EEO	% of total ethanol use	14.7 ± 5.5	45.0 ± 9.7
Acetate rate	g/L/d	-1.0 ± 0.2	-0.8 ± 0.5
Propionate rate	g/L/d	-0.3 ± 0.0	-0.7 ± 0.1
n-Butyrate rate	g/L/d	-0.9 ± 0.1	1.6 ± 1.1
Substrate to product conversions			
Consumed VFA per produced MCFA	mol C/mol C	0.29 ± 0.04	0.20 ± 0.07
Consumed Ethanol per produced MCFA	mol C/mol C	0.87 ± 0.07	1.83 ± 0.31
Consumption / production efficiency			
Ethanol consumption efficiency	mol e %	98.6 ± 5.4	40.3 ± 3.5
VFA consumption efficiency	mol e %	45.8 ± 6.9	7.2 ± 2.3
n-Caproate production efficiency	mol e %	58.7 ± 2.9	12.8 ± 2.1
MCFA production efficiency	mol e %	62.6 ± 2.9	13.3 ± 2.2
NaOH use			
Sodium concentration in influent [AFW]	g/L	4.9 ± 0.1	4.8 ± 0.1
Sodium concentration in reactor	g/L	9.1 ± 0.5	7.0 ± 0.0
Consumed NaOH per produced MCFA	mol/mol	0.92 ± 0.04	1.93 ± 0.31
VSS			
VSS concentration	g/L	0.34 ± 0.23	0.33 ± 0.03
VSS rate	g/L/d	0.02 ± 0.05	0.18 ± 0.33
Growth rate	g/g/d	0.07 ± 0.16	0.54 ± 1.00

4.4 Discussion

4.4.1 Continuous n-caproate production at a high concentration from acidified food waste

In this study, an effective two-stage MCFA production process from food waste and ethanol was developed. The microbiome in the second stage (chain elongation) was able to continuously produce n-caproate at 23.4 ± 1.0 g/L while EEO was limited to 14.7 ± 5.5 % of total ethanol consumption. This was achieved at long HRT (4 d) and at near-neutral pH (6.8) but without in-line product extraction. Thus, a long HRT was shown to be effective for this specific waste stream. The n-caproate production rate was similar for both long and short HRT (~5.5 g/L/d) and was much lower compared to the highest reported n-caproate production rate to date (55.8 g/L/d) [25]. This high production rate, however, occurred at a substantially lower n-caproate concentration (9.3 g/L) than obtained in the present study. An overview of comparable studies that reported high n-caproate concentrations and/ or rates using open cultures is shown in Table 4.2.

Table 4.2: Overview of comparable studies that report high n-caproate concentrations and/or rates using open cultures.

Reactor type	Substrate(s)	pH	HRT	n-Caproate			Reference
				Concentration [g/L]	Rate [g/L/d]	Selectivity [mol e %]	
Continuously stirred anaerobic reactor	AFW and Ethanol	6.8	4 d	23.4	5.5	76.5	This study
Continuously stirred anaerobic reactor	AFW and Ethanol	6.8	1 d	7.1	5.6	44.6	This study
Batch reactor	Lactate	~6.5	N.A.	23.4	1.1	81.4	[34]
Batch reactor	Acetate and ethanol	~6.5	N.A.	21.1	N.D.	65.0	[90]
Continuous upflow anaerobic filter	Acetate and ethanol	6.5–7.2	4 h	9.3	55.8	~78.0	[25]
Continuous upflow anaerobic filter	Acidified food / garden waste and ethanol	6.5–7.0	11 h	12.6	26.0	72.0	[27]
Continuous upflow anaerobic filter	Acetate and ethanol	6.5–7.0	17 h	11.1	15.7	85.0	[24]

N.A. = Not applicable
N.D. = Not determined

A high n-caproate concentration is beneficial for its separation from the fermentation broth. The obtained n-caproate concentration in the present study is more than twice as high as the maximum solubility of the undissociated form of n-caproate, n-caproic acid, in water (~10.8 g/L [94]). Thus, in theory, the high n-caproate concentration allows it to be separated from the effluent by phase separation after lowering the pH to 4.9 or lower. A recent study, executed by Zhu et al. (2015), also reported a high n-caproate concentration (23.4 g/L) using an anaerobic reactor microbiome [34]. The n-caproate was produced from lactate as the sole carbon source in a batch process using an inoculum that was derived from mature pit mud, a microbiome used for the production of Chinese strong-flavored liquor. Their process reached a higher n-caproate selectivity (81.4 mol e %) than the process in the present study at long HRT (76.5 mol e %). However, the process in the present study achieved a slightly higher MCFA selectivity (81.6 mol e %) because it also produced other MCFAs (isocaproate, n-heptanoate and caprylate).

Liu et al. (2017) also reported a high n-caproate concentration (21.2 g/L) from ethanol and acetate using an anaerobic reactor microbiome. They were able to produce this in a batch process upon addition of biochar and 2-bromoethanesulfonate [90]. The maximum n-caproate selectivity was lower (65.0 mol e %) than the maximum n-caproate selectivity in the present study (76.5 mol e %).

The studies by Zhu et al. (2015), and by Liu et al. (2017) already showed that high n-caproate concentrations (>20 g/L) can be reached using anaerobic reactor microbiomes. However, they were using synthetic media and batch systems. As such, the present study does not only show that such high concentrations can be obtained from organic residues, it also shows that this can be obtained in a continuous process and without the use of bioactive compounds such as 2-bromoethanesulfonate. The organic residue that was used, food waste, is a suitable substrate for MCFA production not only because such conversion was recently subjected to a life cycle assessment [35] but also because it is currently being developed to a demonstration factory, processing ~40 ton / day, by ChainCraft in Amsterdam, the Netherlands.

4.4.2 Why was reactor performance so much better at long HRT than at short HRT?

The performance of the chain elongation process was far better at long HRT than at short HRT. A long HRT did not only result in a higher concentration of MCFAs, it also led to a lower rate of syntrophic ethanol oxidation, a net n-butyrate consumption instead of production, and to less NaOH consumption for pH correction. Why was reactor performance so much better at long HRT?

The difference in MCFA concentration can be explained as follows: at long HRT, the microbiome had sufficient time to accumulate MCFAs while these products were washed out (as effluent) at a relatively low rate. This resulted in a high caproate concentration (23.4 ± 1.1 g/L). Vice versa, at short HRT, the microbiome had little time to accumulate MCFAs while these products were washed out at a relatively high rate. This resulted in a considerably lower caproate concentration (7.1 ± 0.9 g/L). Because production of n-caproate occurred at the same volumetric production rate at both long and short HRT (~5.5 g/L/d), it is a logical consequence that n-caproate reached a higher concentration at long HRT than at short HRT. The high n-caproate concentration could also be achieved because the process was not limited by availability of substrates as sufficient ethanol (2.8 ± 1.1 g/L), acetate (4.2 ± 0.8 g/L) and n-butyrate (5.6 ± 0.6 g/L) was observed in the reactor. At short HRT, however, substantially more ethanol (20.1 ± 1.6 g/L), acetate (7.3 ± 0.5 g/L) and n-butyrate (10.8 ± 1.0 g/L) was observed but no higher MCFA production rates. This seems to be limited by the biomass concentration or by the high (i.e. inhibitory) ethanol concentration [57].

Syntrophic ethanol oxidation was more limited at long HRT than at short HRT. Two explanations can be given: firstly, the low ethanol concentration at long HRT may have resulted in a low rate of EEO. Vice versa, the high ethanol concentration at short HRT may have resulted in a high rate of EEO. However, a previous chain elongation study showed that ethanol loading rate and ethanol concentration does not substantially influence reactor performance as long as ethanol is not depleted [88]. Secondly, the high MCFA concentration may have caused an inhibitory effect on (one of) the involved competing syntrophs (i.e. ethanol oxidizers and hydrogenotrophic methanogens). It is known that undissociated MCFAs are toxic to microorganisms because they can damage the cell membrane [95]. The average undissociated MCFA concentration at long HRT (at pH 6.8) was 0.27 g/L. Ge et

al. (2015) determined that chain elongation proceeds until a toxic limit of 0.87 g/L undissociated n-caproic acid is reached [56] although recent work demonstrated chain elongation activity up to 1.46 g/L undissociated n-caproic acid [31]. Because chain elongating microorganisms were producing MCFAs at ~5.8 g/L/d in the present study, evidently these organisms were not rigorously inhibited by the undissociated MCFAs. It is well possible, however, that these undissociated MCFAs (at 0.27 g/L) were selectively inhibitory to either ethanol oxidizers or hydrogenotrophic methanogens. This would explain the limited rate of syntrophic ethanol oxidation at long HRT compared to a short HRT while chain elongation could proceed at a similar rate at both HRTs. It is also possible that the dissociated form of n-caproate was selectively inhibitory to one of the syntrophs. This means that dissociated n-caproate (i.e. the conjugate base) becomes toxic to ethanol oxidizers or hydrogenotrophic methanogens at a concentration around 20 g/L.

The data is not consistent to point out whether hydrogenotrophic methanogens or ethanol oxidizers were more inhibited at long HRT: whereas the first steady state at long HRT (day 28 to day 58) had a pH_2 below the detection limit of the gas chromatograph (< 0.1 %), the second steady state at long HRT (day 138 to day 147) had a pH_2 of up to 30 %. This means that the data from the first steady state suggests that ethanol oxidizers were more inhibited whereas data from the second steady state suggests that hydrogenotrophic methanogens were more inhibited. To what extent n-caproic acid and n-caproate is toxic to hydrogenotrophic methanogens and ethanol oxidizers could be elucidated in further studies. In any way, irrespective how syntrophic ethanol oxidation was limited, it is clear from the results that longer HRTs should be applied in chain elongation processes at near-neutral pH to allow n-caproate accumulation and to limit the rate of syntrophic ethanol oxidation. This limited rate of syntrophic ethanol oxidation results in a more efficient use of ethanol, more VFA consumption and in less base addition for pH control and as such, in a more effective chain elongation process.

4.4.3 Methanogenic UASB sludge can acclimate into a reactor microbiome that is able to produce n-caproate at high concentrations

This study can be compared with a previous study [27]. Both studies focused on two-stage MCFA production from organic residues and ethanol using anaerobic reactor microbiomes. In the previous study, a continuous chain elongation process was operated at similar pH (6.5 - 7.0) but at shorter HRT than in the present

study (11 h instead of 1 and 4 d). This resulted in a lower maximum n-caproate concentration (12.6 g/L) and selectivity (72.0 mol e %). Besides, n-butyrate was produced instead of consumed, indicating that the process was not efficient in ethanol use. A hypothesis is that the process in the previous study could have performed better, including a high n-caproate concentration, if both the HRT and the ethanol concentration in the influent were increased. Of course, the origin of the inoculum may also have an effect on reactor performance because this determines which pathways or microorganisms are introduced and to what extent the initial microbiome is acclimated. The inoculum used by Grootscholten et al. (2014) and also the inoculum used in the present study were both eventually derived from a study executed by Steinbusch et al. (2010), who used granular sludge from an upflow anaerobic sludge blanket (UASB) reactor treating brewery wastewater [23]. This shows that high n-caproate concentrations can be obtained using various types of inocula and not only with mature pit mud (e.g. ref [34]) or with mesophilic sludge from an anaerobic reactor treating paper mill wastewater (e.g. ref [90]). Under the right circumstances (e.g. as described in this study), UASB sludge from a methanogenic reactor will likely acclimate within a matter of weeks to a reactor microbiome that is able to produce n-caproate at high concentrations (> 20 g/L).

4.4.4 Consumption of food waste, ethanol and base in the overall two-stage system

In this study, MCFAs were produced from food waste and ethanol using a two-stage system. In the hydrolysis and acidogenesis stage, part of the food waste was converted into VFAs while some MCFAs were also produced. In the chain elongation stage, a part of the VFAs from the hydrolysis and acidogenesis stage were converted with additional ethanol into MCFAs while some ethanol was also used for ethanol upgrading. Both stages required NaOH addition to keep the pH constant in the reactors.

Based on the results of this study it was possible to calculate how much food waste (expressed as g VS), ethanol and NaOH would be consumed to yield 1000 g MCFAs. This was done for two scenarios; at long and at short HRT in the chain elongation stage. Equations are shown in Table S4.3. Parameters that were used as input for the equations are shown in Table S4.4 and were based on:

I)   Observed conversions and average NaOH consumption in the hydrolysis and acidogenesis stage (VFA yield on VS, MCFA yield on VS, consumed NaOH per consumed VS)

II)   Observed steady state conversions and NaOH consumption in the chain elongation stage (consumed VFAs per produced MCFAs, consumed ethanol per produced MCFAs, consumed NaOH per consumed ethanol)

III)   Average MCFA composition in the chain elongation stage (average carbon atoms per produced MCFAs, average molar weight of produced MCFAs)

A graphical representation on how much food waste (in g VS), ethanol and NaOH would be consumed to yield 1000 g MCFAs at long and short HRT in the chain elongation stage is shown in Figure 4.2.
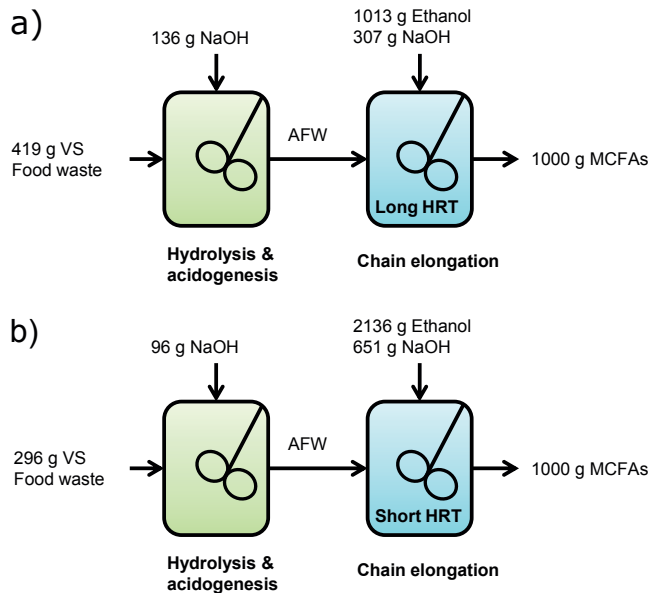

Figure 4.2: Graphical representation on how much food waste (g VS), ethanol and NaOH would be consumed to yield 1000 g MCFAs in the two-stage system at long HRT (a) and at short HRT (b) in the chain elongation stage.

To produce 1000 g MCFAs, the two-stage system with a long HRT in the chain elongation stage would consume 53 % less ethanol, 41 % less NaOH and 42 % more VS compared to a two-stage system with a short HRT in the chain elongation stage. This does not only show that a long HRT in the chain elongation stage result in a more efficient consumption of ethanol and base in the chain elongation stage itself, it also shows that base consumption is hereby reduced in the overall two-stage system. Unfortunately, such quantification on waste-use and chemical-use is not common in chain elongation studies to date.

Addition of ethanol could be minimized or even completely avoided by steering the hydrolysis and acidogenesis stage to MCFAs and/or lactate production. In this study, for example, 1.6 g/L n-caproate was produced in the hydrolysis and acidogenesis stage without addition of an external electron donor. Lim et al. (2008) also demonstrated production of n-caproate (up to 5 g/L) from food waste without an external electron donor [96]. Xu et al. (2017) demonstrated conversion of acid whey waste into MCFAs via lactate [30] using a two-stage system; also without an external electron donor. This shows that the effectiveness of MCFA production processes from diverse organic waste streams can be further improved by optimizing the hydrolysis and acidogenesis stage. Studies should also report on how much base or acid or electricity was used for pH control for a better comparison in terms of effectiveness.

Chemical base consumption could be fully eliminated through membrane electrolysis using electricity and separation of fatty acids, as was demonstrated by Anderson et al. (2015) [97]. They fermented thin stillage into VFAs and MCFAs using a membrane electrolysis system and no chemical pH control. Such system, however, consumes a substantial amount of energy. Based on their experiments, they estimated a power input of 2 kWh per produced kg $COD_{fatty\ acids}$. The developed two-stage system in the present study, at long HRT, consumed 0.22 kg NaOH per produced kg $COD_{fatty\ acids}$. Assuming an electricity consumption of 3 kWh/kg NaOH via the chloralkali process [98], the two-stage system would require less energy for pH control per produced kg COD (0.67 kWh / kg $COD_{fatty\ acids}$) compared to the in-site membrane electrolysis system. However, whereas the membrane electrolysis system already separated fatty acids from the fermentation broth, the two-stage system would require an additional product separation step to be comparable in electricity consumption.

Effective MCFA production from organic waste can be further developed by reducing the need for chemicals and/or electricity. Possibly, also water-use can be reduced too since the two-stage system used a substantial amount of water to dilute the waste before use as fermentation feed. The presented scenario in the present study, as well as the mentioned alternative scenarios (e.g. ref [96], [30] and [97]) can be optimized and assessed with a case-specific life cycle assessment to make a complete justified discussion on the total environmental impact.

4.4.5 Future outlook

In a previous study, it was shown that EEO in a chain elongation process can be limited to 15.9 % of total ethanol consumption by reducing the CO_2 loading rate to 0.5 L_{CO2}/L/d [88]. In the present study, an alternative strategy to suppress EEO is provided: by applying a long HRT, EEO was limited to a similar extent (14.7 %). A major advantage of this strategy is that the n-caproate concentration can become much higher. By further increasing the HRT possibly higher n-caproate concentrations can be reached. This could potentially lead to even more limited rate of EEO and thus base consumption in the chain elongation process. Of course, this is only feasible when the process is not limited in substrates (ethanol and VFAs) and CO_2.

Based on this study and the availability of 88 million ton wet food waste per year in the European Union [6], the developed process has the prospects to produce 29 million ton MCFAs per year. This was calculated using the ratios in Figure 4.2 (at long HRT) and by assuming that wet food waste has the same VS content as in this study; calculations are shown in the Supporting information. The required ethanol (~311 million barrels) would be 37 % of total annual global ethanol production (~844 million barrels [99]). The required electrical power for NaOH production (38.4 tWh) would be 13 % of total annual wind energy production in Europe (305.8 tWh [100]). After selective extraction of the MCFAs, they can be further processed into a fuel (i.e. a mixture of hydrocarbons) via Kolbe electrolysis [85] [101]. Assuming no losses during extraction and a theoretical efficiency of 0.61 $g_{hydrocarbons}/g_{MCFA}$ in the Kolbe electrolysis process and a fuel density of 0.73 g/cm^3, it is possible to produce ~202 million barrels of fuel per year. This is approximately 7 % of the nowadays annual aviation fuel consumption (~2710 million barrels [102]).

4.5   Supporting Information

Table S4.1: Mean steady state values at long HRT (day 28 - 58).

Compound	Concentration [mmol·L^{-1}]	Rate [mmol·L^{-1}·d^{-1}]	Selectivity [mol e %]	Selectivity [mol C %]
Ethanol	61.4 ± 23.6	-130.8 ± 6.9	N.A.	N.A.
Propanol	1.1 ± 1.0	0.3 ± 0.3	0.3	0.2
Acetate	70.6 ± 12.9	-15.9 ± 2.9	N.A.	N.A.
Propionate	6.0 ± 0.8	-4.5 ± 0.1	N.A.	N.A.
Isobutyrate	5.4 ± 0.5	-0.4 ± 0.1	N.A.	N.A.
n-Butyrate	64.1 ± 7.3	-9.9 ± 1.6	N.A.	N.A.
Isovalerate	3.8 ± 0.3	-0.1 ± 0.1	N.A.	N.A.
n-Valerate	16.2 ± 4.4	3.0 ± 1.2	3.9	4.0
Isocaproate	0.9 ± 0.2	0.2 ± 0.1	0.4	0.4
n-Caproate	201.3 ± 8.7	47.1 ± 3.1	76.5	76.2
n-Heptanoate	4.3 ± 1.7	1.1 ± 0.4	2.1	2.0
n-Caprylate	4.7 ± 1.0	1.2 ± 0.3	2.6	2.5
CO_2	52.7 ± 20.1 % *	-22.1 ± 1.8	N.A.	N.A.
CH_4	37.7 ± 14.7 % *	12.8 ± 2.6	5.2	3.5
H_2	<0.1 % *		N.A.	N.A.
Unidentified			9.1	11.2

Table S4.2: Mean steady state values at short HRT (day 79 - 103).

Compound	Concentration [mmol·L^{-1}]	Rate [mmol·L^{-1}·d^{-1}]	Selectivity [mol e %]	Selectivity [mol C %]
Ethanol	437.3 ± 34.0	-267.6 ± 23.5	N.A.	N.A.
Propanol	0.7 ± 0.9	0.7 ± 0.9	0.4	0.3
Acetate	122.1 ± 8.6	-13.1 ± 8.3	N.A.	N.A.
Propionate	15.5 ± 1.0	-9.2 ± 1.5	N.A.	N.A.
Isobutyrate	6.2 ± 0.4	-0.9 ± 0.4	N.A.	N.A.
n-Butyrate	122.8 ± 11.3	18.3 ± 12.4	11.0	12.1
Isovalerate	4.0 ± 0.3	-0.5 ± 0.3	N.A.	N.A.
n-Valerate	9.4 ± 1.1	4.3 ± 0.9	3.2	3.4
Isocaproate	0.4 ± 0.1	0.4 ± 0.1	0.4	0.4
n-Caproate	60.7 ± 7.8	48.1 ± 7.5	44.6	46.0
n-Heptanoate	0.6 ± 0.1	0.6 ± 0.1	0.6	0.6
n-Caprylate	0.5 ± 0.1	0.5 ± 0.1	0.7	0.7
CO_2	5.4 ± 3.0 % *	-37.2 ± 0.1	N.A.	N.A.
CH_4	77.0 ± 42.0 % *	43.8 ± 2.5	10.2	7.0
H_2	<0.1 % *		N.A.	N.A.
Unidentified			29.0	29.5

* Concentrations of gaseous compounds (CO_2, CH_4, H_2) are shown as percentage in the headspace at 1 atm.

Table S4.3: Equations to determine how much food waste (FW; expressed in g volatile solids), ethanol (EtOH) and sodium hydroxide (NaOH) would be consumed to yield 1000 g MCFAs in the two-stage system.

Compound	Unit	Equation
Food waste (FW)	g VS	$FW = \left(\dfrac{1000 \text{ g MCFA}}{\overline{MW}_{MCFA}} \cdot \bar{C}_{MCFA} - Y_{\frac{MCFA}{FW}} \cdot FW \right) \cdot \left| \dfrac{r_{VFA}}{r_{MCFA}} \right| \cdot \dfrac{1}{Y_{\frac{VFA}{FW}}}$
Ethanol (EtOH)	g	$EtOH = \left(\dfrac{1000 \text{ g MCFA}}{\overline{MW}_{MCFA}} \cdot \bar{C}_{MCFA} - Y_{\frac{MCFA}{FW}} \cdot FW \right) \cdot \left| \dfrac{r_{EtOH}}{r_{MCFA}} \right| \cdot \dfrac{MW_{EtOH}}{C_{EtOH}}$
NaOH (Hydrolysis and acidogenesis stage)	g	$NaOH = FW \cdot \dfrac{\Delta NaOH}{\Delta FW}$
NaOH (Chain elongation stage)	g	$NaOH = EtOH \cdot \dfrac{r_{NaOH}}{r_{EtOH}}$

Table S4.4: Parameters that we used as input for the equations in Table S4.3 to determine how much food waste (in g VS), ethanol (EtOH) and sodium hydroxide (NaOH) would be consumed to yield 1000 g MCFAs in the two-stage system.

Parameter description	Symbol	unit	Value HRT = 4 d	Value HRT = 1 d
Hydrolysis and acidification stage				
VFA yield on FW	$Y_{\frac{VFA}{FW}}$	mol C/g VS	$35.14 \cdot 10^{-3}$	$35.14 \cdot 10^{-3}$
MCFA yield on FW	$Y_{\frac{MCFA}{FW}}$	mol C/g VS	$3.39 \cdot 10^{-3}$	$3.39 \cdot 10^{-3}$
Consumed NaOH per consumed FW	$\dfrac{\Delta NaOH}{\Delta FW}$	g/g VS	0.32	0.32
Chain elongation stage [i]				
Consumed VFAs per produced MCFAs	$\dfrac{r_{VFA}}{r_{MCFA}}$	mol C/mol C	0.29	0.20
Consumed ethanol per produced MCFAs	$\dfrac{r_{EtOH}}{r_{MCFA}}$	mol C/mol C	0.87	1.83
Average carbon atoms per produced MCFAs	$\bar{C}_{MCFA}$	C-atoms/mol	6.07	6.03
Average molar weight of produced MCFAs	$\overline{MW}_{MCFA}$	g/mol	117.13	116.61
Consumed NaOH per consumed ethanol	$\dfrac{r_{NaOH}}{r_{EtOH}}$	g/g	0.30	0.30
Constants				
Molar weight of ethanol	MW_{EtOH}	g/mol	46.07	46.07
Carbon atoms per mole ethanol	C_{EtOH}	C-atoms/mol	2	2

[i] Values are based on steady state data.

Future Outlook: Calculations

MCFA production from wet food waste:

88 mln ton wet food waste / yr · (13.8 g VS / 100 g wet food waste)[i] · (1000 g MCFAs / 419 g VS)[i] = 28.9 mln ton MCFAs / yr

Required ethanol for MCFA production:

29 mln ton MCFAs / yr · 1000 · (1013 g ethanol / 1000 g MCFA)[i] / (0.789 kg / L) / (119.2 L / barrel) = 311.1 mln barrels ethanol / yr

Required NaOH for MCFA production:

29 mln ton MCFAs / yr · ((136 g NaOH + 307 g NaOH) / 1000 g MCFA)[1] = 12.8 mln ton NaOH / yr

Required electricity to produce NaOH for MCFA production:

12.8 mln ton NaOH / yr · (3 kWh / kg NaOH)[ii] = 38.4 · 1000 mln kW h / yr = 38.4 TW h / yr

Fuel production from MCFAs:

29 mln ton MCFAs / yr · 1000 · (0.61 g hydrocarbon / g MCFA)[iii] / (0.73 kg / L)[iii] / (119.2 L / barrel) = 202 mln barrels fuel / yr

[i] Values based on this study (Figure 4.2)
[ii] Electricity consumption through the Chlorialkali process
[iii] Assumption / theoretical efficiency
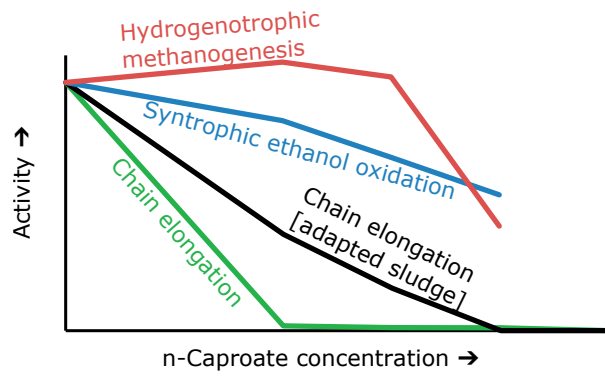
CHAPTER 5

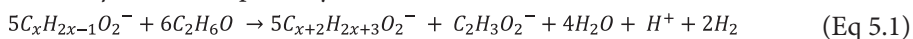# Effect of n-Caproate Concentration on Chain Elongation and Competing Processes

Abstract

Chain elongation is an open-culture fermentation process that facilitates conversion of organic residues with an additional electron donor, such as ethanol, into valuable n-caproate. Open-culture processes are catalyzed by an undefined consortium of microorganisms which typically also bring undesired (competing) processes. Inhibition of competing processes, such as syntrophic ethanol oxidation, will lead to a more selective n-caproate production process. In this study, we investigated the effect of n-caproate concentration on the specific activity of chain elongation and competing processes using batch inhibition assays. With 'synthetic medium sludge' (originally operating at 3.4 g/L n-caproate), syntrophic ethanol oxidation was proportionally inhibited by n-caproate until 45 % inhibition at 20 g/L n-caproate. Hydrogenotrophic methanogenesis was for 58 % inhibited at 20 g/L n-caproate. Chain elongation of volatile fatty acids (volatile fatty acid upgrading; the desired process), was completely inhibited at 20 g/L n-caproate with all tested sludge types. 'Adapted sludge' (operating at 23.2 g/L n-caproate) showed a 10 times higher volatile fatty acid upgrading activity at 15 g/L n-caproate compared to 'non-adapted sludge' (operating at 7.1 g/L n-caproate). This shows that open cultures do adapt to perform chain elongation at high n-caproate concentrations which likely inhibits syntrophic ethanol oxidation through hydrogenotrophic methanogenesis. As such, we provide supporting evidence that the formation of n-caproate inhibits syntrophic ethanol oxidation which leads to a more selective medium chain fatty acid production process.

5.1 Introduction

Organic residual streams, such as food waste, have great potential as alternative resource for production of fuels and chemicals. These residues are conventionally anaerobically digested to produce methane for electric power and/or heat production [17]. Methane, however, has a low monetary value. Producing higher-value products than methane, therefore, is gaining increasing interest. Among these higher-value products, particularly medium chain fatty acids (MCFAs), such as caproic acid and heptanoic acid are interesting because MCFAs can be used for a wide variety of applications (e.g. aviation fuels, lubricants, feed additives). Moreover, like methane, MCFAs are also produced through open-culture anaerobic reactor microbiomes. Open-culture processes are catalysed by an undefined consortium of microorganisms. This is different from pure culture or defined co-culture processes, which are catalysed by only one (or more) known species with known pathways. The advantage of open-culture processes is that they handle a mixture of residual streams without the need for sterilisation. The technological challenge is to control the mixed microbial population within the microbiome to produce MCFAs selectively from the substrates.

MCFA production from organic residues by open-cultures occurs via two subsequent processes which can be combined or performed separately. First, organic residues are hydrolysed by hydrolytic enzymes and acidified by acidogenic bacteria, resulting in production of volatile fatty acids (VFAs) such as acetate, propionate and butyrate. Second, these VFAs are converted together with an electron donor, such as ethanol, into MCFAs through chain elongation. This conversion is performed by chain elongating micro-organisms (e.g. *Clostridium kluyveri*) that use the reverse β-oxidation pathway (Eq 5.1) [21]. Chain elongation with open cultures is an emerging application that can handle many organic feedstocks at various conditions and reactor configurations [18].

Reverse β-oxidation pathway:

$$5C_xH_{2x-1}O_2^- + 6C_2H_6O \rightarrow 5C_{x+2}H_{2x+3}O_2^- + C_2H_3O_2^- + 4H_2O + H^+ + 2H_2 \qquad \text{(Eq 5.1)}$$

Here, we focus on ethanol-based chain elongation which is catalyzed by anaerobic open-cultures. These open-cultures include not only chain elongating microorganisms but also other functional groups of microorganisms. These other functional groups

can degrade the substrates and products into undesired metabolites. This makes their presence and activity detrimental to the MCFA selectivity of chain elongation processes. The challenge, therefore, is to find process conditions that reduce their activity through a selection pressure like inhibition. Inhibition is preferably performed without the use of bioactive chemicals (e.g. 2-bromoethanesulfonate or iodoform as methanogenic inhibitor) so that the non-converted organics from the process can be used as soil fertilizer upon composting. We recognize the following competing processes in chain elongation [27] [88]:

Acetotrophic methanogenesis:
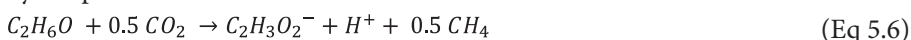$$C_2H_3O_2^- + H^+ \rightarrow CH_4 + CO_2 \qquad \text{(Eq 5.2)}$$

Anaerobic acetate oxidation:
$$C_2H_3O_2^- + H^+ + 2H_2O \rightarrow 4H_2 + 2CO_2 \qquad \text{(Eq 5.3)}$$

Excessive ethanol oxidation (EEO)
$$C_2H_6O + H_2O \rightarrow C_2H_3O_2^- + H^+ + 2H_2 \qquad \text{(Eq 5.4)}$$

Hydrogenotrophic methanogenesis
$$2H_2 + 0.5CO_2 \rightarrow 0.5CH_4 + H_2O \qquad \text{(Eq 5.5)}$$

Syntrophic ethanol oxidation:
$$C_2H_6O + 0.5\,CO_2 \rightarrow C_2H_3O_2^- + H^+ + 0.5\,CH_4 \qquad \text{(Eq 5.6)}$$

Understanding the role of competing processes and how they can be suppressed is essential to establish a selective MCFA production process. For example, acetotrophic methanogenesis degrades acetate into methane and CO_2 (Eq 5.2). This process is performed by acetotrophic methanogens. Acetotrophic methanogenesis was shown to be largely inhibited at slightly acidic pH (5.5) in chain elongating processes [19]. When working at near-neutral pH, which is more favorable for these methanogens, they could be outselected by applying a combination of sufficient hydraulic shear force and a low hydraulic retention time (HRT) to respectively detach and wash out these slow-growing methanogens [24]. Anaerobic oxidation of fatty acids occurs though β-oxidation of fatty acids into acetate and hydrogen (and also CO_2 in the case of propionate oxidation). Acetate can be further oxidized into CO_2 and hydrogen (Eq 5.3). Anaerobic oxidation of

fatty acids is performed by acetogenic bacteria and can be thermodynamically inhibited at a hydrogen partial pressure (pH$_2$) of >0.007 % at standard conditions [88]. Excessive ethanol oxidation (EEO) occurs through direct anaerobic oxidation of ethanol into acetate and hydrogen (Eq 5.4). This process is considered to be performed by ethanol-oxidizing microorganisms which do not perform chain elongation. Suppression of EEO is important not only because this process leads to an inefficient use of ethanol but also because it acidifies the fermentation broth. Because of this acidifying effect, EEO requires extra base addition which increases operating expenses [103]. EEO can be thermodynamically inhibited at a hydrogen partial pressure (pH$_2$) of ≥ 14 % at standard conditions [88]. Such high pH$_2$ pressures, however, are not common in chain elongation processes because hydrogen is typically consumed through hydrogenotrophic methanogenesis (Eq 5.5). In our previous study [88], we showed that EEO and hydrogenotrophic methanogenesis are coupled processes. The overall reaction can be referred to as syntrophic ethanol oxidation (Eq 5.6). Syntrophic ethanol oxidation can be limited by reducing the available amount of CO_2. This has been shown to limit hydrogenotrophic methanogenic activity and the resulting higher pH$_2$ thermodynamically inhibits EEO [27] [29] [103]. CO_2 loading rate may be difficult to control, however, when working with (hydrolyzed and acidified) organic residues. This is because CO_2 is produced during acidification of hydrolyzed residues and the presence of this CO_2 in the feed may complicate the actual CO_2 supply to the chain elongation process. Even though acidification and chain elongation can be separated, dissolved CO_2 could still complicate the control over the actual CO_2 supply. As such, alternative methods to limit EEO in chain elongation are needed.

In a previous study, an alternative method to inhibit EEO may have been shown; by operating a continuous chain elongation process at long HRT (4 d), EEO was limited to 0.9 g/L/d (14.7 % of total ethanol consumption) while n-caproate was produced at a high concentration (23.4 g/L) [103]. In contrast, at short HRT (1 d), EEO occurred at a higher rate (5.6 g/L/d; 45.0 % of total ethanol consumption) while n-caproate was produced at a lower concentration (7.1 g/L). A hypothesis is that the high n-caproate concentration may have had a selective inhibitory effect on one of the competing syntrophs (ethanol oxidizers or hydrogenotrophic methanogens). Note that we refer to n-caproate as both forms together, undissociated n-caproic acid and dissociated n-caproate, and that we refer to each specific form when appropriate.

It is well known that MCFAs are toxic to microorganisms because they can damage the cell membrane [95]. Gram-positive bacteria and methanogens tend to be more easily inhibited by long chain fatty acids (LCFAs) than Gram-negative bacteria [104]. Selective inhibition of MCFAs on competing functional groups of microorganisms may be an alternative strategy to suppress competing processes to enhance the MCFA selectivity. High MCFAs concentrations, however, may also inhibit chain elongation itself. To circumvent potential MCFA toxicity, *in situ* MCFA extraction was applied which showed to enhance n-caproate production [56]. These results were used to clarify that MCFAs inhibit chain elongating microorganisms. A systematic investigation of the inhibitory effect of n-caproate on chain elongation and competing processes in chain elongation microbiomes has not been reported to date.

In this study, we investigated the effect of n-caproate concentration on the specific activities of chain elongation microbiomes in two experiments. Firstly, we studied the effect of n-caproate on the specific activity of five processes: 1) chain elongation (VFA upgrading), 2) syntrophic ethanol oxidation, 3) hydrogenotrophic methanogenesis, 4) acetotrophic methanogenesis, and 5) anaerobic acetate oxidation. This was performed using sludge from a continuous chain elongation process that operated at 3.4 g/L n-caproate. Secondly, we extended the experiment for chain elongation comparing two types of sludge to study the potential adaptation of chain elongation microbiomes to high n-caproate concentrations. One sludge type originally operated at 7.1 g/L caproate (non-adapted sludge) whereas the other sludge type originally operated at 23.2 g/L n-caproate (adapted sludge).

5.2 Materials and methods

An overview of the experimental design is reported in Table 5.1.

5.2.1 Media preparation

All liquid media were initially prepared the same way by adding salts, vitamins, trace elements and yeast extract to deoxygenated water [53]. For $NH_4(H_2)PO_4$, we used 1.8 g/L instead of 3.6 g/L. Buffering agents were also added: 200 mM MES (VWR, the Netherlands), 200 mM BISTRIS (Sigma-Aldrich, the Netherlands) and 10 mM PIPPS (98.4 %, Merck Millipore, USA). For the first experiment, five different media were prepared. Thus, after buffers were added, the mixture was divided into five fractions. The fraction used to monitor chain elongation (VFA upgrading) was supplemented with 11.5 g/L ethanol (Absolute, VWR, France) and 3 g/L propionic acid ($\geq$ 99.5 %, Sigma-Aldrich). With this ethanol concentration, ethanol toxicity is avoided [57]. The fraction used to monitor syntrophic ethanol oxidation was supplemented with 11.5 g/L ethanol. The fraction used to monitor acetotrophic methanogenesis and anaerobic acetate oxidation was supplemented with 2 g/L acetic acid (99.9 %, VWR, France). The fraction used to monitor hydrogenotrophic methanogenesis was not supplemented with a substrate. Each fraction used to monitor a specific process was again divided into 4 smaller fractions to add n-caproic acid ($\geq$ 98 %, Sigma-Aldrich) to concentrations of 0 (control), 10, 15 and 20 g/L. For the second experiment, we added one assay in which n-caproic acid was added up to 25 g/L. Finally, the pH of all assays were adjusted to 6.8 with 5M NaOH.

5.2.2 Methods

Batch inhibition assays were performed in 125 or 250 mL serum bottles. The bottles were filled with 45.0 g medium under anaerobic conditions. After filling, bottles were closed with a rubber stopper and an aluminium crimp seal. The headspaces of the bottles for chain elongation (VFA upgrading), syntrophic ethanol oxidation, acetotrophic methanogenesis and anaerobic acetate oxidation were flushed and pressurized to 1.5 bar with a mixture of N_2/CO_2 (80/20 %). Likewise, the headspaces of the bottles for hydrogenotrophic methanogenesis were flushed and pressurized to 1.5 bar with a mixture of H_2/CO_2 (80/20 %). After preparation, bottles were inoculated with a fresh inoculum (5 mL) using a needle and syringe.

In the first experiment, bottles were inoculated with 'synthetic medium sludge'. Synthetic medium sludge was directly derived from a running continuous chain elongation process that converted synthetic substrates (propionate and ethanol) into MCFAs at 3.4 g/L n-caproate [53]. Based on a carbon flux analysis (e.g. ref [88]), we determined that synthetic medium sludge contained chain elongating microorganisms, ethanol oxidizers and hydrogenotrophic methanogens.

In the second experiment, bottles were inoculated with 'non-adapted sludge' or 'adapted sludge'. Both sludge types were directly derived from a running continuous chain elongation process that converted acidified food waste and ethanol into MCFAs [103]. Whereas non-adapted sludge operated at 7.1 g/L n-caproate (day 103), adapted sludge operated at 23.2 g/L n-caproate (day 124) [103]. Properties of the used inocula, including VSS concentrations, sodium concentrations, n-caproate concentrations and original average specific activities in reactor, are reported in Table 5.2. Specifications on process conditions that conditioned the inocula are reported in the supporting information.

After inoculation, bottles were incubated at 30 °C at 100 rpm in a rotary shaker (New Brunswick Scientific Innova 44). Contents of the bottles were daily analysed on headspace pressure, headspace composition, fatty acids and alcohols. All assays were conducted in duplicate.

5.2.3 Determination of specific activity

The activity of syntrophic ethanol oxidation, acetotrophic methanogenesis and hydrogenotrophic methanogenesis was based on the maximum slope of methane production vs. time divided by the initial VSS concentration. The activity of anaerobic acetate oxidation was based on the maximum slope of hydrogen production vs. time divided by the initial VSS concentration. The activity of chain elongation was based on the maximum slope of n-valerate plus n-heptanoate production vs. time divided by the initial VSS concentration. Chain elongation activity was based on the production of odd-numbered fatty acids and not on production of even-numbered fatty acids. This was performed to determine a measure of chain elongation activity that is independent of other active functional groups of microorganisms. Whereas odd-numbered fatty acids can only be produced through VFA upgrading (chain elongation of added VFAs), even-numbered fatty acids can also be produced through ethanol upgrading (*in situ* ethanol oxidation into

acetate and subsequent chain elongation into even-numbered fatty acids). Because ethanol upgrading is not only mediated by chain elongating microorganisms but also by ethanol oxidizers and hydrogenotrophic methanogens [88], we quantified only the odd numbered chain elongation products (n-valerate and n-heptanoate) by VFA upgrading as a measure for chain elongation activity.

Undissociated n-caproic acid concentrations were calculated from the observed n-caproate concentrations and pH values (during the maximum specific activity) using the Henderson-Hasselbalch equation.

5.2.4 Analytical techniques

Alcohols (C2-C6) and fatty acids (C2-C8) were analyzed by gas chromatography [105]. Gaseous compounds were determined by gas chromatography [106]. Sodium was measured by ion chromatography [107]. VSS measurements were performed in the same way as before [53].

5.3 Results

5.3.1 n-Caproate concentration affects chain elongation and competing processes using 'synthetic medium sludge'

The effect of n-caproate concentration on the maximum specific activities of various processes was investigated with 'synthetic medium sludge' as inoculum. Processes that were investigated were: VFA upgrading, syntrophic ethanol oxidation, hydrogenotrophic methanogenesis, acetotrophic methanogenesis and anaerobic acetate oxidation. Hereby we note that VFA upgrading is the desired chain elongation process that leads to a selective MCFA production process. Results of this batch inhibition assay that showed an effect of n-caproate are graphically summarized in Figure 5.1a and b. Numerical values of average specific activities are reported in Table 5.2 and profiles of product production are presented in the supporting information (Figures S5.1-5.3).

Table 5.1: Experimental design of batch inhibition assays.

Process studied in inhibition assay	Initial aqueous substrate(s) [g/L]	Initial headspace composition [vol %]	Activity based on production of	Inoculum	Initial n-caproate concentration [g/L]	Working volume/ Total bottle volume [mL]
VFA Upgrading	Ethanol [11.5] Propionate [3]	N_2/CO_2 [80/20]	n-Valerate and n-heptanoate	Synthetic medium sludge [iii]	0, 10, 15, 20	50 / 125
Syntrophic ethanol oxidation	Ethanol [11.5]	N_2/CO_2 [80/20]	Methane	Synthetic medium sludge [iii]	0, 10, 15, 20	50 / 125
Hydrogenotrophic methanogenesis	None	H_2/CO_2 [80/20]	Methane	Synthetic medium sludge [iii]	0, 10, 15, 20	50 / 250
Acetotrophic methanogenesis	Acetate [2]	N_2/CO_2 [80/20]	Methane [i]	Synthetic medium sludge [iii]	0, 10, 15, 20	50 / 125
Anaerobic acetate oxidation	Acetate [2]	N_2/CO_2 [80/20]	Hydrogen [ii]	Synthetic medium sludge [iii]	0, 10, 15, 20	50 / 125
VFA Upgrading	Ethanol [11.5] Propionate [3]	N_2/CO_2 [80/20]	n-Valerate and n-heptanoate	Non-adapted sludge [iv]	0, 10, 15, 20, 25	50 / 125
VFA Upgrading	Ethanol [11.5] Propionate [3]	N_2/CO_2 [80/20]	n-Valerate and n-heptanoate	Adapted sludge [v]	0, 10, 15, 20, 25	50 / 125

[i] Can only be quantified when anaerobic acetate oxidation and hydrogenotrophic methanogenesis do not occur.
[ii] Can only be quantified when acetotrophic methanogenesis and hydrogenotrophic methanogenesis do not occur.
[iii] Synthetic medium sludge was grown converting ethanol and propionate into MCFAs at 3.4 g/L caproate.
[iv] Non-adapted sludge was grown converting acidified food waste and ethanol into MCFAs at 7.1 g/L n-caproate.
[v] Adapted sludge was grown converting acidified food waste and ethanol into MCFAs at 23.2 g/L n-caproate.
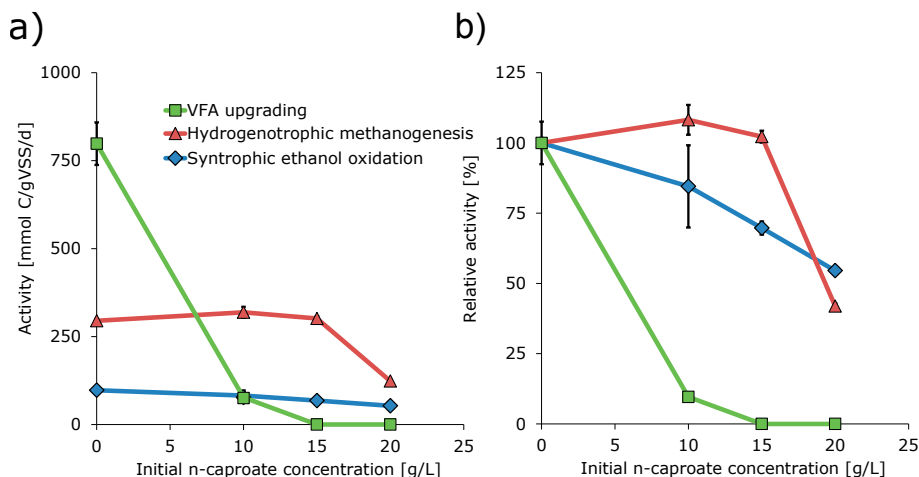
a)

b)

Figure 5.1: Results of batch inhibition assays; initial n-caproate concentration vs. observed activity (a) and relative activity (b) of various processes using synthetic medium sludge as inoculum. Synthetic medium sludge was grown converting synthetic substrates (propionate and ethanol) at 3.4 g/L n-caproate. Values indicate averages of duplicates and bars indicate range of duplicates (often too small to be visual). T = 30 °C, pH = 6.8 (buffered).

The effect of n-caproate on both acetotrophic methanogenesis and anaerobic acetate oxidation could not be determined because these processes did not occur in the controls (0 g/L n-caproate) or in the experimental assays. Likely, acetotrophic methanogens and acetogenic bacteria were not substantially present in the sludge.

Evidently, n-caproate inhibited all other quantified processes in the tested range (Figure 5.1). The activity of VFA upgrading (i.e. specific n-valerate plus n-heptanoate activity) in the control was 798 mmol C/gVSS/d and was for 90 % inhibited at 10 g/L n-caproate. Remarkably, at 15 and 20 g/L n-caproate, VFA upgrading was completely inhibited. VFA upgrading was the most sensitive process for n-caproate inhibition compared to syntrophic ethanol oxidation and hydrogenotrophic methanogenesis. The activity of syntrophic ethanol oxidation in the control was 97 mmol C/gVSS/d and was proportionally inhibited by n-caproate until 45 % inhibition at 20 g/L n-caproate. Syntrophic ethanol oxidation was the least sensitive process to n-caproate inhibition. Hydrogenotrophic methanogenic activity in the control was 295 mmol C/gVSS/d and was not inhibited at 10 and 15 g/L n-caproate. However, at a higher 20 g/L n-caproate, hydrogenotrophic methanogenesis was indeed inhibited with 58 %. Hydrogenotrophic methanogenic activity was always higher than the activity of syntrophic ethanol oxidation.

Up to 15 g/L n-caproate, the relative order of inhibition was VFA upgrading > syntrophic ethanol oxidation with no inhibition for hydrogenotrophic methanogenesis. Within this n-caproate concentration range, syntrophic ethanol oxidation was not limited by hydrogenotrophic methanogenesis. At 20 g/L n-caproate, the relative order of inhibition was VFA upgrading > hydrogenotrophic methanogenesis > syntrophic ethanol oxidation. At this n-caproate concentration, hydrogenotrophic methanogenesis was severely suppressed by n-caproate inhibition. This is in line with earlier work by Hajarnis et al. (1994) who found that pure cultures of hydrogenotrophic methanogens, *Methanobacterium bryantii* and *Methanobacterium formicium*, were inhibited for 96 and 95 % respectively by 20 g/L n-caproate at pH 7.0 [108]. By extrapolating our data, we estimate that, at 25 g/L n-caproate, syntrophic ethanol oxidation may become rate-limited by hydrogenotrophic methanogenesis. This extrapolation provides supportive evidence for the hypothesis that a high n-caproate concentration is a control strategy to suppress syntrophic ethanol oxidation through hydrogenotrophic methanogenesis in chain elongation processes. At high n-caproate concentrations, however, chain elongation itself may also be inhibited; though ethanol may be used more efficiently, as was shown in our previous study [103].

It was remarkable that at 15 and 20 g/L n-caproate, VFA upgrading was not observed, which shows that chain elongating microorganisms were completely inhibited by n-caproate. Previous studies, however, reported chain elongation activity up to considerably higher n-caproate concentrations (i.e. 21 g/L [90], 23 g/L [34] and even up to 25 g/L [103] at similar pH). Probably, the sludge that we used as inoculum was not adapted to such high n-caproate concentrations. The actual inoculum, 'synthetic medium sludge', was indeed derived from a running chain elongation process with a lower n-caproate concentration (3.4 g/L) than that was present in the experimental assays at 15 and 20 g/L n-caproate. Therefore, the sudden increase of n-caproate during inoculation may have resulted in an acute toxic effect to the chain elongating microorganisms.

5.3.2 Comparing VFA upgrading using non-adapted sludge and adapted sludge

To investigate whether sludge can be adapted to perform VFA upgrading (i.e. chain elongation) at high n-caproate concentrations, a follow-up experiment was performed. In this experiment, VFA upgrading activity was compared using an

inoculum that operated at low n-caproate concentration (7.1 g/L; non-adapted sludge) with an inoculum that operated at high n-caproate concentration (23.2 g/L; adapted sludge). Results of this experiment are graphically summarized in Figure 5.2. Numerical values on average specific activities are reported in Table 5.2 and profiles of product production are reported in the supporting information (Figure S5.4 and S5.5). At 10 g/L n-caproate, VFA upgrading activity was a factor 14 higher with adapted sludge (411 mmol C/gVSS/d) than with non-adapted sludge. At 15 g/L, VFA upgrading activity was a factor 10 higher with adapted sludge (181 mmol C/gVSS/d) than with non-adapted sludge. These figures show that the n-caproate tolerance of VFA upgrading activity was clearly increased with adapted sludge. However, at 20 g/L n-caproate the VFA upgrading process was completely inhibited with both adapted sludge and non-adapted sludge.
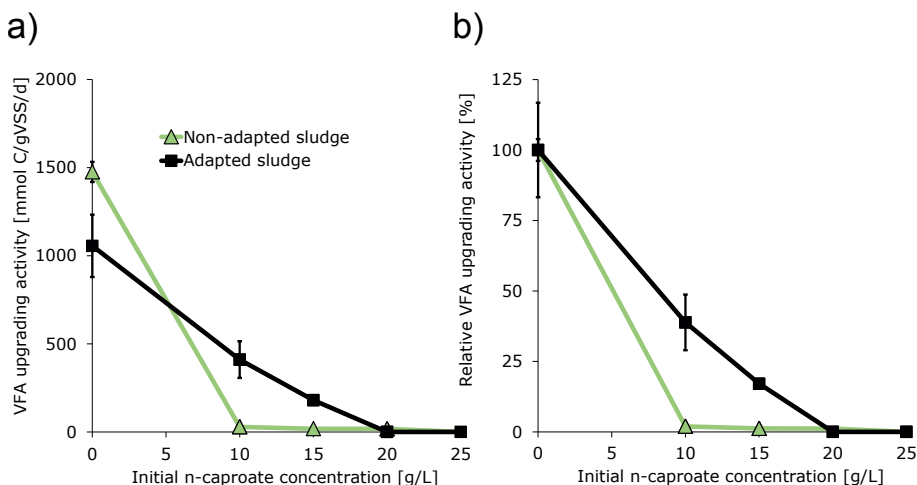

Figure 5.2: Results of batch inhibition assays; initial n-caproate concentration vs. observed activity (a) and relative activity (b) of VFA upgrading using non-adapted and adapted sludge as inoculum. Non-adapted sludge was grown converting acidified food waste and ethanol into MCFAs at 7.1 g/L n-caproate. Adapted sludge was grown converting acidified food waste and ethanol into MCFAs at 23.2 g/L n-caproate. Values indicate averages of duplicates and bars indicate range of duplicates (often too small to be visual). T = 30 °C, pH = 6.8 (buffered).

Table 5.2: Inoculum specifications, average specific activities in batch assays and observed sodium and undissociated n-caproic acid concentrations in batch assays.

| Process | Inoculum name, compounds in inoculum [g/L] and original average specific activity of inoculum in reactor [mmol C/gVSS/d] | | | | | Average specific activity in batch assays [mmol C/gVSS/d] at different initial n-caproate concentrations [g/L]. | | | | |
	Inoculum name	VSS	Sodium	n-Caproate	Activity [iii]	0	10	15	20	25
VFA Upgrading	Synthetic medium sludge	0.6	6.1 ± 0.5	3.4 ± 0.3	1362 ± 106	798	77	0	0	ND
Syntrophic ethanol oxidation	Synthetic medium sludge	0.6	6.1 ± 0.5	3.4 ± 0.3	59 ± 11	97	82	68	53	ND
Hydrogenotrophic methanogenesis	Synthetic medium sludge	0.6	6.1 ± 0.5	3.4 ± 0.3	59 ± 11	295	319	301	124	ND
Acetotrophic methanogenesis	Synthetic medium sludge	0.6	6.1 ± 0.5	3.4 ± 0.3	ND	0	0	0	0	0
Anaerobic acetate oxidation	Synthetic medium sludge	0.6	6.1 ± 0.5	3.4 ± 0.3	ND	0	0	0	0	0
VFA Upgrading	Non-adapted sludge	0.4	7.0 ± 0.0	7.1 ± 0.9	220 ± 95	1476	29	18	17	0
VFA Upgrading	Adapted sludge	0.5	9.1 ± 0.5	23.2 ± 1.9	386 ± 76	1056	411	181	0	0

Solutes in batch assays [g/L]

						0	10	15	20	25
Sodium concentration [i]						2.3 - 3.2	4.0 - 5.0	4.7 - 5.6	5.6 - 6.4	7.1 - 7.1
Undissociated n-caproic acid concentration [ii]						0 - 0.1	0.1 - 0.2	0.1 - 0.3	0.2 - 0.4	0.3 - 0.4

[i] Observed range of initial sodium concentrations in batch assays for different initial n-caproate concentrations.

[ii] Observed range of undissociated n-caproic acid concentrations during batch inhibition assays for different initial n-caproate concentrations.

[iii] Original average reactor activity of inoculum; calculated from reactor data (see supporting information)

ND = Not determined.

± = Standard deviation based on 3 or more measurements.

5.4   Discussion

5.4.1 n-Caproate inhibits the active functional groups in chain elongation microbiomes

In this study, the effect of n-caproate concentration on the specific activity of chain elongation and competing processes was investigated. The specific activity of all active processes decreased with an increasing n-caproate concentration, though the degree in which these processes were inhibited was different for each process. The most plausible explanation for these decreased activities is that n-caproate is inhibitory to the active microorganisms. Such kind of inhibition depends on the MCFA concentration (in this case n-caproate), the chain length, the pH [109] and also on the identity and the degree of adaptation of the microorganism [95]. Evenly, in theory, n-caproate can thermodynamically inhibit its own production. However, we calculated that under the actual conditions, n-caproate did not induce a thermodynamic bottleneck for chain elongation [88].

5.4.2 Both undissociated n-caproic acid and dissociated n-caproate are inhibitory

Evidently, fatty acids in water can appear in their undissociated form or in their dissociated form. The distribution of these two forms depends on the pH and the pK_a of the fatty acid. A low (i.e. acidic) pH yields a high fraction of undissociated fatty acids whereas a neutral and a high pH yields a low fraction of undissociated fatty acids. Undissociated MCFAs are considered to be more inhibitory to microorganisms than dissociated MCFAs [95]. This seems also true for chain elongating microorganisms. Chain elongation studies that operate at slightly acidic pH, therefore, typically report lower MCFA production rates ([29] [56]) compared to studies that operate at near-neutral pH ([25] [26] [53]). For details on mechanisms of (un)dissociated MCFA inhibition, we refer the interested reader to a review article [110].

In this study, we were interested in the inhibitory effect of both n-caproate forms together at constant pH. As such, even though EEO and the reverse β-oxidation pathway release a proton (i.e. acidify the media), we had to minimize undissociation of n-caproate by keeping the pH constant during the assays. This was performed through the use of various buffers.

The assays in our study had an initial pH of 6.8; meaning that 1.1 % of total n-caproate, with a pK_a of 4.85, was undissociated. The lowest observed pH at the end of an assay was 6.5 (data not shown); meaning that, at most, 2 % of total n-caproate was undissociated. Therefore, we conclude that the buffers worked well and the protocol used in this study could thus be used for other batch inhibition assays that require constant pH. We also conclude that VFA upgrading in underlying study was likely not solely inhibited by undissociated n-caproic acid alone. Rather, this process was likely inhibited by a combination of both forms together. This is because the highest observed undissociated n-caproic acid concentration in our study (~0.4 g/L; Table 5.2) was always below the proposed toxic limit of undissociated n-caproic acid for chain elongation (~0.87 g/L [56]). This would mean that, although dissociated MCFAs are considered less toxic than undissociated MCFAs, they are inhibitory too.

5.4.3 The role of exogenous n-caproate and sodium

Before adapted sludge was used as inoculum in the batch inhibition assays, it was active in VFA upgrading (386 mmolC/gVSS/d) at an average n-caproate concentration of 23.2 g/L (Table 5.2). In the batch assays at 20 and 25 g/L n-caproate, however, this sludge showed no VFA upgrading activity (Figure 5.2). We have no mechanistic explanation for this. Possibly, exogenous (i.e. supplied) n-caproate may impose a different inhibitory effect than endogenous (i.e. produced) n-caproate. The exogenous n-caproate in the batch inhibition assays may thus be more toxic to chain elongating microorganisms than endogenous produced n-caproate in the continuous chain elongation process. Earlier work demonstrated a similar, but opposite effect; endogenous ethanol exerted a greater impact on yeast performance than exogenous ethanol [111]. Another example is that *Escherichia coli* was associated with fewer membrane damage with exogenously supplied styrene than with endogenously produced styrene [112]. Hence, these authors stressed the importance of considering the difference between exogenous and endogenous compounds when characterizing the effects of product inhibition.

All assays started with the same initial pH (6.8). Because n-caproic acid was added at different concentrations in the preparation of the media, however, also different amounts of sodium hydroxide were added to adjust the pH. This means that, besides n-caproate, also the sodium concentrations varied among the assays. Indeed, observed initial sodium concentrations were proportional to the initial n-caproate

concentrations (Table 5.2). Sodium can be inhibitory to microorganisms through an increase of osmotic pressure or complete dehydration of microorganisms [113]. To determine whether sodium was inhibitory, observed sodium concentrations were compared (Table 5.2).

Sodium had likely no substantial inhibitory effect on VFA upgrading in all assays. The used inocula were derived from environments with a similar, but often higher, sodium concentration than that was present in the assays. For example, adapted sludge was active in VFA upgrading in the reactor (386 mmolC/gVSS/d) at a high sodium concentration (9.1 g/L) but was completely inhibited in the 20 g/L n-caproate batch assay that contained a lower sodium concentration (6.4 g/L). Some strains of the chain elongating bacterium *C. kluyveri* were derived from brackish sediments [114], underlining that the active chain elongating microorganisms in our batch inhibition assays were likely not rigorously inhibited by sodium but by n-caproate. Also, the synthetic medium sludge was active in hydrogenotrophic methanogenesis in the reactor (59 mmolC/gVSS/d) at a sodium concentration of 6.1 g/L whereas sodium concentrations in the batch inhibition assays were lower or similar (2.3 – 7.1 g/L). Likewise, earlier work showed that hydrogenotrophic methanogens can remain active even up to high sodium chloride concentrations of 1.25M (29 g/L sodium) [115]. This shows that hydrogenotrophic methanogenesis was likely also not rigorously inhibited by sodium but by n-caproate in our batch inhibition assays.

5.4.4 n-Caproate formation may adapt the microbial sludge to perform chain elongation at higher concentrations

In an effective chain elongation process, chain elongation is stimulated while competing processes are suppressed. Whereas chain elongation can be stimulated by adding *C. kluyveri* [116], competing processes can be suppressed in various ways. Past research explained that pH [29], hydraulic shear force in combination with low hydraulic retention time [24] and CO_2 loading rate [88] are control parameters to suppress competing processes. Also, the n-caproate concentration itself may have an effect since earlier work stated that undissociated n-caproic acid does have a microbial toxicity (at pH 5.5) which warranted the need of an continuous extraction unit [56]. In our systematic study, it was shown that exogenous n-caproate does affect the different functional groups of microorganisms which may also be the case with endogenous n-caproate within

bioreactors. With the activity tests, we show that adapted sludge is less inhibited than non-adapted sludge at higher n-caproate concentrations. This difference in n-caproate tolerance between adapted sludge and non-adapted sludge can be explained by a change in physiology of chain elongating microorganisms (e.g. membrane composition, fluidity, integrity, and hydrophobicity) [110]. Another explanation is that the higher caproate concentration in the reactors selected for more n-caproate-tolerant chain elongating microorganisms. Our explanation (i.e. hypothesis) is that the formation of n-caproate in reactor microbiomes does acts as an *in situ* stimulatory agent to form higher n-caproate concentrations which leads towards a further accumulation and possible more selective production of n-caproate.

5.5 Conclusions

In this study, we showed that n-caproate inhibits chain elongation and competing processes in chain elongation microbiomes. Hydrogenotrophic methanogenesis was severely inhibited at 20 g/L n-caproate in batch. This inhibition probably rate-limits syntrophic ethanol oxidation at 25 g/L n-caproate. VFA upgrading was the most sensitive process to n-caproate inhibition but we demonstrated that the n-caproate tolerance of this process is higher with adapted sludge than with non-adapted sludge. Thus, microbiomes can be adapted to perform VFA upgrading at high n-caproate concentrations which likely limits syntrophic ethanol oxidation through hydrogenotrophic methanogenesis. n-Caproate formation is consequently another control parameter to inhibit competing processes to steer to higher n-caproate concentrations.

5.6   Supporting Information
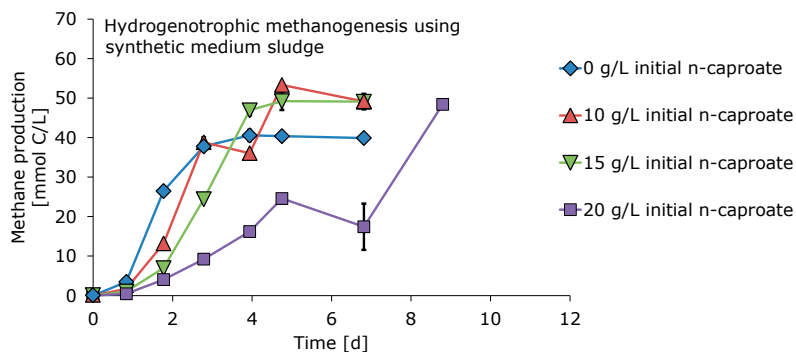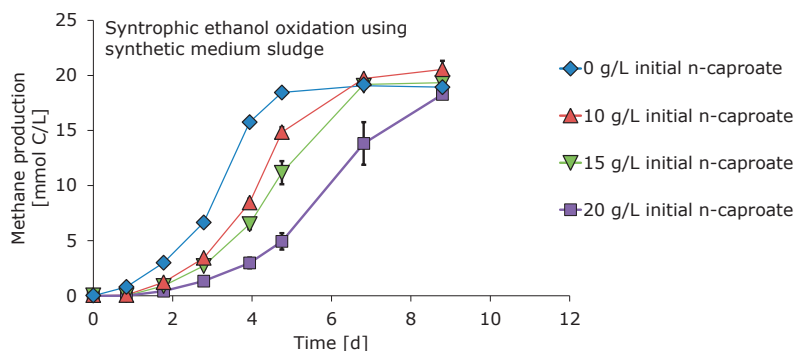
Profiles of product production

Figure S5.1: Methane production by hydrogenotrophic methanogenesis at different initial n-caproate concentrations using synthetic medium sludge. Values indicate averages of duplicates and bars indicate range of duplicates (often too small to be visual). T = 30 °C, pH = 6.8 (buffered).

Figure S5.2: Methane production by syntrophic ethanol oxidation at different initial n-caproate concentrations using synthetic medium sludge. Values indicate averages of duplicates and bars indicate range of duplicates (often too small to be visual). T = 30 °C, pH = 6.8 (buffered).
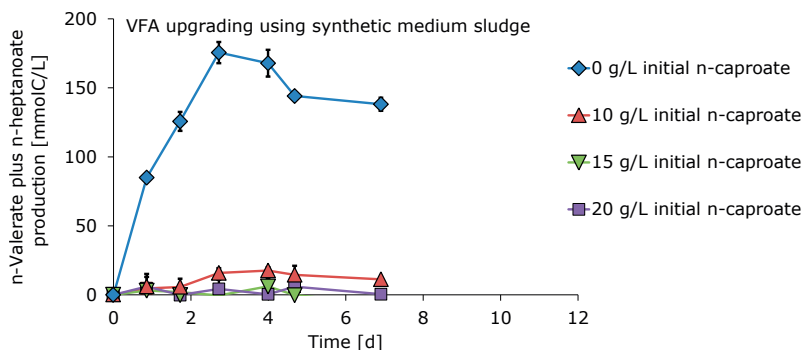
Figure S5.3: n-Valerate plus n-heptanoate production by VFA upgrading at different initial n-caproate concentrations using synthetic medium sludge. Values indicate averages of duplicates and bars indicate range of duplicates (often too small to be visual). T = 30 °C, pH = 6.8 (buffered).
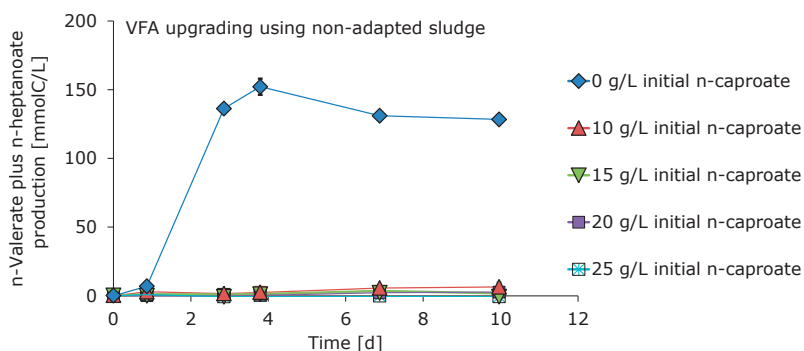

Figure S5.4: n-Valerate plus n-heptanoate production by VFA upgrading at different initial n-caproate concentrations using non-adapted sludge. Values indicate averages of duplicates and bars indicate range of duplicates (often too small to be visual). T = 30 °C, pH = 6.8 (buffered).
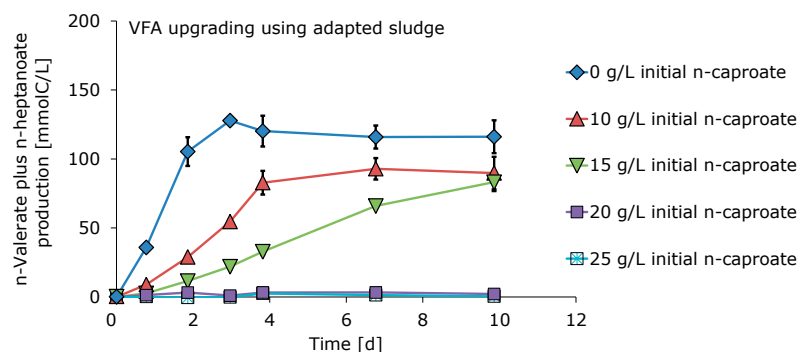

Figure S5.5: n-Valerate plus n-heptanoate production by VFA upgrading at different initial n-caproate concentrations using adapted sludge. Values indicate averages of duplicates and bars indicate range of duplicates (often too small to be visual). T = 30 °C, pH = 6.8 (buffered).

Specifications 'synthetic medium sludge'

Synthetic medium sludge was directly derived from a running continuous chain elongation process that converted synthetic substrates (propionate and ethanol) into MCFAs. The reactor configuration has been described previously [53]. Specifications on process conditions are reported in Table S5.1. Concentrations and rates of substrates and products are reported in Table S5.2.

Table S5.1: Specifications of process conditions that conditioned synthetic medium sludge.

Specification	Unit	Value
Temperature	°C	30
pH	-	6.8
HRT	d	0.7
Substrates in influent	g/L	12.8 [Ethanol]
		13.4 [Propionate]
CO_2 loading rate	L/L/d	2.5
Days after startup	d	377
VSS	g/L	0.61

Table S5.2: Concentrations and rates of substrates and products in the process from which synthetic medium sludge was derived.

Compound	Concentration [$mmol·L^{-1}$]	Rate [$mmol·L^{-1}·d^{-1}$]
Ethanol	6.8 ± 2.9	-400.7 ± 36.7
Propanol	3.5 ± 2.6	5.1 ± 3.5
Acetate	26.0 ± 4.8	38.3 ± 6.7
Propionate	59.1 ± 6.6	-179.9 ± 20.1
Isobutyrate	0.2 ± 0.2	0.3 ± 0.3
n-Butyrate	15.3 ± 1.4	22.6 ± 1.9
Isovalerate	0.7 ± 0.1	1.0 ± 0.1
n-Valerate	88.6 ± 3.1	131.0 ± 11.3
Isocaproate	0.1 ± 0.1	0.1 ± 0.2
n-Caproate	29.3 ± 2.6	43.3 ± 5.4
n-Heptanoate	16.8 ± 2.6	24.9 ± 4.5
n-Caprylate	0.6 ± 0.1	0.8 ± 0.2
CO_2	23.2 ± 12.4 % [i]	-91.3 ± 4.5
CH_4	69.0 ± 26.1 % [i]	35.7 ± 6.4
H_2	2.2 ± 3.7 % [i]	1.1 ± 1.7

[i] Concentrations of gaseous compounds (CO_2, CH_4, H_2) are shown as percentage in the headspace at 1 atm.

Specifications 'synthetic medium sludge'

Specific activity of syntrophic ethanol oxidation of synthetic medium sludge in reactor

- Specific syntrophic ethanol oxidation activity = $1 \cdot r_{CH4}$ / VSS = $1 \cdot 35.7$ mmol/L/d / 0.61 g/L = 59 mmolC/gVSS/d.

Specific VFA upgrading activity of synthetic medium sludge in reactor

- Specific (total) VFA upgrading activity = specific odd-numbered VFA upgrading activity + specific even-numbered VFA upgrading activity = 1362 + 0 = 1362 mmol C/gVSS/d.

    - Specific odd-numbered VFA upgrading activity = $(5 \cdot r_{n\text{-Valerate}} + 7 \cdot r_{n\text{-Heptanoate}})$ / VSS = $(5 \cdot 131.0$ mmol/L/d + $7 \cdot 24.9$ mmol/L/d) / 0.61 g/L = 1362 mmol C/gVSS/d.

    - Specific even-numbered VFA upgrading activity = 0 mmol C/gVSS/d (no even-numbered VFAs were net consumed).

Specifications 'non-adapted sludge'

Non-adapted sludge was directly derived from a running continuous chain elongation process that converted acidified food waste and ethanol into MCFAs [103]. The reactor configuration has been described previously [53]. Specifications on process conditions are reported in Table S5.3. Concentrations and rates of substrates and products are reported in Table S5.4.

Table S5.3: Specifications of process conditions that conditioned non-adapted sludge.

Specification	Unit	Value
Temperature	°C	30
pH	-	6.8
HRT	d	1.0
Substrates in influent	g/L	[Acidified Food Waste] 32.2 [Ethanol]
CO_2 loading rate	L/L/d	1.0
Days after startup	d	103
VSS	g/L	0.35

Table S5.4: Concentrations and rates of substrates and products in the process from which non-adapted sludge was derived.

Compound	Concentration [mmol·L^{-1}]	Rate [mmol·L^{-1}·d^{-1}]
Ethanol	437.3 ± 34.0	-267.6 ± 23.5
Propanol	0.7 ± 0.9	0.7 ± 0.9
Acetate	122.1 ± 8.6	-13.1 ± 8.3
Propionate	15.5 ± 1.0	-9.2 ± 1.5
Isobutyrate	6.2 ± 0.4	-0.9 ± 0.4
n-Butyrate	122.8 ± 11.3	18.3 ± 12.4
Isovalerate	4.0 ± 0.3	-0.5 ± 0.3
n-Valerate	9.4 ± 1.1	4.3 ± 0.9
Isocaproate	0.4 ± 0.1	0.4 ± 0.1
n-Caproate	60.7 ± 7.8	48.1 ± 7.5
n-Heptanoate	0.6 ± 0.1	0.6 ± 0.1
n-Caprylate	0.5 ± 0.1	0.5 ± 0.1
CO_2	5.4 ± 3.0 %[i]	-37.2 ± 0.1
CH_4	77.0 ± 42.0 %[i]	43.8 ± 2.5
H_2	0.0 ± 0.1 %[i]	0.1 ± 0.0

[i] Concentrations of gaseous compounds (CO_2, CH_4, H_2) are shown as percentage in the headspace at 1 atm.

Specifications 'non-adapted sludge'

Specific VFA upgrading activity of non-adapted sludge in reactor

- Specific VFA upgrading activity = specific odd-numbered VFA upgrading activity + specific even-numbered VFA upgrading activity = 71.6 + 148.8 = 220 mmol C/gVSS/d.

  - Specific odd-numbered VFA upgrading activity = $(5 \cdot r_{n\text{-Valerate}} + 7 \cdot r_{n\text{-Heptanoate}})$ / VSS = $(5 \cdot 4.3$ mmol/L/d + $7 \cdot 0.6$ mmol/L/d) / 0.35 g/L = 71.6 mmol C/gVSS/d.

  - Specific even-numbered VFA upgrading activity = $(4 \cdot |r_{acetate}|)$ / VSS = $(4 \cdot |{-13.1}|)$ / 0.35 = 148.8 mmol C/gVSS/d (acetate upgrading to n-butyrate).

Specifications 'adapted sludge'

Adapted sludge was directly derived from a running continuous chain elongation process that converted acidified food waste and ethanol into MCFAs [103]. The reactor configuration has been described previously [53]. Specifications on process conditions are reported in Table S5.5. Concentrations and rates of substrates and products are reported in Table S5.6.

Table S5.5: Specifications of process conditions that conditioned adapted sludge.

Specification	Unit	Value
Temperature	°C	30
pH	-	6.8
HRT	d	4.0
Substrates in influent	g/L	[Acidified Food Waste] 32.2 [Ethanol]
CO_2 loading rate	L/L/d	1.0
Days after startup	d	124
VSS	g/L	0.51

Table S5.6: Concentrations and rates of substrates and products in the process from which adapted sludge was derived.

Compound	Concentration	Rate
	[$mmol·L^{-1}$]	[$mmol·L^{-1}·d^{-1}$]
Ethanol	64.4 ± 35.5	-125.6 ± 26.0
Propanol	5.7 ± 3.7	1.4 ± 1.0
Acetate	31.2 ± 15.2	-26.4 ± 4.7
Propionate	6.4 ± 1.1	-4.6 ± 0.3
Isobutyrate	5.8 ± 0.3	-0.3 ± 0.1
n-Butyrate	90.6 ± 18.4	-3.9 ± 4.5
Isovalerate	4.1 ± 0.3	-0.1 ± 0.1
n-Valerate	13.6 ± 1.7	2.2 ± 0.4
Isocaproate	0.8 ± 0.1	0.1 ± 0.0
n-Caproate	199.9 ± 16.0	46.3 ± 2.8
n-Heptanoate	2.5 ± 0.7	0.5 ± 0.1
n-Caprylate	3.5 ± 1.1	0.8 ± 0.2
CO_2	54.6 ± 25.1 % [i]	-22.5 ± 2.9
CH_4	19.9 ± 21.5 % [i]	6.4 ± 5.8
H_2	11.1 ± 14.0 % [i]	3.7 ± 3.8

[i] Concentrations of gaseous compounds (CO_2, CH_4, H_2) are shown as percentage in the headspace at 1 atm.

Specifications 'adapted sludge'

Specific VFA upgrading activity of adapted sludge in reactor

- Specific VFA upgrading activity = specific odd-numbered VFA upgrading activity + specific even-numbered VFA upgrading activity = 29.0 + 357.5 = 386 mmol C/gVSS/d.

  - Specific odd-numbered VFA upgrading activity = $(5 \cdot r_{n\text{-Valerate}} + 7 \cdot r_{n\text{-Heptanoate}})$ / VSS = $(5 \cdot 2.2$ mmol/L/d + $7 \cdot 0.5$ mmol/L/d) / 0.51 g/L = 29.0 mmol C/gVSS/d.

  - Specific even-numbered VFA upgrading activity = $(6 \cdot |r_{acetate}| + 6 \cdot |r_{n\text{-Butyrate}}|)$ / VSS = $(6 \cdot |{-}26.4$ mmol/L/d $|$ + $6 \cdot |{-}3.9$ mmol/L/d $|)$ / 0.51 g/L = 357.5 mmol C/gVSS/d (acetate upgrading to n-caproate plus n-butyrate upgrading to n-caproate).

CHAPTER 6

General Discussion

6.1   What we did in this thesis and why

In this thesis, we investigated several strategies to control competing processes in ethanol-based open-culture chain elongation. Controlling competing processes is important because they cause limited MCFA selectivities and/or inefficient substrate usages which negatively influences operating expenses. We studied the effect of CO_2 loading rate (Chapter 3), hydraulic retention time (Chapter 4) and n-caproate concentration (Chapter 5) on chain elongation and on competing processes in both batch and continuous reactor experiments. Special attention was given to control the competing process excessive ethanol oxidation (EEO; Eq 6.1). EEO consumes ethanol but does not contribute directly to chain elongation. EEO is an unwanted process because ethanol is a costly substrate. Moreover, its production typically competes for arable land space (first generation bioethanol) or contributes to global warming (synthetic ethanol). Finally, EEO is an acidifying process which requires extra base addition and thus operating expenses.
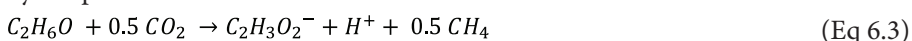
Excessive ethanol oxidation (EEO):
$$C_2H_6O + H_2O \rightarrow C_2H_3O_2^- + H^+ + 2H_2 \qquad \text{(Eq 6.1)}$$

Hydrogenotrophic methanogenesis:
$$2H_2 + 0.5CO_2 \rightarrow 0.5CH_4 + H_2O \qquad \text{(Eq 6.2)}$$

Syntrophic ethanol oxidation:
$$C_2H_6O + 0.5\,CO_2 \rightarrow C_2H_3O_2^- + H^+ + 0.5\,CH_4 \qquad \text{(Eq 6.3)}$$

6.2   Research outcomes and implications

In Chapter 3, we showed that EEO is dependent on hydrogenotrophic methanogenesis (Eq 6.2) and that the overall reaction can be referred to as syntrophic ethanol oxidation (Eq 6.3). By limiting the CO_2 loading rate to a chain elongation process, syntrophic ethanol oxidation is also limited. This means that low CO_2 loading rates must be applied in chain elongation processes from acidified organic waste and additional ethanol in order to minimize use of ethanol and base. Vice versa, at high CO_2 loading rate, syntrophic ethanol oxidation (and thus EEO) was stimulated. This led to an 'ethanol upgrading' process,

in which ethanol was primarily used to upgrade ethanol itself into n-caproate. Although not efficient in ethanol-use, ethanol upgrading could be considered to convert undistilled bioethanol into MCFAs to circumvent distillation of ethanol which is energetically expensive [19]. Next to CO_2 loading rate, we found an alternative strategy to control EEO: by applying a long HRT in a chain elongation process, syntrophic ethanol oxidation was also suppressed (Chapter 4). A major advantage of this strategy over a limited CO_2 loading rate is that the n-caproate concentration can become very high. In fact, here we have reported the highest n-caproate concentration observed in a chain elongation process to date (25.7 g/L). A hypothesis was that the high n-caproate concentration caused the actual inhibition on syntrophic ethanol oxidation. In Chapter 5, we tested this hypothesis by investigating the effect of n-caproate concentration on the specific activity of syntrophic ethanol oxidation, hydrogenotrophic methanogenesis and chain elongation with batch inhibition assays. The results suggest that high n-caproate concentrations inhibit hydrogenotrophic methanogenesis and therefore limit syntrophic ethanol oxidation. As such, accumulation of n-caproate in chain elongation bioreactors inhibits syntrophic ethanol oxidation which leads to a more selective and ethanol-efficient MCFA production process.

In Chapter 2, we presented the discovery of granular sludge formation in a chain elongation process. The granules did contribute to MCFA production through both ethanol and VFA upgrading. However, the formation of granules seems to coincide with high-rate syntrophic ethanol oxidation (Chapter 3 and 4). This type of granular chain elongation sludge, therefore, may be useful in ethanol-upgrading processes but not in processes in which ethanol must be used efficiently.

6.3 Overview of control strategies for chain elongation with open cultures

In Table 6.1, we summarize the desired and competing processes in ethanol-based chain elongation as well as the known corresponding control strategies. These control strategies are based on the results of this thesis and on literature. Note that syntrophic ethanol oxidation (a combination of EEO and hydrogenotrophic methanogenesis) is considered as a competing process when a VFA upgrading process is desired but that it can also be considered as a mediating process when

an ethanol upgrading process is desired. Another side-advantage of syntrophic ethanol oxidation is that it upgrades CO_2 into methane.

Based on the explanations on how the processes were reported to be controlled, we associate the control strategies in Table 6.1 with 'prevented' (process does not occur at all), 'inhibited' (process still occurs but to a limited extent), 'thermodynamically unfavorable' (process is thermodynamic unfavorable but could still occur at local/micro conditions), limited (process still occurs but is limited by substrate availability) or with 'out selected' (process does not occur because the corresponding microorganisms are practically washed out).

6.4   Scenarios that may undermine control strategies

Depending on the feedstock composition and desired processes one can apply different control strategies. These strategies will likely work well with similar substrates and reactor configurations as used in this thesis. However, new circumstances or specific substrates may not always suit the identified control mechanisms. The presented control strategies in Table 6.1, therefore, may not always be applicable. For example, whereas a limited CO_2 loading rate has shown to control EEO under the applied conditions in Chapter 3 and in ref [27] and [29], this control strategy probably won't work properly when other hydrogen sinks than CO_2 are also present. So when sulfate, for example, is present in the medium as well as sulfate reducing bacteria, *in situ* produced hydrogen will likely be used to reduce sulfate into sulfide. This could prevent the accumulation of hydrogen that is required to thermodynamically inhibit EEO.

Other scenarios that undermine the presented control strategies are the adaptation of microorganisms and the introduction of as-yet-uncultured microorganisms. For example, when the open culture contains hydrogenotrophic methanogens that are somehow resilient to high n-caproate concentrations ($\geq$ 25 g/L n-caproate), it is likely that EEO still proceeds at high rates, even beyond these apparent boundary conditions. Also, the desired chain elongation process apparently does not proceed at a temperature higher than or equal to 40 °C [29] and also not at a pH lower than or equal to 4.5 [117]. Although this probably means that chain elongation is prevented at these conditions, we cannot consider this as a hard rule due to the vast diversity and dynamic nature of microorganisms.

Table 6.1: Overview of desired and competing processes in open culture chain elongation bioreactors as well as their corresponding reaction equation and control strategies reported to date.

Process	Reaction equation	Competes for	Process is prevented / inhibited / thermodynamically unfavourable / limited / out selected by
Desired process			
Chain elongation through the reverse β-oxidation pathway	$5C_xH_{2x-1}O_2{}^- + 6C_2H_6O \rightarrow$ $5C_{x+2}H_{2x+3}O_2{}^- + 4H_2O + H^+ + 2H_2$		• Prevented by CO_2 deficiency (≤ 0.07 % at 1 atm) (Chapter 3) • Prevented by toxicity of exogenous n-caproate (~20 g/L) (Chapter 5) • Prevented at thermophilic conditions (≥ 40 °C) [29] • Prevented at acidic pH (< 4.5) [117] • Inhibited at high pH_2 (100 % at 1 atm) [66] • Inhibited at slightly acidic pH (5.5) by toxicity of undissociated n-caproic acid (>7.5 mM) [56]
Competing processes			
Acetotrophic methanogenesis	$C_2H_3O_2{}^- + H^+ \rightarrow CH_4 + CO_2$	Acetate	• Out selected at near-neutral pH by a combination of high shear force and a low HRT (< 4 d) [24] [53] • Out selected by thermal pre-treatment [118] • Inhibited at slightly acidic pH by undissociated fatty acids [19] [56] • Prevented by addition of 2-bromoethanesulfonate [23]
Anaerobic oxidation of VFAs	$C_2H_3O_2{}^- + H^+ + 2H_2O \rightarrow 4H_2 + 2CO_2$	VFAs	• Thermodynamically unfavourable at pH_2 > 0.007 % at 1 atm (Chapter 3)
Anaerobic oxidation of MCFAs	$C_xH_{2x-1}O_2{}^- + 2H_2O \rightarrow$ $C_{x-2}H_{2x-5}O_2{}^- + C_2H_3O_2{}^- + H^+ + 2H_2$	MCFAs	• Thermodynamically unfavourable at pH_2 > 0.006 % at 1 atm (Chapter 3)
Excessive ethanol oxidation	$C_2H_6O + H_2O \rightarrow C_2H_3O_2{}^- + H^+ + 2H_2$	Ethanol	• Thermodynamically unfavourable at pH_2 >14 % at 1 atm (Chapter 3) [27] [29] o By limiting hydrogen sink (hydrogenotrophic methanogenesis) • Slightly inhibited at neutral pH by n-caproate toxicity (Chapter 5)
Hydrogenotrophic methanogenesis	$2H_2 + 0.5CO_2 \rightarrow 0.5CH_4 + H_2O$	Hydrogen	• Inhibited at near- neutral pH by toxicity of n-caproate (20 g/L) (Chapter 5) • Likely prevented at near-neutral pH by toxicity of n-caproate (>25 g/L) (Chapter 5) • Limited by CO_2 availability (~1.1 %) (Chapter 3) [27] [29] • Prevented by addition of 2-bromoethanesulfonate [23] • Inhibited by undissociated butyric acid o At pH < 6; ~15 mmol/L for 90 % inhibition [29]
Syntrophic ethanol oxidation	$C_2H_6O + 0.5CO_2 \rightarrow C_2H_3O_2{}^- + H^+ + 0.5CH_4$	Ethanol	• Likely prevented at near-neutral pH by toxicity of n-caproate (≥ 25 g/L) (Chapter 5) • Limited by CO_2 availability (~1.1 %) (Chapter 3) [27] [29]

6.5 One third of total consumed ethanol is inevitably used for ethanol upgrading

6.5.1 Ethanol-use for ethanol upgrading and VFA upgrading

Ethanol-based chain elongation with open cultures does not only upgrade VFAs into MCFAs, it also upgrades ethanol itself into MCFAs (Figure 6.1). Because ethanol upgrading is inefficient in ethanol-use, it can be considered as an undesired carbon flux. However, although ethanol upgrading can be limited by controlling syntrophic ethanol oxidation, it seems that some extent of ethanol upgrading is inevitable, even when syntrophic ethanol oxidation is completely suppressed. This is because chain elongating microorganisms can upgrade ethanol into MCFAs by 1) oxidizing ethanol into acetate and 2) elongate this acetate with ethanol into MCFAs. Both processes occur through the reverse β-oxidation pathway for chain elongation in which 1 mole of ethanol is anaerobically oxidized into acetate for every 5 chain elongation reactions. Here, we show how much ethanol is used for ethanol upgrading through the reverse β-oxidation pathway without syntrophic ethanol oxidation. We determine this 'minimum ethanol-use for ethanol upgrading' via a theoretical approach and we validate this value by extrapolating our experimental results.
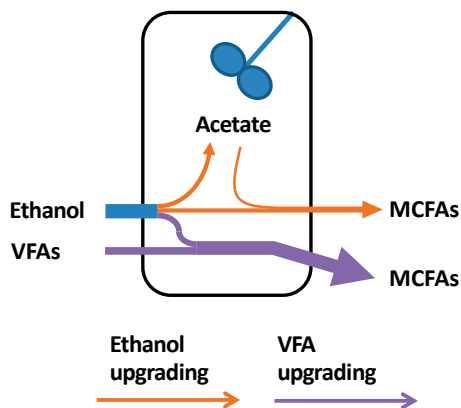

Figure 6.1: Ethanol-based chain elongation typically involves two types of carbon fluxes: ethanol upgrading and VFA upgrading. Ethanol upgrading = *in situ* ethanol oxidation into acetate and subsequent chain elongation into even-numbered fatty acids. VFA upgrading = chain elongation of fed-VFAs.

6.5.2 Minimum ethanol-use for ethanol upgrading: a theoretical approach

Let's consider that 1 mole of acetate, which is derived from primary fermentation, is elongated with 1 mole of ethanol into n-butyrate through the reverse β-oxidation pathway. The ethanol that is consumed here accounts for 'VFA upgrading' because it upgrades a VFA that is externally fed and not internally produced. Inherent to this elongation step, an additional 0.2 mole of ethanol is oxidized into 0.2 mole of acetate (assuming a fixed 5:1 ratio in the reverse β-oxidation pathway). This forms the starting VFA for ethanol upgrading and as such, this ethanol consumption accounts for ethanol upgrading. The resulting acetate is then further elongated with the same molar amount of ethanol (0.2 mole), which also accounts for ethanol upgrading. Along with this elongation step, an additional $(0.2 \cdot 0.2)$ 0.04 mole of ethanol is oxidized into 0.04 mole of acetate. Again, this 0.04 mole acetate is further elongated with the same molar amount of ethanol, and again, acetate is formed. This iterates eventually until 0.5 mole of ethanol-use for ethanol upgrading (Figure 6.2). As such, for every VFA upgrading step, 0.5 mole of ethanol is used for ethanol upgrading. In other words, at least 33.3 % of total used ethanol is inevitably used for ethanol upgrading in ethanol-based chain elongation processes.
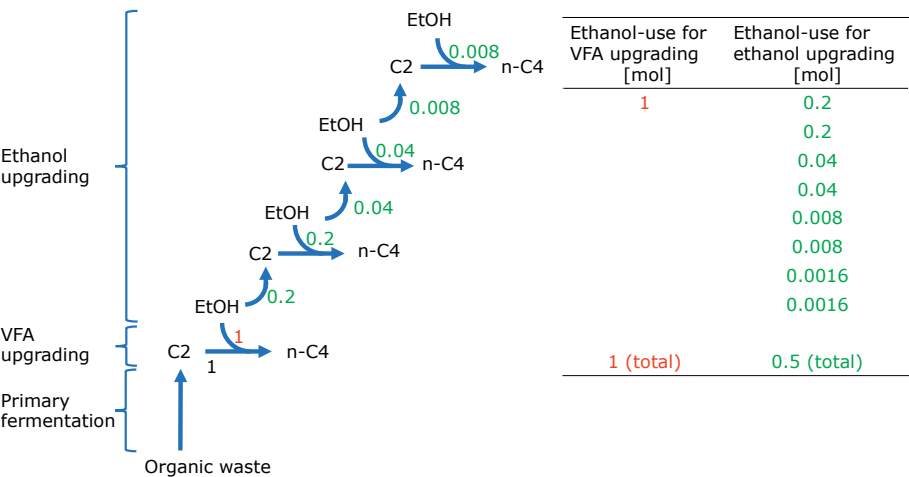

Figure 6.2: Graphical representation how much ethanol is used for both VFA upgrading (red figures) and ethanol upgrading (green figures) in chain elongation without syntrophic ethanol oxidation. In the reverse β-oxidation pathway for chain elongation, 0.2 mole of ethanol is oxidized into acetate (C2) for every chain elongation step.

6.5.3 Minimum ethanol-use for ethanol upgrading: extrapolating experimental results

With the experimental results from Chapter 3, we determined the rate of EEO and the rate of ethanol-use for ethanol upgrading at different CO_2 loading rates. The relative rates are plotted against each other in Figure 6.3. The linear regression line has an intersection with the y-axis (no EEO) at 27.4; meaning that when EEO is completely suppressed, the percentage of ethanol-use for ethanol upgrading is 27.4 %. This value is close to the aforementioned theoretical 33.3 %, underlining that one third of total consumed ethanol inevitably is used for ethanol upgrading, even when the competing processes EEO is completely suppressed.
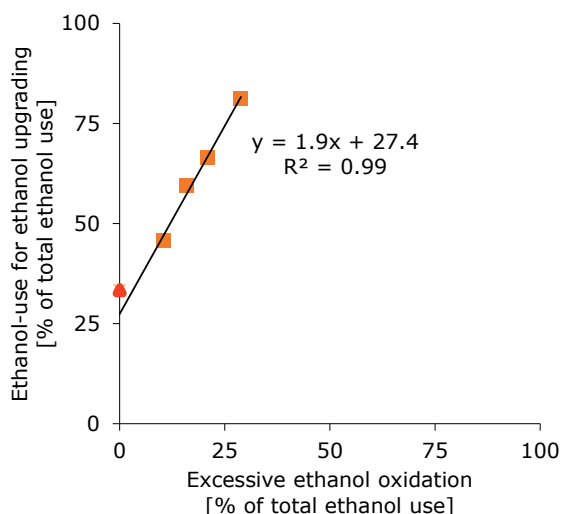

Figure 6.3: Relative rates of excessive ethanol oxidation (EEO) vs. ethanol-use for ethanol upgrading at different CO_2 loading rates. Data is adapted from Chapter 3. The red dot at 0 % EEO indicates the theoretical minimum ethanol-use for ethanol upgrading (33.33 %).

6.6   Outlook

6.6.1   Alternative electron donors from residual biomass

In this thesis, we have shown several strategies to control competing processes in ethanol-based chain elongation with open cultures. To further improve the effectiveness of this technology, ethanol and base consumption should be further reduced since these aspects have most impact on the environment and costs [35].

This could be done by steering the hydrolysis and acidogenesis stage to MCFAs and/or lactate production (e.g. ref [30] and [119]) or by using alternative electron donors for chain elongation such as hydrogen [23], methanol [33], carbon monoxide [67], glucose [66] or propanol [52]. Evidently, these alternative electron donors should also be obtained from residual biomass. Here, we discuss how these alternative electron donors can be produced via the biorefinery platforms (syngas, sugar and carboxylate platform; Chapter 1).

In the syngas platform, dry biomass is gasified into syngas. The primary components of syngas, CO and H_2, can readily be used as electron donor for chain elongation. Alternatively, syngas can be converted into methanol [120], ethanol and propanol [121] which are all suitable electron donors. However, although methanol-based chain elongation is not optimised and typically results in low MCFA production rates (≤ 0.23 g/L/d) and selectivities (≤ 8 % on an electron basis), it could be used for the production of isobutyrate [33] [92].

In the sugar platform, (lignocellulosic) biomass is hydrolyzed into sugars, such as glucose and xylose, as intermediate platform chemicals. Glucose could readily be used as electron donor for chain elongation but whether xylose is also suitable remains to be investigated. If this C5 sugar is suitable, lignocellulosic hydrolysates are interesting alternative feedstocks for chain elongation. Alternatively, lignocellulosic sugars could be fermented into ethanol or lactate as electron donor for chain elongation.
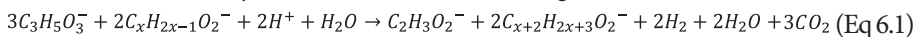
In the carboxylate platform, wet biomass is typically hydrolyzed and acidified into volatile fatty acids (VFAs), such as acetate, propionate and butyrate, as intermediates. However, it is also possible to steer such hydrolysis and acidification towards electron donors for chain elongation such as hydrogen [122] or lactate. Lactate seems interesting as this could be produced in high concentrations from organic waste. For example, Kim et al. (2016) acidified food waste at thermophilic conditions (50 °C) at pH 5.0 which resulted in lactate production until 40 g/L [123].

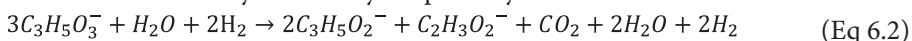### 6.6.2 Lactate as electron donor for chain elongation

Lactate is a promising alternative electron donor for chain elongation. Zhu et al. (2015) fermented lactate into MCFAs and reported a MCFA production

rate of 2.5 g/L/d, a MCFA concentration of 23.4 g/L and a MCFA selectivity of 81.4 % on an electron basis [34]. These figures are similar as in our developed ethanol-based chain elongation process with acidified food waste, in which we reported an average MCFA production rate of 5.8 g/L/d at a MCFA concentration of 24.7 g/L and a MCFA selectivity of 81.4 % on an electron basis (Chapter 4). Lactate-based chain elongation, therefore, is certainly no less than ethanol-based chain elongation. Another advantage of lactate is that it could fully eliminate the addition of an external electron donor. Xu et al. (2017) fed acid whey waste to a two-stage conversion, resulting in a lactate production of ~37 g/L/d in the first stage (50 °C, pH 5.0, HRT = 1.17 d) and a MCFA production of ~2.2 g/L/d in the second stage (30 °C, pH 5.0, HRT = 3.55) [30]. Due to the lactate production in the first stage, they did not need an external electron donor. However, not all residual biomass streams may be suitable for lactate production. Another advantage of lactate-based chain elongation is that it consumes a proton (Eq 6.1), instead of produces a proton, which is the case in ethanol-based chain elongation. Lactate based chain elongation, therefore, allows further minimization of base-use. By combining both ethanol and lactate as electron donor, one could possibly fully eliminate base-use in chain elongation processes.

Overall stoichiometry of lactate-based chain elongation:
$$3C_3H_5O_3^- + 2C_xH_{2x-1}O_2^- + 2H^+ + H_2O \rightarrow C_2H_3O_2^- + 2C_{x+2}H_{2x+3}O_2^- + 2H_2 + 2H_2O + 3CO_2 \quad \text{(Eq 6.1)}$$

Overall stoichiometry of the acrylate pathway:
$$3C_3H_5O_3^- + H_2O + 2H_2 \rightarrow 2C_3H_5O_2^- + C_2H_3O_2^- + CO_2 + 2H_2O + 2H_2 \qquad \text{(Eq 6.2)}$$

Unfortunately, lactate is also prone to competing processes. Kucek et al. (2016) demonstrated continuous conversion of lactate to n-caproate [20] but also reported that part of the lactate was converted into propionate through the acrylate pathway (Eq 6.2). Similar as EEO, this acrylate pathway can be considered as a competing process. It seems, however, that this process can also be controlled since Xu et al. (2017) mentioned that, based on their MCFA selectivity of up to 66 %, it is possible to steer microbiomes towards chain elongation rather than the acrylate pathway. This indicates that also the acrylate pathway, like EEO, can be controlled.

6.7   Concluding remarks

Chain elongation with open cultures can effectively convert biomass residues into precursors for fuels and chemicals. Such processes are important to reduce both the dependency of petrochemical resources and land-use for non-food applications. The attractiveness of the process is that it operates under mild temperature and pressure conditions. It also does not need an expensive catalyst or genetically modified microorganisms. Furthermore, as shown in this thesis, chain elongation with open cultures can produce MCFAs at high rates and concentrations under practical circumstances in a continuous process. To control competing processes in chain elongation, one does not need to add toxic chemicals or apply expensive heat shocks. In fact, competing processes can be controlled in relatively simple ways such as a limited CO_2 availability or by operating the process at high MCFA concentrations. Still, the addition of base and ethanol can be further reduced to decrease operating expenses and to lower the environmental impact. Fortunately, there are possibilities to do so by, for example, steering hydrolysis and acidification towards lactate or by selecting alternative electron donors from biomass residues.

References

1. Wilbrand K: Potential of Fossil Kerosene. In *Biokerosene: Status and Prospects.* Edited by Kaltschmitt M, Neuling U. Berlin, Heidelberg: Springer Berlin Heidelberg; 2018: 43-57

2. Luo L, van der Voet E, Huppes G: Life cycle assessment and life cycle costing of bioethanol from sugarcane in Brazil. *Renewable Sustainable Energy Rev* 2009, 13:1613-1619.

3. Mekhilef S, Siga S, Saidur R: A review on palm oil biodiesel as a source of renewable fuel. *Renewable Sustainable Energy Rev* 2011, 15:1937-1949.

4. G Cassman K, Liska AJ: Food and fuel for all: realistic or foolish? *Biofuels, Bioprod Biorefin* 2007, 1:18-23.

5. Sheil D, Casson A, Meijaard E, Van Noordwjik M, Gaskell J, Sunderland-Groves J, Wertz K, Kanninen M: The impacts and opportunities of oil palm in Southeast Asia: What do we know and what do we need to know? : Center for International Forestry Research (CIFOR), Bogor, Indonesia; 2009.

6. Stenmarck Å, Jensen C, Quested T, Moates G. Estimates of European Food Waste Levels 2016. https://www.eu-fusions.org/phocadownload/Publications/Estimates%20of%20European%20food%20waste%20levels.pdf (accessed 25 Oktober 2017).

7. Straw. https://www.wallpaperflare.com/photography-of-brown-hay-wallpaper-24797 (accessed 21 March 2018).

8. Food Scraps. http://maxpixel.freegreatpicture.com/Shells-Potato-Dish-Potato-Skins-Waste-344185 (accessed 21 March 2018).

9. Sewage Sludge. https://www.shutterstock.com/g/wang%20wentong (accessed 21 March 2018).

10. Potato Peels. http://maxpixel.freegreatpicture.com/Shells-Potato-Dish-Potato-Skins-Waste-344185 (accessed 21 March 2018).

11. EC (European Commission). Communication from the commission to the European parliament, the council, the European economic and social committee and the committee of the regions *Closing the loop - An EU action plan for the Circular Economy* [Online], 2015. http://eur-lex.europa.eu/legal-content/EN/TXT/?uri=CELEX:52015DC0614 (accessed 30-01-2018).

12. de Jong E, Higson A, Walsh P, Wellisch M: Biorefineries: Adding Value to the Sustainable Utilisation of Biomass. IEA Bioenergy Task 42; 2012.

13. Hayes DJ: An examination of biorefining processes, catalysts and challenges. *Catal Today* 2009, 145:138-151.

14. Agler MT, Wrenn BA, Zinder SH, Angenent LT: Waste to bioproduct conversion with undefined mixed cultures: the carboxylate platform. *Trends Biotechnol* 2011, 29:70-78.

15. Ramirez J, Brown R, Rainey T: A Review of Hydrothermal Liquefaction Bio-Crude Properties and Prospects for Upgrading to Transportation Fuels. *Energies* 2015, 8:6765.

16. Moscoviz R, Trably E, Bernet N, Carrere H: The environmental biorefinery: state-of-the-art on the production of hydrogen and value-added biomolecules in mixed-culture fermentation. *Green Chem* 2018, 20:3159-3179.

17. Weiland P: Biogas production: current state and perspectives. *Appl Microbiol Biotechnol* 2010, 85:849-860.

18. Angenent LT, Richter H, Buckel W, Spirito CM, Steinbusch KJJ, Plugge CM, Strik DPBTB, Grootscholten TIM, Buisman CJN, Hamelers HVM: Chain Elongation with Reactor Microbiomes: Open-Culture Biotechnology To Produce Biochemicals. *Environ Sci Technol* 2016, 50:2796-2810.

19. Agler MT, Spirito CM, Usack JG, Werner JJ, Angenent LT: Chain elongation with reactor microbiomes: Upgrading dilute ethanol to medium-chain carboxylates. *Energy Environ Sci* 2012, 5:8189-8192.

20. Kucek LA, Nguyen M, Angenent LT: Conversion of l-lactate into n-caproate by a continuously fed reactor microbiome. *Water Res* 2016, 93:163-171.

21. Seedorf H, Fricke WF, Veith B, Bruggemann H, Liesegang H, Strittmatter A, Miethke M, Buckel W, Hinderberger J, Li F, et al: The genome of *Clostridium kluyveri*, a strict anaerobe with unique metabolic features. *Proc Natl Acad Sci USA* 2008, 105:2128-2133.

22. Balat M: Production of bioethanol from lignocellulosic materials via the biochemical pathway: A review. *Energy Convers Manage* 2011, 52:858-875.

23. Steinbusch KJJ, Hamelers HVM, Plugge CM, Buisman CJN: Biological formation of caproate and caprylate from acetate: fuel and chemical production from low grade biomass. *Energy Environ Sci* 2011, 4:216-224.

24. Grootscholten TIM, Steinbusch KJJ, Hamelers HVM, Buisman CJN: Chain elongation of acetate and ethanol in an upflow anaerobic filter for high rate MCFA production. *Bioresour Technol* 2012, 135:440-445.

25. Grootscholten TIM, Steinbusch KJJ, Hamelers HVM, Buisman CJN: Improving medium chain fatty acid productivity using chain elongation by reducing the hydraulic retention time in an upflow anaerobic filter. *Bioresour Technol* 2013, 136:735-738.

26. Grootscholten TIM, Steinbusch KJJ, Hamelers HVM, Buisman CJN: High rate heptanoate production from propionate and ethanol using chain elongation. *Bioresour Technol* 2013, 136:715-718.

27. Grootscholten TIM, Strik DPBTB, Steinbusch KJJ, Buisman CJN, Hamelers HVM: Two-stage medium chain fatty acid (MCFA) production from municipal solid waste and ethanol. *Appl Energy* 2014, 116:223-229.

28. Grootscholten TIM, dal Borgo FK, Hamelers HVM, Buisman CJN: Promoting chain elongation in mixed culture acidification reactors by addition of ethanol. *Biomass Bioenergy* 2013, 48:10-16.

29. Agler MT, Spirito CM, Usack JG, Werner JJ, Angenent LT: Development of a highly specific and productive process for n-caproic acid production: applying lessons from methanogenic microbiomes. *Water Sci Technol* 2014, 69:62-68.

30. Xu J, Hao J, Guzman JJL, Spirito CM, Harroff LA, Angenent LT: Temperature-Phased Conversion of Acid Whey Waste Into Medium-Chain Carboxylic Acids via Lactic Acid: No External e-Donor. *Joule* 2017, 2:280 - 295.

31. Andersen SJ, De Groof V, Khor WC, Roume H, Props R, Coma M, Rabaey K: A Clostridium Group IV Species Dominates and Suppresses a Mixed Culture Fermentation by Tolerance to Medium Chain Fatty Acids Products. *Front Bioeng Biotechnol* 2017, 5:8.

32. Hegner R, Koch C, Riechert V, Harnisch F: Microbiome-based carboxylic acids production: from serum bottles to bioreactors. *RSC Adv* 2017, 7:15362-15371.

33. Chen WS, Ye Y, Steinbusch KJJ, Strik DPBTB, Buisman CJN: Methanol as an alternative electron donor in chain elongation for butyrate and caproate formation. *Biomass Bioenergy* 2016, 93:201-208.

34. Zhu X, Tao Y, Liang C, Li X, Wei N, Zhang W, Zhou Y, Yang Y, Bo T: The synthesis of n-caproate from lactate: A new efficient process for medium-chain carboxylates production. *Sci Rep* 2015, 5:14360.

35. Chen W-S, Strik DPBTB, Buisman CJN, Kroeze C: Production of Caproic Acid from Mixed Organic Waste- An Environmental Life Cycle Perspective. *Environ Sci Technol* 2017, 51:7159-7168.

36. Barker H, Kamen M, Bornstein B: The synthesis of butyric and caproic acids from ethanol and acetic acid by *Clostridium kluyveri* 1945, 31:373.

37. van der Star WRL, Abma WR, Blommers D, Mulder J-W, Tokutomi T, Strous M, Picioreanu C, van Loosdrecht MCM: Startup of reactors for anoxic ammonium oxidation: Experiences from the first full-scale anammox reactor in Rotterdam. *Water Res* 2007, 41:4149-4163.

38. Lettinga G: Anaerobic digestion and wastewater treatment systems. *Antonie van leeuwenhoek* 1995, 67:3-28.

39. Yu HQ, Mu Y: Biological hydrogen production in a UASB reactor with granules. II: Reactor performance in 3-year operation. *Biotechnol Bioeng* 2006, 94:988-995.

40. Tomlinson N, Barker HA: Carbon dioxide and acetate utilization by *Clostridium kluyveri*. I. Influence of nutritional conditions on utilization patterns. *J Biol Chem* 1954, 209:585-595.

41. Hulshoff Pol L: The phenomenon of granulation of anaerobic sludge. PhD dissertation, Agricultural University of Wageningen, the Netherlands., 1989.

42. Ngian K, Lin S, Martin W: Effect of mass transfer resistance on the Lineweaver–Burk plots for flocculating microorganisms. *Biotechnol Bioeng* 1977, 19:1773-1784.

43. Hulshoff Pol L, de Castro Lopes S, Lettinga G, Lens P: Anaerobic sludge granulation. *Water Res* 2004, 38:1376-1389.

44. Liu Y, Tay J-H: The essential role of hydrodynamic shear force in the formation of biofilm and granular sludge. *Water Res* 2002, 36:1653-1665.

45. Fang HH, Liu H, Zhang T: Characterization of a hydrogen-producing granular sludge. *Biotechnol Bioeng* 2002, 78:44-52.

46. Zhang ZP, Show KY, Tay JH, Liang DT, Lee DJ, Jiang WJ: Rapid formation of hydrogen-producing granules in an anaerobic continuous stirred tank reactor induced by acid incubation. *Biotechnol Bioeng* 2007, 96:1040-1050.

47. Hou Y-p, Peng D-c, Wang B-b, Zhang X-y, Xue X-d: Effects of stirring strategies on the sludge granulation in anaerobic CSTR reactor. *Desalin Water Treat* 2014, 52:6348-6355.

48. Phillips JR, Klasson KT, Clausen EC, Gaddy JL: Biological production of ethanol from coal synthesis gas. *Appl Biochem Biotechnol* 1993, 39-40:559-571.

49. Sutton NB, Grotenhuis T, Rijnaarts HHM: Impact of organic carbon and nutrients mobilized during chemical oxidation on subsequent bioremediation of a diesel-contaminated soil. *Chemosphere* 2014, 97:64-70.

50. Anneken DJ, Both S, Christoph R, Fieg G, Steinberner U, Westfechtel A: Fatty Acids. In *Ullmann's Encyclopedia of Industrial Chemistry.* Wiley-VCH Verlag GmbH & Co. KGaA; 2000

51. Gervajio GC: Fatty Acids and Derivatives from Coconut Oil. In *Bailey's Industrial Oil and Fat Products.* John Wiley & Sons, Inc.; 2005

52. Coma M, Vilchez-Vargas R, Roume H, Jauregui R, Pieper DH, Rabaey K: Product Diversity Linked to Substrate Usage in Chain Elongation by Mixed-Culture Fermentation. *Environ Sci Technol* 2016, 50:6467-6476.

53. Roghair M, Strik DPBTB, Steinbusch KJJ, Weusthuis RA, Bruins ME, Buisman CJN: Granular sludge formation and characterization in a chain elongation process. *Process Biochem* 2016, 51:1594-1598.

54. Steinbusch KJJ, Hamelers HVM, Buisman CJN: Alcohol production through volatile fatty acids reduction with hydrogen as electron donor by mixed cultures. *Water Res* 2008, 42:4059-4066.

55. Kleerebezem R, Van Loosdrecht MCM: A generalized method for thermodynamic state analysis of environmental systems. *Crit Rev Env Sci Technol* 2010, 40:1-54.

56. Ge S, Usack JG, Spirito CM, Angenent LT: Long-term n-caproic acid production from yeast-fermentation beer in an anaerobic bioreactor with continuous product extraction. *Environ Sci Technol* 2015, 49:8012-8021.

57. Lonkar S, Fu Z, Holtzapple M: Optimum alcohol concentration for chain elongation in mixed-culture fermentation of cellulosic substrate. *Biotechnol Bioeng* 2016, 113:2597-2604.

58. Sander R: Compilation of Henry's law constants for inorganic and organic species of potential importance in environmental chemistry. Max-Planck Institute of Chemistry, Air Chemistry Department Mainz, Germany; 1999.

59. Schmidt JE, Ahring BK: Effects of hydrogen and formate on the degradation of propionate and butyrate in thermophilic granules from an upflow anaerobic sludge blanket reactor. *Appl Environ Microbiol* 1993, 59:2546-2551.

60. Schink B: Energetics of syntrophic cooperation in methanogenic degradation. *Microbiol Mol Biol Rev* 1997, 61:262-280.

61. Stams AJM, Plugge CM: Electron transfer in syntrophic communities of anaerobic bacteria and archaea. *Nat Rev Microbiol* 2009, 7:568-577.

62. Plugge CM, Zhang W, Scholten JCM, Stams AJM: Metabolic flexibility of sulfate-reducing bacteria. *Front Microbiol* 2011, 2:81.

63. Savant DV, Shouche YS, Prakash S, Ranade DR: *Methanobrevibacter acididurans* sp. nov., a novel methanogen from a sour anaerobic digester. *Int J Syst Evol Microbiol* 2002, 52:1081-1087.

64. Ishii S, Kosaka T, Hori K, Hotta Y, Watanabe K: Coaggregation facilitates interspecies hydrogen transfer between Pelotomaculum thermopropionicum and Methanothermobacter thermautotrophicus. *Appl Environ Microbiol* 2005, 71:7838-7845.

65. Kouzuma A, Kato S, Watanabe K: Microbial interspecies interactions: recent findings in syntrophic consortia. *Front Microbiol* 2015, 6:477.

66. Schoberth S, Gottschalk G: Considerations on the energy metabolism of *Clostridium kluyveri*. *Archiv für Mikrobiologie* 1969, 65:318-328.

67. Diender M, Stams AJM, Sousa DZ: Production of medium-chain fatty acids and higher alcohols by a synthetic co-culture grown on carbon monoxide or syngas. *Biotechnol Biofuels* 2016, 9:82.

68. Kleerebezem R, Joosse B, Rozendal R, Van Loosdrecht MCM: Anaerobic digestion without biogas? *Rev Environ Sci Biotechnol* 2015, 14:787-801.

69. Weusthuis RA, Aarts JMMJG, Sanders JPM: From biofuel to bioproduct: is bioethanol a suitable fermentation feedstock for synthesis of bulk chemicals? *Biofuels, Bioprod Biorefin* 2011, 5:486-494.

70. Harvey BG, Meylemans HA: 1-Hexene: A renewable C6 platform for full-performance jet and diesel fuels. *Green Chem* 2014, 16:770-776.

71. Min K, Khan A, Kwon M, Jung Y, Yun Z, Kiso Y: Acidogenic fermentation of blended food-waste in combination with primary sludge for the production of volatile fatty acids. *J Chem Technol Biotechnol* 2005, 80:909-915.

72. Ni BJ, Liu H, Nie YQ, Zeng RJ, Du GC, Chen J, Yu HQ: Coupling glucose fermentation and homoacetogenesis for elevated acetate production: Experimental and mathematical approaches. *Biotechnol Bioeng* 2011, 108:345-353.

73. Luo G, Johansson S, Boe K, Xie L, Zhou Q, Angelidaki I: Simultaneous hydrogen utilization and *in situ* biogas upgrading in an anaerobic reactor. *Biotechnol Bioeng* 2012, 109:1088-1094.

74. Raes SMT, Jourdin L, Buisman CJN, Strik DPBTB: Continuous Long-Term Bioelectrochemical Chain Elongation to Butyrate. *ChemElectroChem* 2017, 4:386-395.

75. Ramiro-Garcia J, Hermes G, Giatsis C, Sipkema D, Zoetendal E, Schaap P, Smidt H: NG-Tax, a highly accurate and validated pipeline for analysis of 16S rRNA amplicons from complex biomes [version 1; referees: 2 approved with reservations, 1 not approved]. *F1000Research* 2016, 5.

76. van den Bogert B, de Vos WM, Zoetendal EG, Kleerebezem M: Microarray analysis and barcoded pyrosequencing provide consistent microbial profiles depending on the source of human intestinal samples. *Appl Environ Microbiol* 2011, 77:2071-2080.

77. Daims H, Brühl A, Amann R, Schleifer K-H, Wagner M: The domain-specific probe EUB338 is insufficient for the detection of all Bacteria: development and evaluation of a more comprehensive probe set. *Syst Appl Microbiol* 1999, 22:434-444.

78. Lu Y, Ramiro-Garcia J, Vandermeeren P, Herrmann S, Cichocka D, Springael D, Atashgahi S, Smidt H: Dechlorination of three tetrachlorobenzene isomers by contaminated harbor sludge-derived enrichment cultures follows thermodynamically favorable reactions. *Appl Microbiol Biotechnol* 2017, 101:2589-2601.

79. Quast C, Pruesse E, Yilmaz P, Gerken J, Schweer T, Yarza P, Peplies J, Glöckner FO: The SILVA ribosomal RNA gene database project: improved data processing and web-based tools. *Nucleic Acids Res* 2013, 41:D590-D596.

80. Edgar RC: Search and clustering orders of magnitude faster than BLAST. *Bioinf* 2010, 26:2460-2461.

81. Caporaso JG, Kuczynski J, Stombaugh J, Bittinger K, Bushman FD, Costello EK, Fierer N, Peña AG, Goodrich JK, Gordon JI, et al: QIIME allows analysis of high-throughput community sequencing data. *Nat Methods* 2010, 7:335-336.

82. Großkopf R, Janssen PH, Liesack W: Diversity and structure of the methanogenic community in anoxic rice paddy soil microcosms as examined by cultivation and direct 16S rRNA gene sequence retrieval. *Appl Environ Microbiol* 1998, 64:960-969.

83. Lane DJ: 16S/23S rRNA sequencing. In *Nucleic acid techniques in bacterial systematics.* Edited by Stackebrandt E, Goodfellow M. New York, NY: John Wiley & Sons, Inc.; 1991: 115-175

84. Coma M, Martinez-Hernandez E, Abeln F, Raikova S, Donnelly J, Arnot TC, Allen MJ, Hong DD, Chuck CJ: Organic waste as a sustainable feedstock for platform chemicals. *Faraday Discuss* 2017, 202:175-195.

85. Khor WC, Andersen S, Vervaeren H, Rabaey K: Electricity-assisted production of caproic acid from grass. *Biotechnol Biofuels* 2017, 10:180.

86. Evans NP, Collins DA, Pierson FW, Mahsoub HM, Sriranganathan N, Persia ME, Karnezos TP, Sims MD, Dalloul RA: Investigation of Medium Chain Fatty Acid Feed Supplementation for Reducing Salmonella Typhimurium Colonization in Turkey Poults. *Foodborne Pathogens and Disease* 2017, 14:531-536.

87. Hanczakowska E, Szewczyk A, Świątkiewicz M, Okon K: Short- and medium-chain fatty acids as a feed supplement for weaning and nursery pigs. *Polish Journal of Veterinary Sciences* 2013, 16:647-654.

88. Roghair M, Hoogstad T, Strik DPBTB, Plugge CM, Timmers PHA, Weusthuis RA, Bruins ME, Buisman CJN: Controlling ethanol use in chain elongation by CO2 loading rate. *Environ Sci Technol* 2018, 52:1496-1505.

89. López-Garzón CS, Straathof AJJ: Recovery of carboxylic acids produced by fermentation. *Biotechnol Adv* 2014, 32:873-904.

90. Liu Y, He P, Shao L, Zhang H, Lü F: Significant enhancement by biochar of caproate production via chain elongation. *Water Res* 2017, 119:150-159.

91. Syngellakis S: *Biomass to Biofuels.* Southampton ; Boston: WIT Press; 2015.

92. Chen WS, Huang S, Strik DPBTB, Buisman CJN: Isobutyrate biosynthesis via methanol chain elongation: Converting organic wastes to platform chemicals. *J Chem Technol Biotechnol* 2016, 92:1370–1379.

93. APHA: *Standard Methods for the Examination of Water and Wastewater, 20th Edition.* Washington DC: APHA American Public Health Association; 1998.

94. Yalkowsky SH, He Y, Jain P: *Handbook of Aqueous Solubility Data.* Boca Raton, FL: CRC press; 2016.

95. Royce LA, Liu P, Stebbins MJ, Hanson BC, Jarboe LR: The damaging effects of short chain fatty acids on Escherichia coli membranes. *Appl Microbiol Biotechnol* 2013, 97:8317-8327.

96. Lim S-J, Kim BJ, Jeong C-M, Choi J-d-r, Ahn YH, Chang HN: Anaerobic organic acid production of food waste in once-a-day feeding and drawing-off bioreactor. *Bioresour Technol* 2008, 99:7866-7874.

97. Andersen SJ, Candry P, Basadre T, Khor WC, Roume H, Hernandez-Sanabria E, Coma M, Rabaey K: Electrolytic extraction drives volatile fatty acid chain elongation through lactic acid and replaces chemical pH control in thin stillage fermentation. *Biotechnol Biofuels* 2015, 8:221.

98. Euro Chlor. The European Chlor-Alkali industry: an electricity intensive sector exposed to carbon leakage. 2010. http://www.eurochlor.org/media/9385/3-2-the_european_chlor-alkali_industry_-_an_electricity_intensive_sector_exposed_to_carbon_leakage.pdf (accessed 24 October 2017).

99. Renewable Fuels Association (RFA). Industry statistics: World Fuel Ethanol Production 2016. https://www.ethanolrfa.org/resources/industry/statistics/ (accessed 24 Oktober 2017).

100. International Energy Agency (IEA). OECD Europe: Electricity and Heat for 2015 *Statistics* [Online], 2015. http://www.iea.org/statistics/statisticssearch/report/?year=2015&country=OECDEUR&product=ElectricityandHeat (accessed 26 October 2017).

101. Urban C, Xu J, Strauber H, dos Santos Dantas TR, Muhlenberg J, Hartig C, Angenent LT, Harnisch F: Production of drop-in fuels from biomass at high selectivity by combined microbial and electrochemical conversion. *Energy Environ Sci* 2017, 10:2231-2244.

102. International Air Transport Association (IATA). Economic performance of the airline industry: 2017 Mid-year report. 2017. https://www.iata.org/whatwedo/Documents/economics/IATA-Economic-Performance-of-the-Industry-mid-year-2017-report.pdf (accessed 25 October 2017).

103. Roghair M, Liu Y, Strik DPBTB, Weusthuis RA, Bruins ME, Buisman CJN: Development of an Effective Chain Elongation Process From Acidified Food Waste and Ethanol Into n-Caproate. *Front Bioeng Biotechnol* 2018, 6:50.

104. Roy F, Albagnac G, Samain E: Influence of Calcium Addition on Growth of Highly Purified Syntrophic Cultures Degrading Long-Chain Fatty Acids. *Appl Environ Microbiol* 1985, 49:702-705.

105. Sudmalis D, Gagliano MC, Pei R, Grolle K, Plugge CM, Rijnaarts HHM, Zeeman G, Temmink H: Fast anaerobic sludge granulation at elevated salinity. *Water Res* 2017, 128:293-303.

106. Roman P, Bijmans MFM, Janssen AJH: Influence of methanethiol on biological sulphide oxidation in gas treatment system. *Environ Technol* 2016, 37:1693-1703.

107. Rodríguez Arredondo M, Kuntke P, ter Heijne A, Hamelers HVM, Buisman CJN: Load ratio determines the ammonia recovery and energy input of an electrochemical system. *Water Res* 2017, 111:330-337.

108. Hajarnis SR, Ranade DR: Inhibition of methanogens by n- and iso-volatile fatty acids. *World J Microbiol Biotechnol* 1994, 10:350-351.

109. Liu P, Chernyshov A, Najdi T, Fu Y, Dickerson J, Sandmeyer S, Jarboe L: Membrane stress caused by octanoic acid in Saccharomyces cerevisiae. *Appl Microbiol Biotechnol* 2013, 97:3239-3251.

110. Jarboe LR, Royce LA, Liu P: Understanding biocatalyst inhibition by carboxylic acids. *Front Microbiol* 2013, 4:272.

111. Zhang Q, Wu D, Lin Y, Wang X, Kong H, Tanaka S: Substrate and Product Inhibition on Yeast Performance in Ethanol Fermentation. *Energy Fuels* 2015, 29:1019-1027.

112. Lian J, McKenna R, Rover MR, Nielsen DR, Wen Z, Jarboe LR: Production of biorenewable styrene: utilization of biomass-derived sugars and insights into toxicity. *J Ind Microbiol Biotechnol* 2016, 43:595-604.

113. Hierholtzer A, Akunna JC: Modelling sodium inhibition on the anaerobic digestion process. *Water Sci Technol* 2012, 66:1565-1573.

114. Kenealy WR, Waselefsky DM: Studies on the substrate range of *Clostridium kluyveri*; the use of propanol and succinate. *Arch Microbiol* 1985, 141:187-194.

115. Liu Y, Boone DR: Effects of salinity on methanogenic decomposition. *Bioresour Technol* 1991, 35:271-273.

116. Reddy MV, Hayashi S, Choi D, Cho H, Chang Y-C: Short chain and medium chain fatty acids production using food waste under non-augmented and bio-augmented conditions. *J Cleaner Prod* 2018, 176:645-653.

117. Ganigué R, Sánchez-Paredes P, Bañeras L, Colprim J: Low Fermentation pH Is a Trigger to Alcohol Production, but a Killer to Chain Elongation. *Front Microbiol* 2016, 7:702.

118. Steinbusch KJJ, Arvaniti E, Hamelers HVM, Buisman CJN: Selective inhibition of methanogenesis to enhance ethanol and n-butyrate production through acetate reduction in mixed culture fermentation. *Bioresour Technol* 2009, 100:3261-3267.

119. Nzeteu CO, Trego AC, Abram F, O'Flaherty V: Reproducible, high-yielding, biological caproate production from food waste using a single-phase anaerobic reactor system. *Biotechnol Biofuels* 2018, 11:108.

120. Galadima A, Muraza O: From synthesis gas production to methanol synthesis and potential upgrade to gasoline range hydrocarbons: A review. *J Nat Gas Sci Eng* 2015, 25:303-316.

121. Liu K, Atiyeh HK, Stevenson BS, Tanner RS, Wilkins MR, Huhnke RL: Continuous syngas fermentation for the production of ethanol, n-propanol and n-butanol. *Bioresour Technol* 2014, 151:69-77.

122. Guo XM, Trably E, Latrille E, Carrère H, Steyer J-P: Hydrogen production from agricultural waste by dark fermentation: A review. *Int J Hydrogen Energy* 2010, 35:10660-10673.

123. Kim M-S, Na J-G, Lee M-K, Ryu H, Chang Y-K, Triolo JM, Yun Y-M, Kim D-H: More value from food waste: Lactic acid and biogas recovery. *Water Res* 2016, 96:208-216.

Mark Roghair

Process Engineer

Personal info

Date of birth	24 February 1986
Place of birth	's-Gravenhage, the Netherlands
Nationality	Dutch
Marital status	Living together
Children	1 son

Education

2010 - 2012	**MSc in Biotechnology**, *Wageningen University & Research*, Wageningen Specialization in Process Technology
2006 - 2010	**BaSc in Biotechnology,** *Van Hall Larenstein*, Leeuwarden Major in Process Engineering
1998 - 2006	**Pre-university education**, *Alfrink College,* Zoetermeer & *ID College*, Gouda Profile: Science and Health

Experience

2018 – Present	**Process Engineer**, *DMT Environmental Technology,* Joure Developing existing and new environmental technological processes
2013 - 2017	**PhD Student**, *Wageningen University & Research,* Wageningen Developing control strategies for ethanol-based chain elongation processes
2012	**Intern and Bioprocess Technologist**, *Waste2Chemical* (Now: *Chaincraft*), Wageningen Laboratory research on fermentation of bio-based products from agro-food residues
2011 - 2012	**MSc Thesis**, *Wageningen University & Research,* Wageningen Investigating the inactivation of probiotics during spray drying using a single droplet drying approach
2010	**BaSc Thesis**, *Virginia Tech*, Blacksburg (USA) Investigating the potential of biochar as a nutrient source and inhibitor-reducer in xylose to xylitol fermentation

Acknowledgements

I would like to thank my teachers,

Kirsten, thanks for having me as an intern at Waste2Chemical in 2012. This is where my chain elongation adventure started. Thanks for your support and advices during the first years of my PhD. David, thanks for your patience. My learning curve in writing was somewhat flat but you never seemed to be bothered by this. Thanks for bringing the work to a much higher level than I was initially aiming at. Thanks for your faith and for all the freedom that you gave me; thanks for letting me go to Leeuwarden. Ruud, thanks for your very critical remarks in the draft versions of the manuscripts. Thanks for the beers in cafe de Zaaier. I hope you'll be a full professor soon. Marieke, thanks for all your advices during our meetings. You always brought joy and a very positive vibe to the meetings. Thanks for inviting me to go to Brazil. It was awesome, and I will never forget it. Cees, thanks for having me as a PhD student. It was an honour. Also, thanks for having me in Wetsus and thanks for not letting me become a post-doc. My parents, the very first and most important teachers in my life; thank you for all your time and efforts. Especially, thank you for your love.

I would like to thank my colleagues,

Hans, thanks for your support in the lab and for the good times during the borrels. Jan, thanks for maintaining the lab and lab-equipment so well. Livio, thanks for analysing the vast number of samples I brought to you. Ilse, thanks for your support in analytical work. Bert, thanks for moving the reactor setups from Wageningen to Leeuwarden and back. Vinnie, thanks for your technical support in the lab. Jean, thanks for the nice talks. Katja, thanks for the cigarette breaks. Hardy, Jan and Bruna; it was a joy to organize the ETEI2015 conference with you. Koen, it was awesome to be in the borrel committee with you and Hans; good times! In fact, being in the ETE department was always a joy to me. Thank you very much, Yvonne, Ingo, Leire, Nora, Arnoud, Dainis, Romana, Roxani, Sanne, Ludo, Dandan, Miriam for the talks and gezelligheid in the office/lab and during the borrels/coffeebreaks. Thanks, Liesbeth and Gea, for the administrative work. Michael, Tim, Coen, Julius and Yuchen; thank you for your hard work, dedication and for your contribution to the experimental work. You guys are true heroes! Also, I'd like to thank co-authors Caroline and Peer for their efforts.

List of publications

Perdana J, Bereschenko L, **Roghair M**, Fox MB, Boom RM, Kleerebezem M, Schutyser MA: Novel method for enumeration of viable Lactobacillus plantarum WCFS1 cells after single-droplet drying. *Appl Environ Microbiol* 2012, 78:8082-8088.

Roghair M, Strik DPBTB, Steinbusch KJJ, Weusthuis RA, Bruins ME, Buisman CJN: Granular sludge formation and characterization in a chain elongation process. *Process Biochem* 2016, 51:1594-1598.

Roghair M, Hoogstad T, Strik DPBTB, Plugge CM, Timmers PHA, Weusthuis RA, Bruins ME, Buisman CJN: Controlling ethanol use in chain elongation by CO_2 loading rate. *Environ Sci Technol* 2018, 52:1496-1505.

Roghair M, Liu Y, Strik DPBTB, Weusthuis RA, Bruins ME, Buisman CJN: Development of an Effective Chain Elongation Process From Acidified Food Waste and Ethanol Into n-Caproate. *Front Bioeng Biotechnol* 2018, 6:50.

Roghair M, Liu Y, Adiatma JC, Weusthuis RA, Bruins ME, Buisman CJN, Strik DPBTB: Effect of n-Caproate Concentration on Chain Elongation and Competing Processes. *ACS Sustainable Chem Eng* 2018, 6:7499-7506.

**Netherlands Research School for the
Socio-Economic and Natural Sciences of the Environment**

D I P L O M A

For specialised PhD training

The Netherlands Research School for the
Socio-Economic and Natural Sciences of the Environment
(SENSE) declares that

Mark Roghair

born on 24 February 1986 's-Gravenhage, the Netherlands

has successfully fulfilled all requirements of the
Educational Programme of SENSE.

Wageningen, 16 November 2018

On behalf of the SENSE board   the SENSE Director of Education

Prof. dr. Huub Rijnaarts   Dr. Ad van Dommelen

The SENSE Research School has been accredited by the Royal Netherlands Academy of Arts and Sciences (KNAW)

K O N I N K L I J K E   N E D E R L A N D S E
A K A D E M I E   V A N   W E T E N S C H A P P E N

The SENSE Research School declares that **Mark Roghair** has successfully fulfilled all
requirements of the Educational PhD Programme of SENSE with a
work load of 32.2 EC, including the following activities:

SENSE PhD Courses

o   Environmental research in context (2014)
o   Research in context activity: 'Co-organizing the conference Environmental Technology
    for Impact (ETEI2015), around the themes: Biorecovery, Water Reuse and Urban
    Systems Engineering (29-30 April 2015, Wageningen)'

Other PhD and Advanced MSc Courses

o   PhD Competence Assessment course, Wageningen University (2013)
o   Workshop OLI Stream Analyzer, Wageningen University (2013)
o   Training course 1, BE Basic Innovation centre, The Netherlands (2013)
o   Voice matters - Pitch training for PhD pitch presentations, Wageningen University (2014)
o   Techniques for writing and presenting a scientific paper, Wageningen University (2016)

External training at a foreign research institute

o   PhD Study trip, Brasil (2013)
o   Course on SuperPro Designer, Intelligen, Ghent, Belgium (2017)

Management and Didactic Skills Training

o   Assisting practicals of the BSc course 'Biorefinery' (2013)
o   Supervising case studies in the BSc course 'Introduction to Environmental Sciences'
    (2014)
o   Supervising five MSc students (2013-2017)

Oral Presentations

o   *Medium chain α,ω-di-ester production from non-food feedstock for biomaterials.* BE-
    Basic conference, 31 March-1 April 2015 , Noordwijkerhout, The Netherlands
o   *Granular sludge formation and characterization in a chain elongation process.* 1st
    International Conference on Bioresource Technology for Bioenergy, Bioproducts &
    Environmental Sustainability (BIORESTEC), 23-26 October 2016, Sitges, Spain

SENSE Coordinator PhD Education

Dr. Peter Vermeulen